REFERENCES

Albery, W.J., Li , F.B., and Mount ,A.R. (1991) Electrochemical polymerization of poly(thiophene-3-acetic acid), poly(thiophene-co-thiophene-3-acetic acid) and determination of their molar mass. Journal Electroanalytical Chemistry, 310, 239-253.

Albery ,W.J., and Li, F.B. (1991) Electrochimica Acta, 37, 293.

Anquetil, P.A., Yu, H., Madden, J.D., Madden, P.G., Swager, T.M., and Hunter, I.W. (2002) Thiophene-based conducting polymer molecular actuators. Proceedings of SPIE, 4695, 424-434.

Andreani, F., Salatelli, E., Lanzi, M., Bertinelli, F., Fichera, A.M., and Gazzano, M. (2000) Synthesis and characterization of neutral newly substituted polyalkylthiophenes. Polymer, 41, 3147–3157.

Bantaculo, R. V., Alguno, A. C., Vequizo, R. M., and Dahili, A. S. (2001) A Structural Study of Polythiophene Coupling through α and β Carbon: An AB Initio Evaluation. NECTEC Technical Journal, 9, 176-181.

Bell, R.G. (2001) British Zeolite Association.

Benco, L., Bucko, T., Hafner, J., and Toulhoat, H. (2005) A Density Fuctional Theory Study of Molecular and Dissociative Adsorption of H_2 on Active Sites in Mordenite. Journal of Physical Chemistry B, 109, 22491-22501.

Bordiga, S., Palomino, G. T., Paze, C., and Zecchina, A. (2000) Vibrational spectroscopy of H2, N2, CO and NO adsorbed on H, Li, Na K-exchanged ferrierite. Microporous and Mesoporous Materials. 34, 67-80.

Burroughes, J. H., Bradley, D. D. C., Brown, A. R., Marks, R. N., Mackay, K., Friend, R. H., Burns, P. L., and Holmes, A. B. (1990) LEDs based on conjugated polymers. Nature, 347, 539.

Chandrasekhar, P. (1999) Fundamnetals and Applications of Conducting Polymers Handbook. USA: Kluwer Academic Publishers.

Chen, T-A., Wu, X., and Rieke, R.D. (1995) Regiocontrolled Synthesis of Poly(3-alkythiophenes) Mediated by Rieke Zinc: Their Characterization and Solid-State Properties. J. Am. Chem. Soc., 117, 233-244.

Chotpattananont, D., Sirivat, A., and Jamieson, A. (2004) Scaling of Yield Stress of Polythiophene Suspensions under Electric Field. Macromolecular Materials and Engineering, 289, 434-441.

Chotpattananont, D., Sirivat, A., and Jamieson, A. (2004) Electrorheological properties of perchloric acid-doped polythiophene suspension. Colloid polymer science, 282, 357-365.

Chiang, C.K., Fincher, C.R., Park, Y.W., Heeger, A.J., Shirakawa, H., Louis, E.J., Gau, S.C., and MacDiarmid, A.G. (1977) Electrical Conductivity in Doped Polyacetylene. Physical Review Letter, 39, 1098-1101.

Chiang, C.K., Druy, M.A., Gau, S.C., Heeger, A.J., Louis, E.J., MacDiarmid, A.G., Park, Y.W., Shirakawa, H. (1978) Synthesis of highly conducting films of derivatives of polyacetylene, (CH)x. J. Am. Chem. Soc., 100, 1013-1015.

Chuapradit, C., Ruangchuay, L., Wannatong, R., and Chotpattananont, D., Hismtup, P., Sirivat, A., Schwank, J. (2005) Polyaniline/zeolite LTA composites and electrical conductivity response towards CO. Polymer, 46, 947-953.

Demanze, F., Yassar, A., and Garnier, F. (1996) Alternating Donor-Acceptor Substitutions in Conjugated Polythiophenes. Macromolecules, 29, 4267-4273.

Densakulprasert, N., Wannatong, L., Chotpattananont, D., Hiamtup, P., Sirivat, A., and Schwank, J. (2005) Electrical conductivity of polyaniline/zeolite composites and synergetic interaction with CO. Materials Science and Engineering B, 117, 276-282.

De Paoli, M.A. and Gazotti, W.A. (2002) Electrochemistry, Polymers and Opto-Electronic Devices: A Combination with a Future. Journal of the Brazilian Chemical Society, 13, 410-424.

De Souza, J.M., and Pereira, E.C. (2001) Luminescene of poly(3-thiophene acetic acid) in alcohols and aqueous solutions of poly(vinyl alcohol). Synthetic Metals, 118, 167-170.

Dietrich, M., Heinze, J., Heywang, G., and Jonas, F. (1994) Electrochemical and spectroscopiccharacterization of polyalkylenedioxythiophenes. Journal Electroanalytical Chemistry, 369, 87.

Donsld, W. (1974) Zeolite Molecular Sieves. Florida: Robert E. Krieger.

Ferrari, A.M., Neyman, K.M., and Rösch, N. (1997) CO interaction with Alkali Metal Cations in Zeolites: A Density Functional Model Cluster. J. Phys. Chem. B, 101, 9292-9298.

Frolov, S. V., Fujii, A., Chinn, D., Hirohata, M., Hidayat, R., Taraguchi, M., Masuda, T., Yoshino, K., and Vardeny, Z. V. (1998) Microlasers and Micro-LEDs from Disubstituted Polyacetylene. Advanced Materials, 10, 869-872.

Gazotti, W. A., Casalbore-Miceli, G., Geri, A., and De Paoli, M. —A. (1998) A Solid-State Electrochromic Device Based on Two Optically Complementary Conducting Polymers. Advanced Materials, 10, 60-64.

Günzler, H., and Gremlich, H-U. (2002) IR Spectroscopy: An Introduction. Germany: Wiley-VCH.

Hatano, M., Kambara, S., and Okamoto, S. (1961) Paramagnetic and electric properties of polyacetylene. Journal of Polymer Science, 51, S26-S29.

Hotovy, I., Huran, J., Siciliano, P., Capone, S., Spiess, L., and Rechacekm, V. (2004) Enhancement of H_2 sensing properties of NiO-base thin films with a Pt surface modification. Sensor and Actuators B, 103, 300-311.

Kaneyasu, K., Ostsuka, K., Setoguchi, Y., Sonoda, S., Nakahara, T., Aso, I., Nakagaichi, N. (2000) A carbon dioxide gas sensor based on solid electrolyte for air quality control. Sensor and Actuators B, 66, 56-58.

Kiattibutr, P., Tarachiwin, L., Ruangchuay, L., Sirivat, A., and Schwank, J. (2002) Electrical conductivity responses of polyaniline films to SO_2-N_2 mixtures: effect of dopant type and doping level. Reactive & Fuctional Polymers, 53, 29-37.

Kim, B., Chen, Li., Gong, J., and Osada, Y. (1999) Titration Behavior and Spectral Transitions of Water-Soluble. Macromolecules, 32, 3964-3969.

Kim, B., Chen, L., Gong, J., and Osada, Y. (1999) Titration Behavior and Transitions of Water-Soluble Polythiophene Carboxylic Acids. Macromolecules, 32, 3964-3969.

Kumar, D., and Sharma, R.C. (1998) Advances in conductive polymers. European Polymer Journal, 34, 1053-1060

Lee, C. H., Yu, G., Zhang, C., and Heeger, A. J. (1994) Dual-function semiconducting polymer devices: Light-emitting and photodetecting diodes. Applied Physics Letters., 64, 1540-1542.

Liaw, D.J., Laiw, B.Y., Gong, J.P., and Osada, Y. (1999) Synthesis and properties of poly(3-thiopheneacetic acid) and its networks via electropolymerization. Synthetic Metals, 99, 53-59.

Masuda, H., Asano, D. K., and Kaeriyama, K. (1999) Synthesis of poly(3-alkoxymethylthiophenes). Synthetic Metals, 101, 73-74.

M, J., Souza, de., and Pereira, E.C. (2001) Luminescence of poly(3-thiopheneacetic acid) in alcohols and aqueous solutions of poly(vinyl alcohol). Synthetic Metals, 118, 167-170.

Msuda, H., Asano, D.K., and Kaeriyama, K. (2001) Preparation and properties of polthiophene derivatives. Synthetic Metals, 119, 167-168.

Mu, S., and Park, S.M. (1995) Preparation and characterization of polythiophene in aqueous solutions. Synthetic Metals, 69, 311-312.

Patil, A. O., Heeger, A. J., and Wudl, F. (1988) Optical properties of conducting polymers. Chemical Review, 88, 183-200.

Pei, Q., Yu, G.; Zhang, C., Yang, Y., and Heeger, A. J. (1995) Polymer light-emitting electrochemical cells. Science, 269, 1086.

Pei, Q., Yang, Y., Yu, G., Zhang, C., and Heeger, A. J. (1996) Polymer Light-Emitting Electrochemical Cells: In Situ Formation of a Light-Emitting p-n Junction. J. Am. Chem. Soc., 118, 3922-3929.

Prissanaroon, W., Ruangchuay, L., Sirivat, A., and Schwank, J. (2000) Electrical conductivity response of dodecylbenzene sulfonic acid-doped polypyrrole film to SO_2-N_2 mixtures. Synthetic Metals, 114 , 65-72.

Ribeiro, A. S., Gazotti Jr, W.A., Santos Filho, P.F., and De Paoli, M.A. (2004) New functionalized 3-(alkyl)thiophene derivatives and spectroelectrochemical characterization of its polymers. Synthetic Metals, 145, 43-49.

Ruangchuay, L., Sirivat, A., and Schwank, J. (2004) Electrical conductivity response of polypyrrole to acetone vapor: effect of dopant anions and interaction mechanisms. Synthetic Metals, 140, 15-21.

Sakurai, Y., Jung, H., Shimanouchi, T., Inoguchi, T., Morita, S., Kuboi, R., Natsukawa, K. (2002) Novel array-type gas sensors using conducting polymers, and their performance for gas identification. Sensor and Actuators B, 83, 270-275.

Sasaki, I., Tsuchiya, H., and Nishioka, M. (2002) Gas sensing with zeolite-coat quartz crystal microbalances-principal component analysis approach. Sensor and Actuators B, 85, 26-33.

Savenije, T. J., Warman, J. M., and Goossens, A. (1998) Visible light sensitisation of titanium dioxide using a phenylene vinylene polymer. Chemicals Physics Letters, 287, 148-153.

Schottland, P., Bouguettaya, M., and Chevrot, C. (1999) Soluble polythiophene derivatives for NO_2 sensing applications. Synthetic Metals, 102, 1325.

Shirakawa, H., Louis, E.J., MacDiarmid, A.G., Chiang, C.K., Heeger, A.J. (1977) J. Chem. Soc. Chem. Commun, 578.

Skoog, D.A., and Leary, J.J. (1992) Principles of Instrumental Analysis Fouth edition. Tokyo: Saunders College Publishing.

Souza, J.M., and Pereira, E.C. (2001) Luminescence of poly(3-thiopheneacetic acid) in alcohols and aqueous solution of poly(vinyl alcohol). Synthetic Metals, 118, 167-170.

Szostak, R. (1989) Molecular Sieves, Principles of Synthesis and Identification. New York: Van Nostrand Reinhold

Tananka, F., Kawai, T., Kojima, S., and Yoshino, K. (1999) Electrical and optical properties of poly(3-alkoxythiophene) and their application for gas sensor. Synthetic Metals, 102, 1358-1359.

Torsi, L., Tafuri, A., Cioffi, N., Gallazzi, M.C., Sassella, A., Sabbatini, L., and Zambonin, P.G. (2003) Regioregular polythiophene field-effect transistors employed as chemical sensors. Sensors and Actuators B, 93, 257-262.

Torsi, L., Tanese, M.C., Ciofi, N., Gallazzi M.C., Sabbatini,L., and Zambonin, P.G. (2004) Alkoxy-substituted polyterthiophene thin-film-transistors as alcohol sensors. Sensors and Actuators B, 98, 204-207.

Triebe, R.W., and Tezel, F.H. (1995) Adsorption of nitrogen, carbon monoxide, carbon dioxide and nitric oxide on molecular sieves. Gas Separation & Purification, 9, 223-230.

Vamvounis, G., Yu, J., and Holdcroft, S. (2004) Photo-physial and eletro-optical properties of polythiophenes bearing tetrahydropyran side groups. European Polymer Journal, 40, 2659-2664.

Van Vught, F.A. (2000) Transparent and conductive polymer layers by gas plasma techniques. The Netherlands: L.M.H. Groenewoud.

Wang, F., Lai, Y-H., and Han, M-Y. (2004) Stimuli-Responsive Conjugated Copolymers Having Electro-Active Azulene and Bithiophene Units in the Polymer Skeleton: Effect of Protonation and p-Doping on conducting Properties. Macromolecules, 37, 3222-3230.

Wang, Y-D., Ma, C-L., Wu, X-H., S, X-D., and Li, H-D. (2002) Electrical and gas-sensing properties of mesostructured tin oxide-base H_2 sensor. Sensor and Actuators B, 85, 270-276.

Weitkamp, J., and Puppe, L. (1999) Catalysis and Zeolite (Fundamenttals and Appication). New York: Springer.

Yu, G., Gao, J., Hummelen, J. C., Wudl, F., and Heeger, A. J. (1995) Science, 270, 1789.

Yu, G.; Heeger, and A. J. (1997) High efficiency photonic devices made with semiconducting polymers. Synthetic Metals, 85, 1183.

Yu, G., Pakbaz, K., and Heeger, A. J. (1994) J. Electron. Mater., 23, 925.

Yu, G., Wang, J., McElvain, J., and Heeger, A. J. (1998) Large-Area, Full-Color Image Sensors Made with Semiconducting Polymers. Advanced Materials, 10, 1431-1434.

APPENDICES

Appendix A Identification of Characteristic Peaks of FT-IR Spectrum of Undoped and Doped Poly(3-thiopheneacetic acid)

FT-IR spectrometer (Thermo Nicolet, Nexus 670) was used to investigate spectra of poly(3-thiophenemethyl acetate) (P3TMA), undoped and doped poly(3-thiophene acetic acid) (P3TAA). The spectrometer was operated in the absorption mode with 32 scans and a resolution of ±4 cm^{-1}, covering a wavenumber range of 4000-400 cm^{-1}. Optical grade KBr was used as the background material and the polymers were mixed with dried KBr at a ratio 1:20. In order to investigate the spectrum of Pth_200:1 and zeolite L, mordenite and beta, before, expose and after exposed with H_2 gas, gas cell with ZnSe window was used.

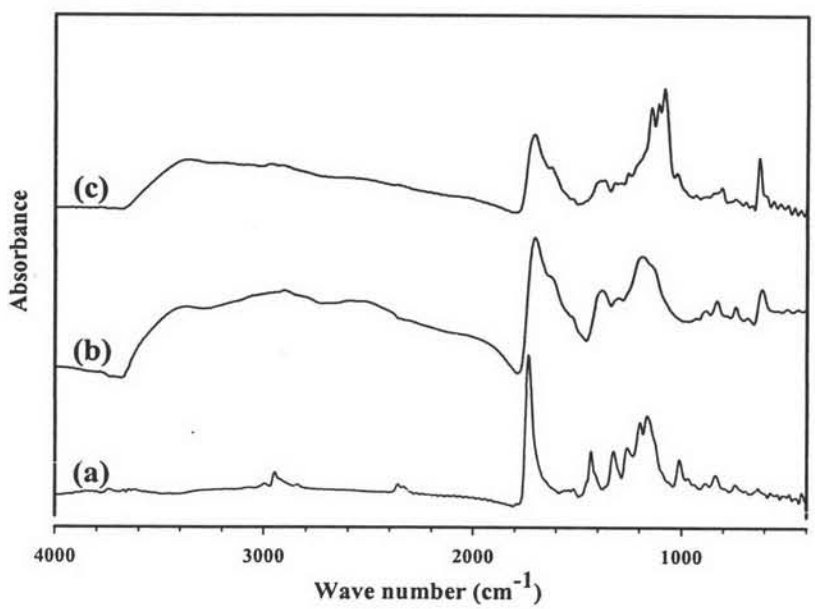

Figure A1 The FT-IR spectra of: a) poly(3-thiophenemethyl acetate); b) undoepd poly(3-thiophene acetic acid); and c) poly(3-thiopheneacetic acid) doped with $HClO_4$ at mole ratio of acid to monomer unit of 200:1.

In Figure A1, distinct peaks of P3TMA and P3TAA appeared between 3400-2400 cm^{-1}. A broad peak is characteristic of hydroxy fuctional group of P3TAA which ensures us a successful synthesization of this polymer by oxidation polymerization. After doping with perchloric acid, some characteristic peaks of acid appeared on FT-IR spectra. There are appearances of a lower absorbance at 3400-2400 cm^{-1} and a sharp peak at 1200 cm^{-1}.

The assignments of peaks in the spectrum are shown in Table A1. The characteristic peaks of P3TAA appears at 3200-3000 cm^{-1} and can be assigned to the stretching vibration of the C-H bond on the thiophene ring; peaks at 3000-2800 cm^{-1} represent the aliphatic C-H bonds; a peak at 1700 cm^{-1} represents the C=O stretching vibration; a peak at 1400 cm^{-1} represents the thiophene ring stretching vibration; and peaks at 1300-1200 cm^{-1} represent the C-O stretching vibration. The important feature peak is the extremely broad O-H absorption occurring in the region from 3400 to 2400 cm^{-1}, which is attributed to the strong hydrogen bonding of the dimer. In the same region, the C-H stretching vibrations occurs (Kim *et al.*, 1999).

Table A1 The FT-IR absorption spectrum of undoped and doped PTAA with $HClO_4$

Wavenumber (cm^{-1})	Assignments	References
3400-2400	O-H stretching vibration	Kim *et al.* (1999)
3200-3000	C-H stretching of thiophene ring	Kim *et al.* (1999)
3000-2800	C-H stretching of aliphatic	Kim *et al.* (1999)
1700	C=O stretching vibration	Kim *et al.* (1999)
1400	Thiophene ring stretching vibration	Kim *et al.* (1999)
1300-1200	C-O stretching vibration	Kim *et al.* (1999)
835	C-H stretching, out of plane of thiophene ring	Kim *et al.* (1999)

Appendix B Identification Thermal Property of Undoped and Doped P3TAA

Undoped and doped poly(3-thiopheneacetic acid) (P3TAA) at 200:1 mole ratio of dopant to monomer unit were determined by a thermal gravimetric analyzer (DuPont, model TGA 2950). Measurements were carried out with the temperature scan from 30 to 800°C and a heating rate of 10°C/min. The samples were weighed in the range of 5-20 mg and loaded into a platinum pan, and then it was heated under air flow. Three transitions were observed in undoped and dope poly (3-thiopheneacetic acid). The first transition can be referred to the losses of water and residue solvent. The other transitions can be referred to the side chain degradation and the backbone degradation, respectively (Chotpattananont *et al.*, 2004; Hu *et al.*, 2000). After the doping, the thermal stability decreased as compared to undoped P3TAA.

Table B1 Degradation steps of undoped and doped P3TAA

Sample	T_d onset (°C)		% Weight loss		% residue
	1	2	1	2	
Pth_u	186	356	21.79	63.03	7.667
Pth_200:1	104	300	16.94	69.76	4.711

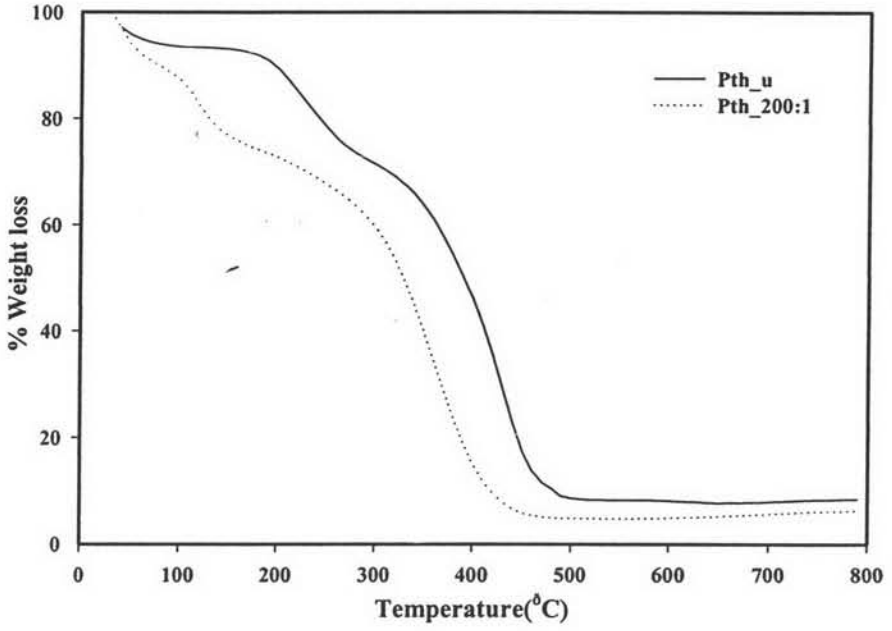

Figure B1 TGA thermograms of undoped and doped P3TAA with $HClO_4$.

Appendix C Identification of Characteristic Peaks of Undoped and Doped Poly(3-thiopheneacetic acid) by UV-Visible Spectroscopy

UV-Vis absorption spectrophotometer (Shimadzu, UV-2550) was used to investigate spectra of undoped and doped polythiophene in the absorbance mode, wavelength range of 200-800 nm with medium scan speed and a slit width of 1.0 nm. Both polymers were dissolved in DMSO at the concentration of 2.8134×10^{-6} M. The absorbance of solution in a quatz cell was measured and we used DMSO as a reference solvent.

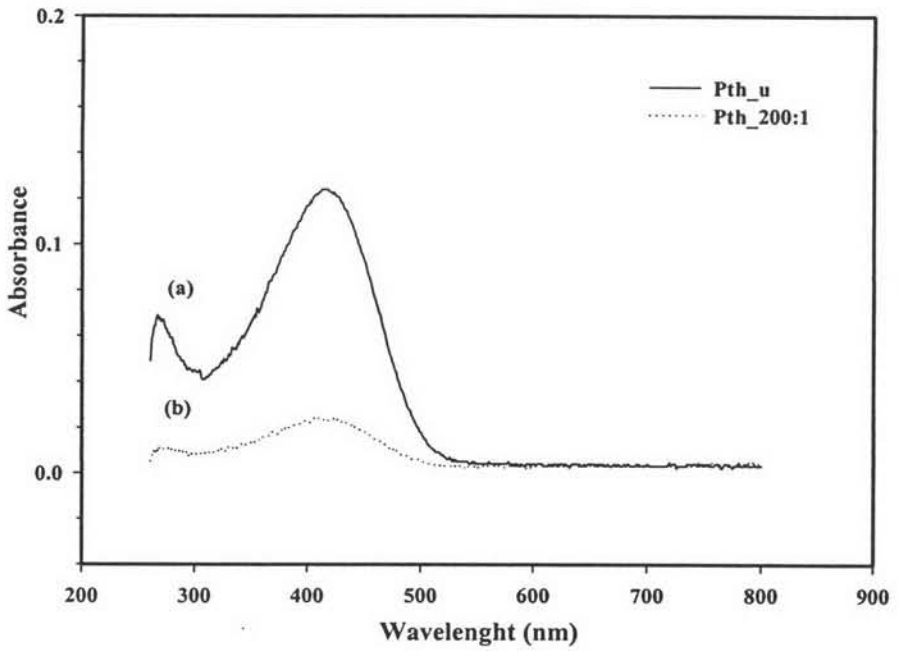

Figure C1 The UV-Visible spectra of: a) undoped poly(3-thiopheneacetic acid); b) doped with $HClO_4$ at 200:1 mole ratio of acid to monomer.

Table C1 The UV_Visible spectrum of undope (Pth_u) and dope polythiophene at the doping mole ratio of $HClO_4$:Pth (Pth_200:1)

Pth_u		Pth_200:1	
Wavelength	Absorbance	Wavelength	Absorbance
None	None	701	0.004
417	0.124	410	0.024
267	0.069	270	0.018

In Table C2, the UV-Visible spectra of undoped and doped poly(3-thiopheneacetic acid) from the references are shown. The wavelength in [ ] refers to the assignments as cited from the references.

Table C2 Assignments of UV-Visible peaks of undoped and doped polythiophenes

Wavelength (nm)	Assignments	References
264±5 [264]	π-π* transitions of the bithiophene unit	Wang *et al.* (2004)
435±10 [435]	π-π* transitions of the conjugated polymer chains	Demanze *et al.* (1996)
735±5 [735]	localized of polaron state	Demanze *et al.* (1996)

Appendix D Determination of Particle size and Size distribution of Undoped and Doped poly(3-thiopheneacetic acid)

Particle size analyser (Malvern, Masterizer X Version 2.15) was used to measure the particle size of undoped and dope polythiophene. Polythiophene was grounded and sieved with mesh size 38 μm before measurment were taken.

Table D1 Summary data of particle size of undoped and dope poly(3-thiopheneacetic acid)

Samples	Particle diameter (μm)				
	1	2	3	Avg.	STD
Pth_U	19.28	19.40	20.05	19.58	0.41
Pth_200:1	20.56	20.81	21.11	20.83	0.28

Table D2 Summary data of particle size of Zeolite

Samples	Particle diameter (μm)				
	1	2	3	Avg.	STD
L	7.57	7.99	7.57	7.71	0.24
MOR	16.64	16.95	16.69	16.76	0.17
BEA	2.41	2.44	2.38	2.41	0.03

Table D3 The raw data of particle size of undoped poly(3-thiopheneacetic acid)

Particle size diameter (μm)		Undope polythiophene					
Size Low	Size high	In %	Under %	In %	Under %	In %	Under %
0.50	1.32	0.19	0.19	0.19	0.20	0.19	0.20
1.32	1.60	0.60	0.79	0.64	0.83	0.63	0.82
1.60	1.95	0.90	1.69	0.96	1.79	0.94	1.76
1.95	2.38	1.07	2.76	1.15	2.95	1.11	2.87
2.38	2.90	1.22	3.98	1.31	4.25	1.26	4.13
2.90	3.53	1.49	5.47	1.56	5.82	1.52	5.65
3.53	4.30	1.98	7.45	2.03	7.85	2.00	7.65
4.30	5.24	2.76	10.21	2.76	10.61	2.76	10.41
5.24	6.39	3.79	14.00	3.72	14.33	3.78	14.19
6.39	7.78	4.93	18.93	4.75	19.08	4.87	19.06
7.78	9.48	6.02	24.95	5.73	24.81	5.90	24.97
9.48	11.55	7.30	32.24	6.89	31.70	7.08	32.05
11.55	14.08	8.89	41.14	8.40	40.10	8.54	40.59
14.08	17.15	10.68	51.81	10.17	50.27	10.20	50.80
17.15	20.9	12.16	63.97	11.77	62.03	11.62	62.42
20.90	25.46	12.35	76.30	12.28	74.3	11.94	74.35
25.46	31.01	10.40	86.70	10.82	85.11	10.35	84.69
31.01	37.79	6.60	93.31	7.44	92.56	6.97	91.66
37.79	46.03	2.83	96.14	3.74	96.29	3.37	95.03
46.03	56.09	0.88	97.02	1.46	97.77	1.28	96.32
56.09	68.33	0.78	97.80	0.83	98.59	0.98	97.30
68.33	83.26	1.18	98.98	0.81	99.40	1.35	98.65
83.26	101.44	0.85	99.82	0.51	99.91	1.08	99.72
101.44	123.59	0.17	100.00	0.09	100.00	0.27	100.00
123.59	150.57	0.00	100.00	0.00	100.00	0.00	100.00
150.57	183.44	0.00	100.00	0.00	100.00	0.00	100.00
183.44	223.51	0.00	100.00	0.00	100.00	0.00	100.00
223.51	272.31	0.00	100.00	0.00	100.00	0.00	100.00
272.31	331.77	0.00	100.00	0.00	100.00	0.00	100.00
331.77	404.21	0.00	100.00	0.00	100.00	0.00	100.00
404.21	429.47	0.00	100.00	0.00	100.00	0.00	100.00
492.47	600.00	0.00	100.00	0.00	100.00	0.00	100.00

Table D4 The raw data of particle size of doped poly(3-thiopheneacetic acid)

Particle size diameter (μm)		**Dope polythiophene with $HClO_4$ at 200:1 mole ratio**					
Size Low	Size high	In %	Under %	In %	Under %	In %	Under %
0.50	1.32	0.17	0.17	0.17	0.17	0.16	0.17
1.32	1.60	0.51	0.68	0.50	0.66	0.48	0.64
1.60	1.95	0.74	1.41	0.71	1.38	0.69	1.34
1.95	2.38	0.85	2.27	0.82	2.20	0.81	2.14
2.38	2.90	0.96	3.22	0.92	3.13	0.91	3.05
2.90	3.53	1.18	4.40	1.14	4.27	1.13	4.18
3.53	4.30	1.63	6.03	1.60	5.87	1.59	5.78
4.30	5.24	2.40	8.44	2.37	8.25	2.36	8.14
5.24	6.39	3.49	11.93	3.47	11.72	3.47	11.60
6.39	7.78	4.77	16.70	4.76	16.49	4.76	16.37
7.78	9.48	6.05	22.75	6.08	22.56	6.08	22.45
9.48	11.55	7.42	30.16	7.49	30.05	7.53	29.98
11.55	14.08	8.83	39.00	8.99	39.05	9.06	39.04
14.08	17.15	10.17	49.17	10.44	49.48	10.53	49.56
17.15	20.9	11.16	60.33	11.50	60.98	11.55	61.11
20.90	25.46	11.32	71.64	11.59	72.56	11.52	72.63
25.46	31.01	10.25	81.88	10.20	82.76	10.00	82.63
31.01	37.79	7.90	89.78	7.41	90.17	7.16	59.79
37.79	46.03	4.94	94.71	4.22	94.38	4.03	93.82
46.03	56.09	2.49	97.21	1.94	96.33	1.90	95.72
56.09	68.33	1.18	98.39	1.09	97.42	1.20	96.92
68.33	83.26	0.81	99.20	1.15	98.58	1.34	98.26
83.26	101.44	0.62	99.83	1.06	99.63	1.24	99.51
101.44	123.59	0.17	100.00	0.37	100.00	0.49	100.00
123.59	150.57	0.00	100.00	0.00	100.00	0.00	100.00
150.57	183.44	0.00	100.00	0.00	100.00	0.00	100.00
183.44	223.51	0.00	100.00	0.00	100.00	0.00	100.00
223.51	272.31	0.00	100.00	0.00	100.00	0.00	100.00
272.31	331.77	0.00	100.00	0.00	100.00	0.00	100.00
331.77	404.21	0.00	100.00	0.00	100.00	0.00	100.00
404.21	429.47	0.00	100.00	0.00	100.00	0.00	100.00
492.47	600.00	0.00	100.00	0.00	100.00	0.00	100.00

Table D5 The raw data of particle size of Zeolite L

Particle size diameter (μm)		**Zeolite L**					
Size Low	Size high	In %	Under %	In %	Under %	In %	Under %
0.05	0.12	0.00	0.00	0.00	0.00	0.00	0.00
0.12	0.15	0.00	0.00	0.04	0.04	0.00	0.00
0.15	0.19	0.40	0.04	0.25	0.29	0.02	0.03
0.19	0.23	0.30	0.34	0.61	0.90	0.28	1.30
0.23	0.28	0.79	1.13	1.17	2.07	0.74	1.04
0.28	0.35	1.52	2.66	1.98	4.05	1.45	2.50
0.35	0.43	2.50	5.16	3.00	7.50	2.41	4.90
0.43	0.53	3.66	8.81	4.17	11.22	3.53	8.44
0.53	0.65	4.83	13.64	5.32	16.54	4.68	13.11
0.65	0.81	5.76	19.39	6.18	22.72	5.60	18.71
0.81	1.00	6.13	25.52	6.43	29.15	5.98	24.69
1.00	1.23	5.85	31.37	6.00	35.15	35.67	30.41
1.23	1.51	5.36	36.73	5.37	40.52	5.26	35.67
1.51	1.86	5.26	42.00	5.14	45.66	5.18	40.84
1.86	2.30	5.36	47.36	5.11	50.77	5.29	46.14
2.30	2.83	5.35	52.71	4.95	55.71	5.29	51.42
2.83	3.49	5.24	57.96	4.67	60.39	5.15	56.57
3.49	4.30	5.11	63.07	4.35	64.73	4.94	61.51
4.30	5.29	5.11	68.18	4.11	68.84	4.80	66.31
5.29	6.52	5.23	73.41	4.03	72.87	4.84	71.15
6.52	8.04	5.36	78.77	4.08	76.95	5.02	76.17
8.04	9.91	5.22	83.99	4.08	81.03	5.15	81.32
9.91	12.21	4.58	88.57	3.83	84.86	4.94	86.27
12.21	15.04	3.37	91.94	3.17	88.03	4.13	90.39
15.04	18.54	1.81	93.75	2.17	90.21	2.66	93.06
18.54	22.84	0.35	94.10	1.18	91.38	0.95	94.00
22.84	28.15	0.00	94.10	0.68	92.06	0.00	94.01
28.15	34.69	0.00	94.10	0.92	92.99	0.00	94.01
34.69	42.75	0.00	94.11	1.75	94.74	0.00	94.01
42.75	52.68	0.51	94.62	2.46	97.19	0.40	94.41
52.68	64.92	2.14	96.75	2.04	99.23	2.09	96.51
64.92	80.00	3.26	100.00	0.77	100.00	3.50	100.00

Table D6 The raw data of particle size of Zeolite Mordenite

Particle size diameter (μm)		Zeolite Mordenite					
Size Low	Size high	In %	Under %	In %	Under %	In %	Under %
0.05	0.12	0.00	0.00	0.00	0.00	0.00	0.00
0.12	0.15	0.00	0.00	0.00	0.00	0.00	0.00
0.15	0.19	0.00	0.00	0.00	0.00	0.00	0.00
0.19	0.23	0.00	0.00	0.00	0.00	0.00	0.00
0.23	0.28	0.00	0.00	0.00	0.00	0.00	0.00
0.28	0.35	0.00	0.00	0.00	0.00	0.00	0.00
0.35	0.43	0.00	0.00	0.00	0.00	0.00	0.00
0.43	0.53	0.00	0.00	0.00	0.00	0.00	0.00
0.53	0.65	0.35	0.35	0.32	0.32	0.34	0.34
0.65	0.81	0.57	0.92	0.56	0.88	0.56	0.90
0.81	1.00	0.65	1.56	0.63	1.52	5.67	1 53
1.00	1.23	0.68	2.24	0.66	2.18	0.63	2.20
1.23	1.51	0.78	3.02	0.75	2.93	0.67	2.97
1.51	1.86	0.92	3.94	0.88	3.81	0.76	3.87
1.86	2.30	1.13	5.08	1.10	4.91	0.90	4.99
2.30	2.83	1.40	6.47	1.36	6.27	1.12	6.38
2.83	3.49	1.80	8.27	1.77	8.04	1.39	8.18
3.49	4.30	2.41	10.68	2.39	10.43	1.80	10.59
4.30	5.29	3.36	14.04	3.33	13.77	2.41	13.94
5.29	6.52	4.67	18.71	4.64	18.41	3.35	18.58
6.52	8.04	6.28	24.99	6.22	24.63	4.64	24.80
8.04	9.91	7.97	32.97	7.87	32.49	6.23	32.71
9.91	12.21	9.48	42.45	9.33	41.82	7.91	42.15
12.21	15.04	10.67	53.12	10.53	52.35	0.68	52.83
15.04	18.54	11.31	64.42	11.20	63.55	11.35	64.18
18.54	22.84	10.91	75.33	10.87	74.42	10.97	75.14
22.84	28.15	9.44	84.77	9.53	83.94	9.52	84.66
28.15	34.69	7.08	91.85	7.26	91.20	7.17	91.82
34.69	42.75	4.63	96.48	4.85	96.05	4.70	96.53
42.75	52.68	2.55	99.03	2.76	98.82	2.57	99.10
52.68	64.92	0.96	99.99	1.18	99.99	0.89	99.99
64.92	80.00	0.00	100.00	0.00	100.00	0.00	100.00

Table D7 The raw data of particle size of Zeolite Beta

Particle size diameter (μm)		**Zeolite Beta**					
Size Low	Size high	In %	Under %	In %	Under %	In %	Under %
0.05	0.12	0.00	0.00	0.00	0.00	0.00	0.00
0.12	0.15	0.00	0.00	0.00	0.00	0.00	0.00
0.15	0.19	0.00	0.00	0.00	0.00	0.00	0.00
0.19	0.23	0.00	0.00	0.00	0.00	0.00	0.00
0.23	0.28	0.00	0.00	0.00	0.00	0.00	0.00
0.28	0.35	0.00	0.00	0.00	0.01	0.00	0.01
0.35	0.43	0.85	0.85	0.99	0.99	1.03	1.03
0.43	0.53	2.40	3.26	2.41	3.41	2.52	3.56
0.53	0.65	4.21	7.46	4.08	7.48	4.28	7.83
0.65	0.81	5.95	13.41	5.76	13.25	6.03	13.86
0.81	1.00	7.17	20.58	7.02	20.26	7.31	21.16
1.00	1.23	7.60	28.18	7.52	27.78	7.74	28.91
1.23	1.51	7.87	36.05	7.82	35.61	7.95	36.86
1.51	1.86	9.10	45.15	9.08	44.68	9.14	46.00
1.86	2.30	10.78	55.93	10.76	55.45	10.77	56.78
2.30	2.83	11.69	67.62	11.69	67.14	11.63	68.40
2.83	3.49	11.14	78.75	11.17	78.30	11.00	79.39
3.49	4.30	9.11	87.86	9.18	87.48	8.92	88.32
4.30	5.29	6.29	94.14	6.39	93.86	6.10	94.41
5.29	6.52	3.52	97.67	3.62	97.49	3.38	97.79
6.52	8.04	1.54	99.21	1.61	99.11	1.46	99.26
8.04	9.91	0.53	99.74	0.57	99.69	0.50	99.76
9.91	12.21	0.18	99.92	0.21	99.89	0.17	99.93
12.21	15.04	0.08	99.99	0.09	99.99	0.07	100.00
15.04	18.54	0.01	100.00	0.01	100.00	0.00	100.00
18.54	22.84	0.00	100.00	0.00	100.00	0.00	100.00
22.84	28.15	0.00	100.00	0.00	100.00	0.00	100.00
28.15	34.69	0.00	100.00	0.00	100.00	0.00	100.00
34.69	42.75	0.00	100.00	0.00	100.00	0.00	100.00
42.75	52.68	0.00	100.00	0.00	100.00	0.00	100.00
52.68	64.92	0.00	100.00	0.00	100.00	0.00	100.00
64.92	80.00	0.00	100.00	0.00	100.00	0.00	100.00

Appendix E Characteristic Peaks of poly (3-thiophene methyl acetate) and poly (3-thiopheneacetic acid) by ^{1}H-NMR

Proton Nuclear Magnetic Resonance used to identify our successful synthesis of poly (3-thiopheneacetic acid). The different characteristic peaks of both polythiophene derivatives are shown in the figures E1 and E2. The position at 12.6 ppm is the important feature peak of poly(3-thiopheneacetic acid) and this peak disappears in case of poly(3-thiophene methyl acetate) (Kim, *et al.*, 1999).

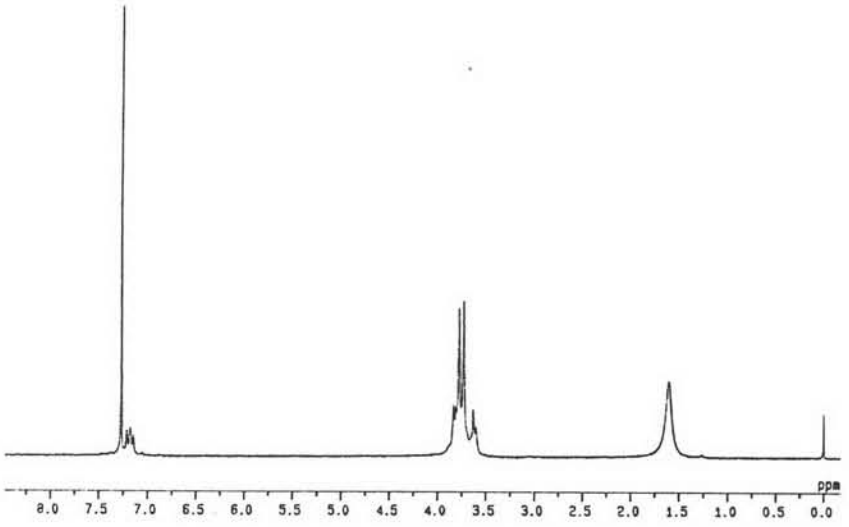

Figure E1 ^{1}H-NMR characteristic peaks of poly(3-thiophenemethyl acetate).

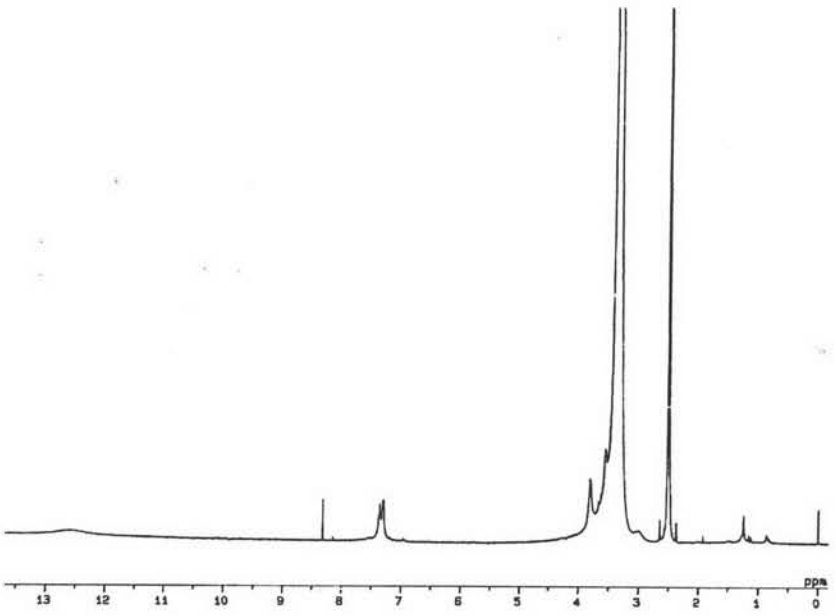

Figure E2 ^{1}H-NMR characteristic peaks of poly(3-thiophene acetic acid).

Table E1 The raw data of ^{1}H-NMR of poly(3-thiophene methyl acetate) and poly(3-thiopheneacetic acid

	Characteristic	Chemical shift (ppm)	Intensity (%)	Reference (Kim *et al.*, 1999)
Solvent	TMS	0.006	7.442	
	$CDCl_2$	7.30-7.24	100.000	
	H_2O	1.75-1.48	16.768	
	DMSO	2.75-2.38	100.000	
Polythiophene P3TMA	m,thiophene ring proton, 1H (δ, 7.23-7.11)	7.2206	1.405	7.26-7.03
		7.2133	2.853	
		7.2072	5.251	
		7.1980	3.510	
		7.1974	3.458	
		7.1895	2.242	
		7.1809	3.582	
		7.1742	4.998	
		7.1675	6.002	
		7.1565	2.718	
		7.1425	3.180	
		7.1376	4.247	
		7.1321	2.821	
	s, thiophene ring $-CH_2-$, 2H (δ, 3.85-3.70)	3.8525	2.849	3.68
		3.8397	5.035	
		3.8281	11.180	
		3.8239	9.955	
		3.8147	7.917	
		3.8086	9.000	
		3.8049	10.643	
		3.7994	10.422	
		3.7909	9.611	
		3.7811	15.326	
		3.7708	32.925	
		3.7750	28.066	
		3.7641	23.768	

		3.7482	10.754	
		3.7348	15.437	
		3.7232	34.143	
		3.7171	25.969	
		3.7146	19.756	
	s,-CH_3,3H	3.6536	3.808	3.64
		3.6292	6.217	
	(δ, 3.64-3.58)	3.6219	10.226	
		3.6164	8.456	
		3.6054	4.971	
		3.5957	5.501	
		3.5914	6.394	
		3.5847	4.319	
		3.5780	2.659	
		3.5712	1.745	
P3TAA	s, -COOH,1H	12.8456	0.033	12.60
	(δ, 12.80-12.30)	12.7437	0.038	
		12.5674	0.041	
		12.4746	0.039	
		12.3685	0.035	
		12.2727	0.030	
		12.1812	0.027	
		12.0378	0.022	
	m, thiophene ring	7.3591	0.035	7.55-7.28
	proton, 1H	7.3426	0.171	
	(δ, 7.40-7.25)	7.3298	0.035	
		7.2975	0.181	
		7.2865	0.035	
		7.2822	0.035	
		7.2767	0.189	
		7.2529	0.045	
		7.2145	0.014	
		7.1571	0.005	
	m, thiophene ring	4.2802	0.014	3.88-3.37
	$-CH_2-$,2H	4.1485	0.021	
	(δ, 3.80-3.37)	4.0490	0.032	
		3.8263	0.035	

		3.7982	0.284	
		3.7738	0.035	
		3.4553	0.628	
		3.3839	5.510	
		3.3736	11.289	
		3.3656	26.223	
		3.3632	36.558	
		3.3589	68.251	
		3.3540	100.000	
		3.3491	66.095	
		3.3406	21.319	
		3.3125	3.261	

Appendix F Identification of Crytallinity of Undoped and Dope of P3TAA and Structure of Zeolite by X-ray Diffraction

Powders of polymer and zeolite were packed onto a glasss plate and data were collected after X-ray passed though the sample. Properties of polythiophene can be investigated by the peaks of graph. The areas of sharp peak and broad peak can be identified as the crystal part and the amorphous part, respectively. The structure of zeolite can be considered from the position of each peak.

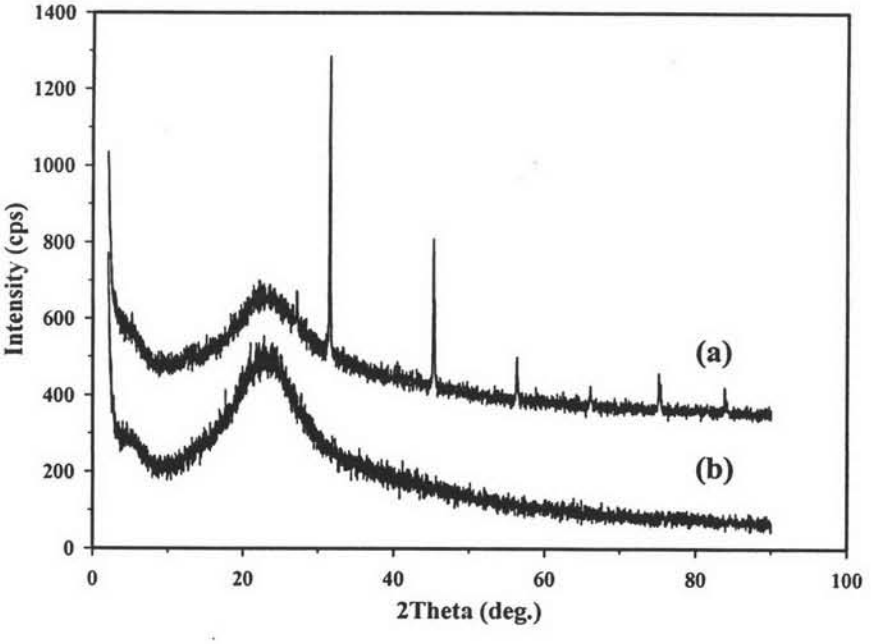

Figure F1 XRD pattern of: a) undope and b) dope poly(3-thiphene acetic acid) with $HClO_4$.

From Figure F1 undoped polythiophene shows some sharp peaks and those peaks disappear after doping with $HClO_4$. So $HClO_4$ decrease crystallinity of poltythiophene.

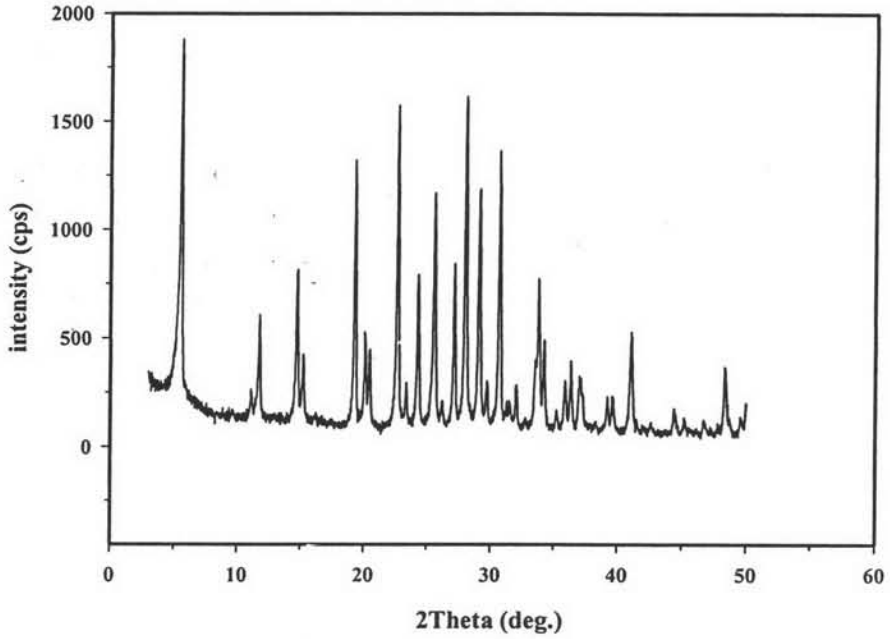

Figure F2 XRD pattern of Zeolite L.

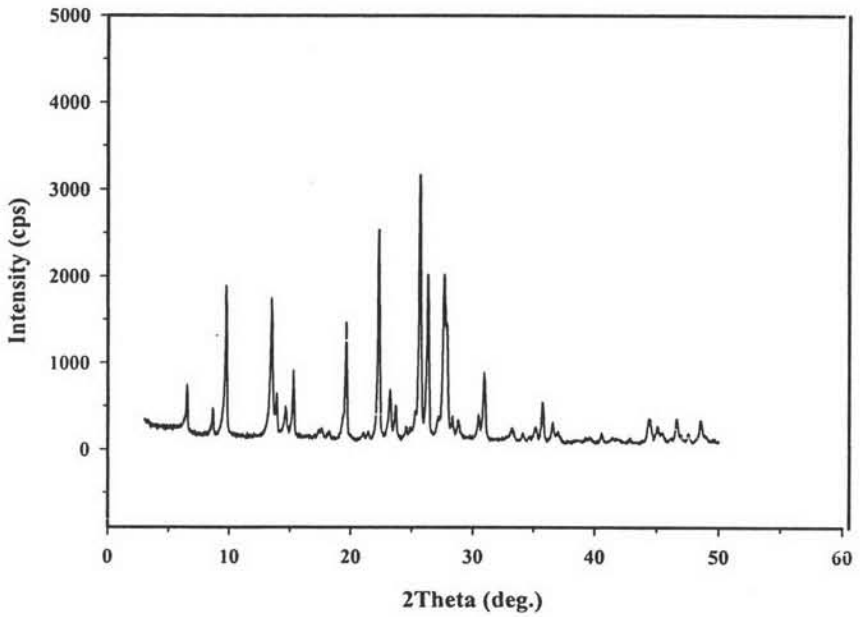

Figure F3 XRD pattern of Zeolite Mordenite.

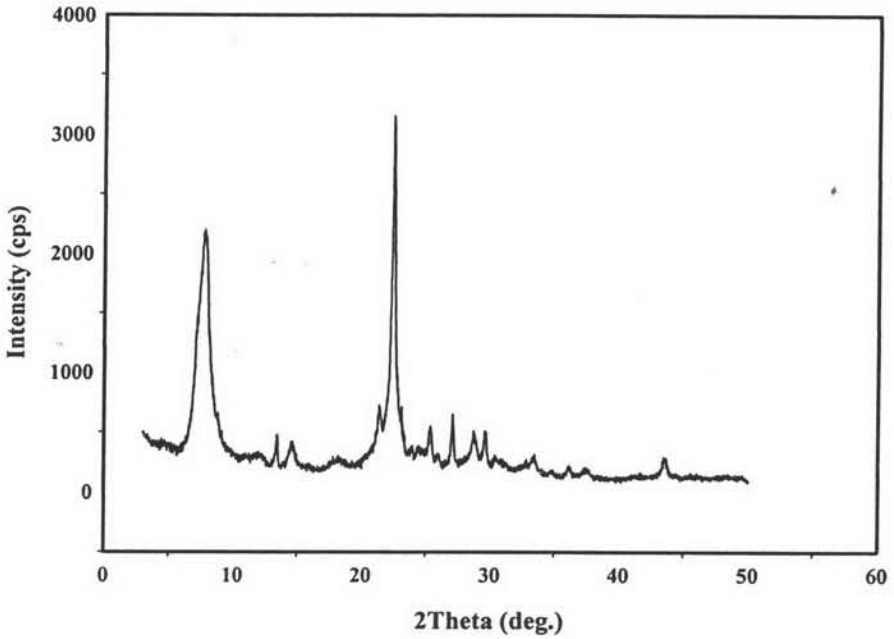

Figure F4 XRD pattern of Zeolite Beta.

Table F1 Law data of XRD analysis of undoped and doped poly(3-thiopheneacetic acid)

	%Crystalline	2Theta	d-value	Intensity	I/I0
Pth_u	3.16	22.92	3.8769	1696	2
		27.28	3.2664	1600	2
		31.66	2.8238	4609	2
		45.40	1.996	2117	2
		56.36	1.6311	888	2
		66.16	1.4113	571	2
		75.22	1.2622	626	2
		83.94	1.1518	467	2
Pth_200:1		23.12	3.8438	2084	2

Table F2 Law data of XRD analysis of Zeolite L

Law data				Reference*	
2Theta	**d-value (A)**	**Intensity**	**I/I_0**	***hkl***	**d-value (A)**
5.56	15.8817	7776	100	100	15.80
11.08	7.9788	1105	16	200	7.89
11.76	7.5189	2530	15	001	7.49
14.70	6.0211	3355	25	201	5.98
15.20	5.8241	1776	24	111	5.75
19.30	4.5952	5509	72	220	4.75
20.08	4.4184	2205	30	310	4.39
20.46	4.3372	1800	24	301	4.33
22.68	3.9174	6559	86	221	3.91
23.36	3.8049	1234	16	311	3.78
24.30	3.6598	3263	42	320	3.66
25.56	3.4822	4876	64	410	3.48
26.20	3.3985	880	12		
27.14	3.2829	3513	46	321	3.26
28.04	3.1796	6726	88	212	3.17
29.10	3.0661	4871	64	330	3.07
29.74	3.0016	1126	16	420	3.02
30.70	2.9099	5663	74	222	2.91
31.24	2.8608	826	12		
31.50	2.8378	884	12		
32.04	2.7911	1188	16		
33.78	2.6120	3205	42	600	2.65
34.22	2.6182	2046	28	430	2.62
35.20	2.5475	700	10		
35.88	2.5007	1271	18		
36.32	2.4715	1634	22		
37.02	2.4263	1359	18		
39.22	2.9510	955	14		
39.58	2.2751	976	14		

Table F3 Law data of XRD analysis of Zeolite Mordenite

Law data				Reference*	
2Theta	**d-value (A)**	**Intensity**	**I/I_0**	***hkl***	**d-value (A)**
6.50	13.5869	3121	24	110	13.590
8.64	10.2259	1976	16	20	10.250
9.74	9.0733	7880	60	200	9.072
13.46	6.5729	7271	56	111	6.584
13.88	6.3749	2692	22	130	6.371
14.62	6.0539	2013	16	21	6.056
15.26	5.8014	3812	30	201	5.782
17.58	5.0407	1013	8	221	5.039
18.22	4.8650	909	8	131	4.861
19.62	4.5209	6109	48	330	4.512
21.02	4.2229	826	8	41	4.210
21.46	4.1373	871	8	420	4.119
22.30	3.9833	10559	82	150	4.077
23.24	3.8243	2805	22	241	3.830
23.72	3.7479	2105	18	112	3.640
24.88	3.5758	1050	10	510	3.561
25.30	3.5173	1859	16	22	3.521
25.66	3.4688	13134	100	202	3.486
26.32	3.3833	8421	66	60	3.410
27.16	3.2805	152	14	222	3.272
27.68	3.2201	8434	66		3.221
28.34	3.1466	1605	14	530	28.340
30.46	2.9322	1680	14		2.942
30.92	2.8896	3696	30		2.895
33.20	2.6962	1050	8		2.701
34.12	2.5503	809	8		2.633
35.16	2.5503	1080	10		2.565
35.72	2.5116	2255	18		2.521
36.56	2.4558	1317	12		2.436
37.00	2.4276	850	8		2.436

Table F4 Law data of XRD analysis of Zeolite Beta

Law data				Reference*	
2Theta	**d-value (A)**	**Intensity**	**I/I_0**	***hkl***	**d-value (A)**
7.78	11.3542	9088	70		11.50
13.46	6.5729	1988	16	004	6.85
14.66	3.0674	1763	14		4.75
18.34	4.8335	1159	10	300	4.75
21.38	4.1526	3009	24	300	4.17
22.46	3.9553	12996	100	302	3.98
25.38	3.5064	2288	18	304	3.54
26.00	3.4242	1338	12		3.42
27.08	3.2901	2709	22	008	3.33
28.70	3.1079	2105	18		3.12
29.62	3.0134	2100	18	306	29.62
30.36	2.9417	1284	10		2.90
32.84	2.72496	1134	10		2.74
33.44	2.6774	1321	12		2.69
34.70	2.58303	776	6		2.58
36.14	2.4833	926	8		2.49
37.58	2.3914	780	6		2.41
43.48	2.0796	1217	10		2.08

* Szostak R. (1992) and Donald W. (1974)

Appendix G Calculation of Doping Level of Poly (3-thiopheneacetic acid)

Doping level of poly (3-thiopheneacetic acid) can be determined by Electron Dispersive Spectroscopy (EDS) (Pentafet Link, Oxford). The amounts of each element were obtained such as carbon (C), oxygen (O), sulfur (S) and chlorine (Cl) in mole percent. Calculation of % doping level was by the equation (G.1)

$$\%\ \text{doping level of Pth\_HClO}_4 = \frac{\%Cl_{HClO_4}}{\%S} \times \frac{M_S}{M_{ClO_4^-}} \times 100 \qquad \text{(G.1)}$$

Table G1 Doping level of poly (3-thiopheneacetic acid) with $HClO_4$

Doping ratio	% Mole of Cl				% Mole of S				% Doping level
(N_{acid}/N_{Pth})	1	2	3	Avg.	1	2	3	Avg.	
Pth_200:1	0.73	0.86	0.94	0.84	1.35	1.82	1.10	1.42	20.14 ± 6.75

Appendix H Identification Morphology of Materials

Undoped and doped poly(3-thiopheneacetic acid), zeolite and composites were observed for their morphology by scanning electron microscopy (SEM). Polythiophene and zeolites exist as powder and composites exist as pellets. Sample was coated with gold for improving conductivity. Morphology of samples appears in these pictures. In the figures H1 and H2 there appears irregular shapes and distribution of particle size of undoped and dope poly(3-thiopheneacetic acid) powders.

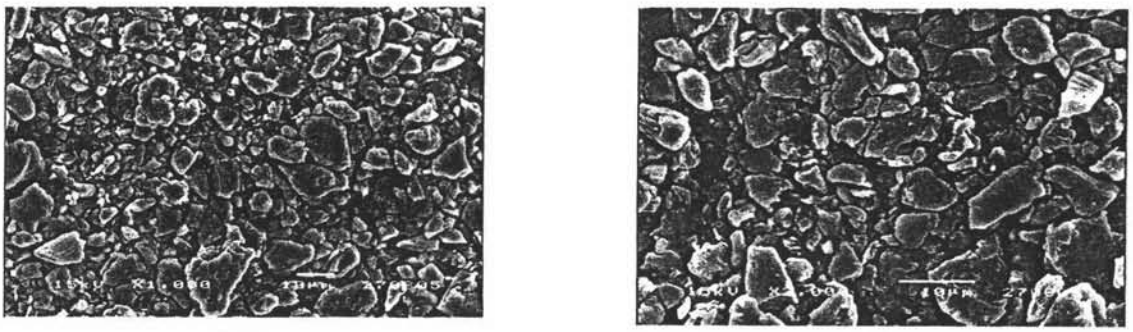

(a) **(b)**

Figure H1 SEM photographs of undope poly(3-thiopheneacetic acid) at magnification (a)1000 and (b)2000.

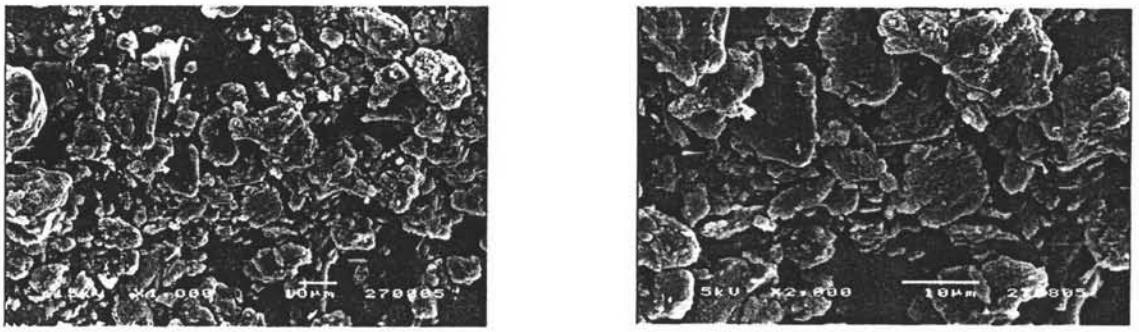

(a) **(b)**

Figure H2 SEM photographs of dope poly(3-thiopheneacetic acid) at magnification (a)1000 and (b)2000.

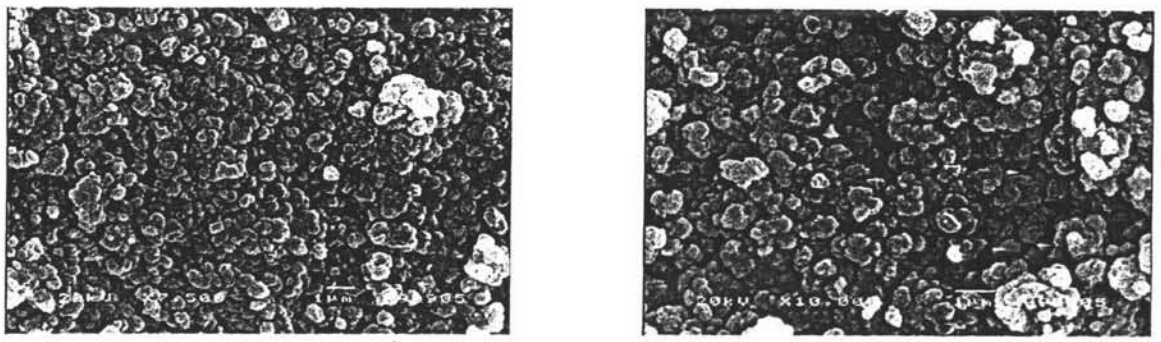

(a) (b)

Figure H3 SEM photographs: Zeolite L at magnification (a) 7500 and (b) 10000.

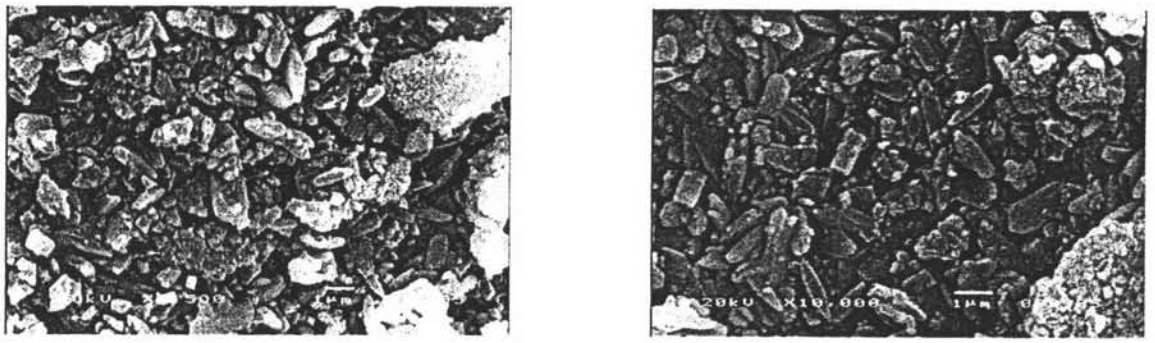

(a) (b)

Figure H4 SEM photographs: Zeolite Modenite at magnification (a) 7500 and (b) 10000.

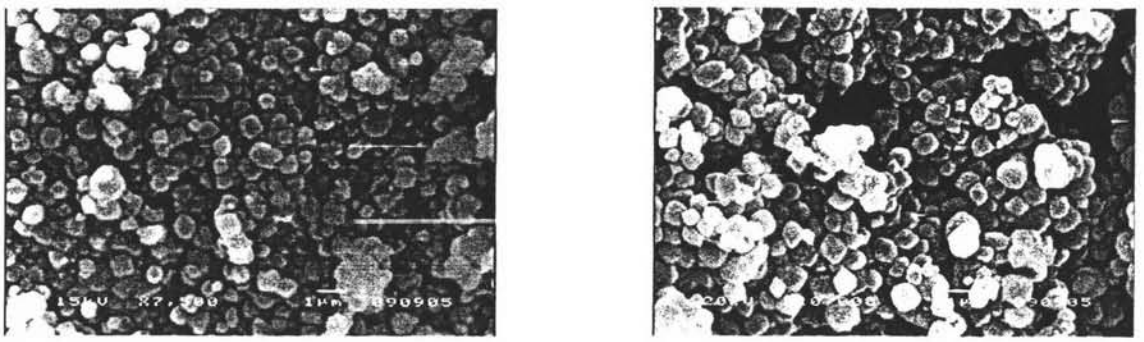

(a) (b)

Figure H5 SEM photographs: Zeolite Beta at magnification (a) 7500 and (b) 10000.

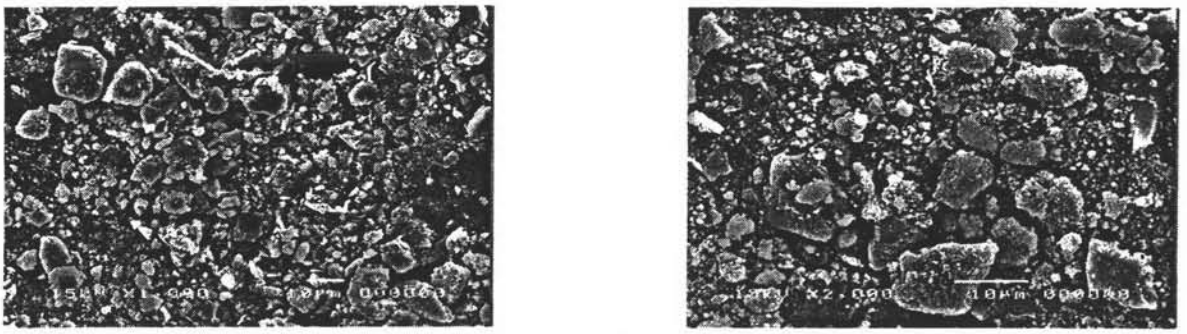

(a) (b)

Figure H6 SEM photographs: Pth_200:1/L_20 at magnification (a) 1000 and (b)2000.

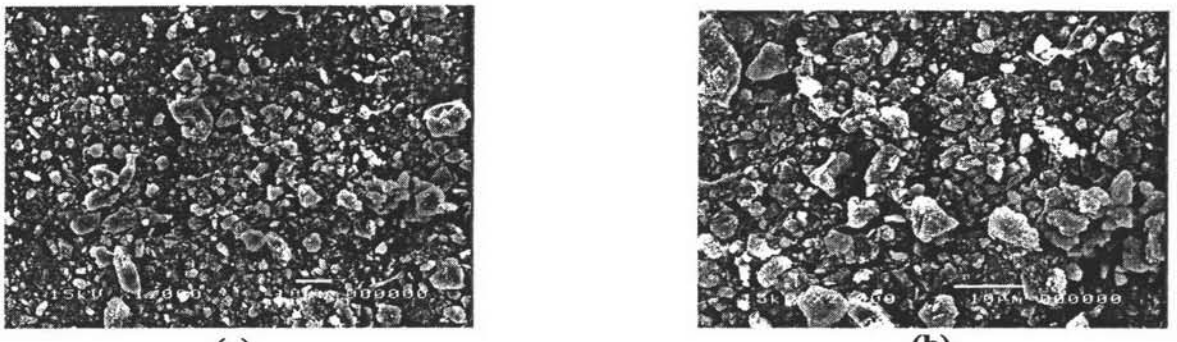

(a) (b)

Figure H7 SEM photographs : Pth_200:1/MOR_20 at magnification (a)1000 and (b) 2000.

(a) (b)

Figure H8 SEM photographs: Pth_200:1/BEA_20 at magnification(a)1000 and(b) 2000.

(a) (b)

Figure H9 SEM photographs: Pth_200:1/MOR_10 at magnification (a) 1000 and (b) 2000.

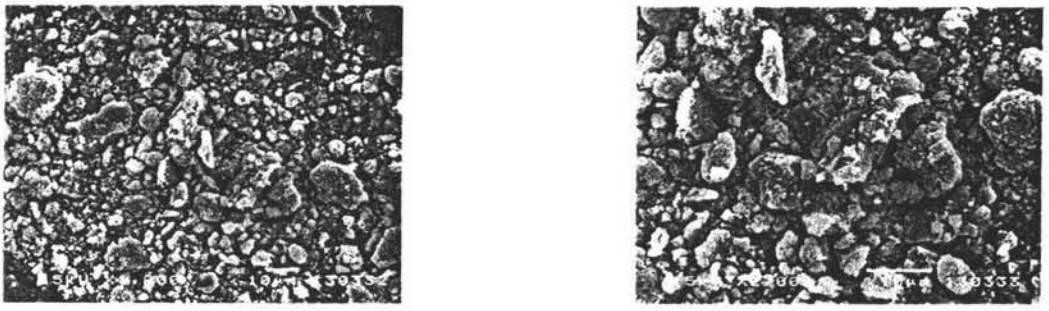

(a) (b)

Figure H10 SEM photographs:Pth_200:1/MOR_30 atmagnification (a) 1000 and (b) 2000.

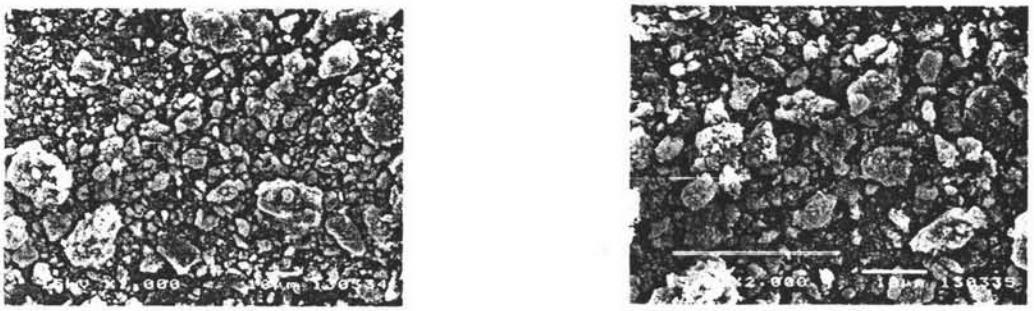

(a) (b)

Figure H11 SEM photographs:Pth_200:1/MOR_40 at magnification (a) 1000 and (b) 2000.

(a) (b)

Figure H12 SEM photographs:Pth_200:1/MOR_50 at agnification (a) 1000 and (b) 2000.

Appendix I Determination of the Correction Factor (K)

The electrical conductivity of conductive polymer can be mesured by using two-point probe meter. The surface of sample contact with two probes of source meter (Keithley, Model 6517A). A constant voltage is applied and a current is measured.

The geometrical correction factor was taken into account of geometric effects, depending on the configuration and probe tip spacing.

$$K = \frac{w}{l} \qquad \text{(I.1)}$$

K is geometrical correction factor, w is width of probe tip spacing (cm), l is the length between probes (cm).

In this measurement, the constant K value was determined by using standard materials where specific resistivity values were known; we used silicon wafer chips (SiO_2). In our case, the sheet resistivity was measured by using our custom made two-point probe and then the geometric correction factor was calculated by equation (I.2) as follows:

$$K = \frac{\rho}{R \times t} = \frac{I \times \rho}{V \times t} \qquad \text{(I.2)}$$

K is geometric correction factor, ρ is resistivity of standard silicon wafer, which was calibrated by using a four point probe at King Mongkut's Institute Technology of Lad Krabang (Ω.cm), t is film thickness (cm), R is film resistance (Ω), I is measure current (A), and V is voltage drop (V).

Standard Si wafers were cleaned to remove organic impurities prior to be used according to the standard RCA method (Kern, 1993).

Materials

Acetones (Scharlau, 99.5%), Methanol (CARLO ERBA, 99.9%), Ammonium hydroxide (Merk, 99.9%), Hydrogen peroxide (CARLO ERBA, 30% in water), and dilute (2%) Hydrofuric acid

Experiment

The cleaning procedures contain 3 steps: the solvent clean, the RCA01 and the HF dip. The first step is the solvent clean step, employed to remove oils and organic residues that appeared on Si wafer surface. The Si wafer was placed into the acetone at 55°C for 10 min, removed and placed in methanol for 2-5 min, subsequently rinsed with deionized water and blown dried with nitrogen gas. The second step is the RCA clean, to remove organic residues from silicon wafers. This process oxidized the silicon wafer and left a thin oxide on the surface of the wafer. RCA solution was prepared with 5 parts of water (H_2O), 1 part of 27% ammonium hydroxide (NH_4OH), and 1 part of 30% hydrogen peroxide (H_2O_2). 65 ml of NH_4OH (27%) was added into 325 ml of deionized water in a beaker and then heated to 70 ± 5°C. The mixture would bubble vigorously after 1-2 min, indicated that it was ready to use. Silicon wafer was soaked in the solution for 15 min, consequently overflowed with deionized water in order to rinse and remove the solution. The third step is the HF dip, which was carried out to remove native silicon dioxide from wafer. 480 ml of deionised water was added to the polypropylene bottle and then added to 20 ml HF. Wafer was soaked in this solution for 2 min, removed and checked for hydrophobicity by performing the wetting test. Deionized water was poured onto the surface wafer; the clean silicon surface would shows that the beads of water would roll off. Clean Si wafer was further blown dried with nitrogen and stored in a clean and dry environment.

Table I1 Determination the correction factor of four point probe

Probe	K (correction factor)				
	1	2	3	Average	STD
1	2.20E-04	2.20E-04	2.20E-04	2.20E-04	5.56E-08
2	4.26E-04	4.28E-04	4.29E-04	4.27E-04	1.19E-06

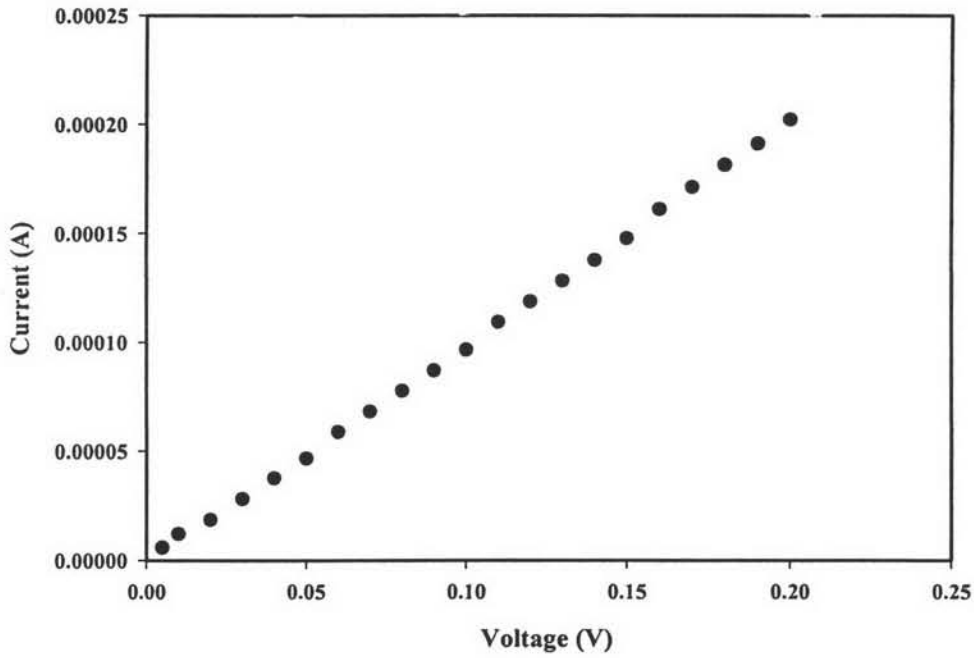

Figure I1 The calibration data of Si-wafer: K tay which specific resistivity (ρ) 0.01647 Ω.cm, thickness 0.0724 cm, 24-25°C, 55-59 %R.H.

Table I2 Determination the correction factor of probe 1 with standard Si wafer (specific resistivity 0.01647 Ω.cm, thickness 0.0724 cm, 24-25°C, 55-59% R.H)

Volt Applied (mV)			Current (mA)		
1	2	3	1	2	3
0.005	0.005	0.005	5.82E-06	5.78E-06	5.71E-06
0.01	0.01	0.01	1.19E-05	1.20E-05	1.21E-05
0.02	0.02	0.02	1.85E-05	1.85E-05	1.85E-05
0.03	0.03	0.03	2.80E-05	2.79E-05	2.80E-05
0.04	0.04	0.04	3.75E-05	3.75E-05	3.75E-05
0.05	0.05	0.05	4.68E-05	4.65E-05	4.65E-05
0.06	0.06	0.06	5.88E-05	5.88E-05	5.89E-05
0.07	0.07	0.07	6.81E-05	6.83E-05	6.84E-05
0.08	0.08	0.08	7.78E-05	7.78E-05	7.78E-05
0.09	0.09	0.09	8.69E-05	8.70E-05	8.71E-05
0.10	0.10	0.10	9.67E-05	9.65E-05	9.65E-05
0.11	0.11	0.11	1.09E-04	1.09E-04	1.09E-04
0.12	0.12	0.12	1.19E-04	1.19E-04	1.19E-04
0.13	0.13	0.13	1.28E-04	1.28E-04	1.28E-04
0.14	0.14	0.14	1.38E-04	1.38E-04	1.38E-04
0.15	0.15	0.15	1.47E-04	1.48E-04	1.48E-04
0.16	0.16	0.16	1.61E-04	1.61E-04	1.61E-04
0.17	0.17	0.17	1.71E-04	1.71E-04	1.71E-04
0.18	0.18	0.18	1.81E-04	1.81E-04	1.81E-04
0.19	0.19	0.19	1.91E-04	1.91E-04	1.91E-04
0.20	0.20	0.20	2.02E-04	2.02E-04	2.02E-04

Table I3 Determination the correction factor of probe 2 with standard Si wafer (specific resistivity 0.01647 Ω.cm, thickness 0.0724 cm, 24-25°C, 55-59% R.H)

Volt Applied (mV)			Current (mA)		
1	2	3	1	2	3
0.005	0.005	0.005	8.81E-06	8.88E-06	8.99E-06
0.010	0.010	0.010	1.97E-05	2.01E-05	2.01E-05
0.015	0.015	0.015	2.91E-05	2.91E-05	2.92E-05
0.020	0.020	0.020	3.58E-05	3.58E-05	3.58E-05
0.025	0.025	0.025	4.16E-05	4.16E-05	4.15E-05
0.030	0.030	0.030	5.47E-05	5.49E-05	5.49E-05
0.035	0.035	0.035	6.70E-05	6.71E-05	6.72E-05
0.040	0.040	0.040	7.39E-05	7.40E-05	7.40E-05
0.045	0.045	0.045	8.71E-05	8.70E-05	8.70E-05
0.050	0.050	0.050	9.39E-05	9.38E-05	9.40E-05
0.060	0.060	0.060	1.18E-04	1.19E-04	1.19E-04
0.070	0.070	0.070	1.40E-04	1.40E-04	1.40E-04
0.080	0.080	0.080	1.62E-04	1.62E-04	1.62E-04
0.090	0.090	0.090	1.85E-04	1.85E-04	1.85E-04
0.100	0.100	0.100	2.08E-04	2.08E-04	2.08E-04
0.110	0.110	0.110	2.40E-04	2.40E-04	2.40E-04
0.120	0.120	0.120	2.65E-04	2.65E-04	2.65E-04
0.130	0.130	0.130	2.90E-04	2.90E-04	2.90E-04
0.140	0.140	0.140	3.16E-04	3.16E-04	3.18E-04

Appendix J Conductivity Measurement

The specific conductivity can be mesured with a two point probe connect to a source meter (Keithley, Model 6517A), and in contact with sample surface and a constant voltage is applied. So a responsive current was measured under the atmospheric pressure, 54-60% relative humidity and 24-25°C. At a responsive current varies linearly does not change with voltage this region is called the linear ohmic regime which can be identified by plotting the applied voltage versus the current. The applied voltage and the current change in the linear ohmic regime were converted to the electrical conductivity of the polymer by using equation (J.1) as follows:

$$\sigma = \frac{1}{\rho} = \frac{1}{R_s \times t} = \frac{I}{K \times V \times t} \qquad \text{(J.1)}$$

where σ is specific conductivity (S/cm), ρ is specific resistivity (Ω.cm), R_s is sheet resistivity (Ω), I is measure current (A), K is geometric correction factor, V is applied voltage (voltage drop) (V), t is pellet thickness (cm).

In this mesurement, the geometric correction factor (K) of probe A is 2.8×10^{-5} and the thickness of sample pellets was mesured by using a thickness gauge.

In addition the conductivity of matrixes can be measure by using the resistivity testing fixture (Keithley, Model 8009) connected to a source meter (Keithley, Model 6517A) for a constant voltage source and reading resultant current under the atmospheric pressure, 54-60% relative humidity and 24-25°C. The conductivity of matrixes can calculate by using equation (J.2 – J.3) as follows:

$$K_v = \frac{\pi \times \left(D + \left[\beta \times g\right]\right)^2}{4} \qquad \text{(J.2)}$$

where K_v is effective area of the guarded electrode for the particular electrode arrangement employed (cm^2), D is diameter of the guarded electrode (cm), β is effective

area coefficient (cm^2) (β is always zero), g is distance between the guarded electrode and the ring electrode (cm).

$$\sigma = \frac{1}{\rho} = \frac{t \times I}{22.9 \times V} \qquad \text{(J.3)}$$

where σ is specific conductivity (S/cm), ρ is specific resistivity (Ω.cm), I is measure current (A), V is applied voltage (voltage drop) (V), t is sheet thickness (cm).

Table J1 Determination the specific conductivity (S/cm) of undoped and doped poly(3-thiopheneacetic acid)

Code	Specific conductivity (S/cm)			AVG	STD
Pth_u	2.69E-04	2.73E-04	2.69E-04	2.70E-04	2.43E-06
Pth_200:1	4.84E-02	4.84E-02	4.89E-02	4.85E-02	3.23E-04

Table J2 Determination the specific conductivity (S/cm) of Zeolite

Code	Specific conductivity (S/cm)		AVG	STD
L	1.75E-03	1.16E-03	1.45E-03	4.21E-04
MOR	4.80E-03	5.56E-03	5.18E-03	5.35E-04
BEA	9.29E-04	9.62E-04	9.46E-04	2.35E-05

Table J3 The raw data of the determination of linear regime of undoped poly(3-thiopheneacetic acid) at 24-25°C, 54-60% R.H.

Sample	Thickness	Applied voltage (V)			Measured Current (A)			Conductivity (S/cm)		
	(cm)	1	2	3	1	2	3	1	2	3
Pth_u	1) 0.01097	5.00	5.00	5.00	1.08E-10	1.07E-10	1.03E-10	1.22E-04	1.23E-04	1.17E-04
	2) 0.01077	10.00	10.00	10.00	1.08E-10	1.09E-10	1.06E-10	6.14E-05	6.27E-05	6.04E-05
	3) 0.01090	15.00	15.00	15.00	1.10E-10	1.09E-10	1.09E-10	4.15E-05	4.21E-05	4.14E-05
		20.00	20.00	20.00	1.13E-10	1.10E-10	1.12E-10	3.19E-05	3.19E-05	3.19E-05
		25.00	25.00	25.00	1.15E-10	1.15E-10	1.15E-10	2.61E-05	2.66E-05	2.63E-05
		30.00	30.00	30.00	1.18E-10	1.17E-10	1.16E-10	2.22E-05	2.25E-05	2.21E-05
		35.00	35.00	35.00	1.19E-10	1.19E-10	1.19E-10	1.93E-05	1.96E-05	1.94E-05
		40.00	40.00	40.00	1.22E-10	1.22E-10	1.22E-10	1.72E-05	1.76E-05	1.73E-05
		45.00	45.00	45.00	1.24E-10	1.24E-10	1.24E-10	1.57E-05	1.59E-05	1.58E-05
		50.00	50.00	50.00	1.27E-10	1.27E-10	1.27E-10	1.44E-05	1.46E-05	1.44E-05
		55.00	55.00	55.00	2.59E-09	2.56E-09	2.54E-09	2.66E-04	2.68E-04	2.63E-04
		60.00	60.00	60.00	2.77E-09	2.76E-09	2.74E-09	2.61E-04	2.65E-04	2.60E-04
		65.00	65.00	65.00	2.97E-09	2.98E-09	2.97E-09	2.58E-04	2.64E-04	2.60E-04
		70.00	70.00	70.00	3.35E-09	3.36E-09	3.35E-09	2.71E-04	2.77E-04	2.73E-04
		75.00	75.00	75.00	3.58E-09	3.59E-09	3.59E-09	2.70E-04	2.76E-04	2.72E-04
		80.00	80.00	80.00	3.87E-09	3.83E-09	3.82E-09	2.74E-04	2.76E-04	2.72E-04
		85.00	85.00	85.00	4.12E-09	4.10E-09	4.11E-09	2.75E-04	2.78E-04	2.75E-04
		90.00	90.00	90.00	4.36E-09	4.33E-09	4.34E-09	2.74E-04	2.77E-04	2.75E-04
		95.00	95.00	95.00	4.54E-09	4.51E-09	4.52E-09	2.70E-04	2.74E-04	2.71E-04
		100.00	100.00	100.00	4.74E-09	4.78E-09	4.72E-09	2.69E-04	2.76E-04	2.69E-04

Table J4 The raw data of the determination of linear regime of doped poly(3-thiopheneacetic acid) at 24-25°C, 54-60% R.H

Sample	Thickness	Applied voltage (V)			Measured Current (A)			Conductivity (S/cm)		
	(cm)	1	2	3	1	2	3	1	2	3
Pth_200:1	1) 0.0284	0.10	0.10	0.10	2.12E-08	2.13E-08	2.18E-08	6.84E-02	6.85E-02	7.08E-02
	2) 0.0285	0.20	0.20	0.20	3.04E-08	3.06E-08	3.10E-08	4.91E-02	4.92E-02	5.03E-02
	3) 0.0283	0.30	0.30	0.30	4.41E-08	4.46E-08	4.50E-08	4.74E-02	4.79E-02	4.86E-02
		0.35	0.35	0.35	5.04E-08	5.02E-08	5.00E-08	4.65E-02	4.62E-02	4.63E-02
		0.40	0.40	0.40	5.48E-08	5.45E-08	5.48E-08	4.42E-02	4.38E-02	4.44E-02
		0.45	0.45	0.45	6.04E-08	6.16E-08	6.30E-08	4.34E-02	4.41E-02	4.54E-02
		0.50	0.50	0.50	7.17E-08	7.16E-08	7.20E-08	4.63E-02	4.61E-02	4.67E-02
		0.55	0.55	0.55	7.67E-08	7.71E-08	7.748E-08	4.50E-02	4.51E-02	4.57E-02
		0.60	0.60	0.60	9.40E-08	9.46E-08	9.38E-08	5.06E-02	5.08E-02	5.07E-02
		0.65	0.65	0.65	9.58E-08	9.54E-08	9.63E-08	4.76E-02	4.72E-02	4.80E-02
		0.70	0.70	0.70	1.04E-07	1.06E-07	1.08E-07	4.79E-02	4.88E-02	5.01E-02
		0.75	0.75	0.75	1.15E-07	1.16E-07	1.17E-07	4.97E-02	4.99E-02	5.05E-02
		0.80	0.80	0.80	1.24E-07	1.23E-07	1.21E-07	5.00E-02	4.94E-02	4.92E-02
		0.85	0.85	0.85	1.28E-07	1.29E-07	1.30E-07	4.87E-02	4.87E-02	4.95E-02
		0.90	0.90	0.90	1.45E-07	1.46E-07	1.47E-07	5.20E-02	5.24E-02	5.31E-02
		0.95	0.95	0.95	1.56E-07	1.56E-07	1.54E-07	5.30E-02	5.27E-02	5.27E-02
		1.00	1.00	1.00	1.61E-07	1.59E-07	1.59E-07	5.20E-02	5.13E-02	5.14E-02
		1.50	1.50	1.50	2.32E-07	2.34E-07	2.40E-07	5.00E-02	5.03E-02	5.19E-02
		2.00	2.00	2.00	3.23E-07	3.23E-07	3.24E-07	5.22E-02	5.20E-02	5.25E-02
		2.50	2.50	2.50	3.92E-07	3.87E-07	3.83E-07	5.07E-02	4.99E-02	4.96E-02
		3.00	3.00	3.00	4.32E-07	4.32E-07	4.34E-07	4.65E-02	4.64E-02	4.69E-02
		3.50	3.50	3.50	5.26E-07	5.28E-07	5.29E-07	4.85E-02	4.85E-02	4.90E-02
		4.00	4.00	4.00	6.02E-07	5.96E-07	5.90E-07	4.86E-02	4.80E-02	4.78E-02
		4.50	4.50	4.50	6.34E-07	6.36E-07	6.41E-07	4.55E-02	4.55E-02	4.62E-02
		5.00	5.00	5.00	7.57E-07	7.58E-07	7.58E-07	4.89E-02	4.88E-02	4.92E-02
		5.50	5.50	5.50	7.97E-07	8.12E-07	8.19E-07	4.68E-02	4.75E-02	4.83E-02
		6.00	6.00	6.00	9.37E-07	9.35E-07	9.29E-07	5.05E-02	5.02E-02	5.02E-02
		6.50	6.50	6.50	1.04E-06	1.07E-06	9.29E-07	5.18E-02	5.30E-02	4.63E-02
		7.00	7.00	7.00	1.15E-06	1.14E-06	1.13E-06	5.31E-02	5.25E-02	5.24E-02

Table J5 The raw data of the determination of linear regime of Zeolite L at 24-25°C, 54-60% R.H.

Sample	Thickness	Applied voltage (v)		Measure Current (A)		Conductivity (S/cm)	
	(cm)	1	2	1	2	1	2
L	1) 0.02847	5.00	5.00	4.77E-08	1.87E-08	1.54E-03	5.97E-04
	2) 0.02892	6.00	6.00	6.05E-08	2.54E-08	1.63E-03	6.75E-04
		7.00	7.00	6.85E-08	3.25E-08	1.58E-03	7.40E-04
		8.00	8.00	8.00E-08	3.91E-08	1.62E-03	7.79E-04
		9.00	9.00	9.44E-08	4.69E-08	1.70E-03	8.30E-04
		10.00	10.00	1.07E-07	5.52E-08	1.73E-03	8.80E-04
		11.00	11.00	1.19E-07	6.46E-08	1.75E-03	9.36E-04
		12.00	12.00	1.32E-07	7.41E-08	1.77E-03	9.84E-04
		13.00	13.00	1.42E-07	8.18E-08	1.77E-03	1.00E-03
		14.00	14.00	1.52E-07	9.15E-08	1.76E-03	1.04E-03
		15.00	15.00	1.60E-07	1.01E-07	1.73E-03	1.07E-03
		16.00	16.00	1.67E-07	1.10E-07	1.69E-03	1.09E-03
		17.00	17.00	1.73E-07	1.19E-07	1.65E-03	1.12E-03
		18.00	18.00	1.78E-07	1.29E-07	1.60E-03	1.14E-03
		19.00	19.00	1.81E-07	1.42E-07	1.54E-03	1.19E-03
		20.00	20.00	1.80E-07	1.47E-07	1.46E-03	1.17E-03
		21.00	21.00	1.86E-07	1.56E-07	1.43E-03	1.18E-03
		22.00	22.00	1.91E-07	1.61E-07	1.40E-03	1.17E-03
		23.00	23.00	1.94E-07	1.68E-07	1.37E-03	1.17E-03
		24.00	24.00	1.98E-07	1.74E-07	1.34E-03	1.15E-03
		25.00	25.00	2.04E-07	1.77E-07	1.32E-03	1.13E-03
			26.00		1.86E-07		1.14E-03
			27.00		1.93E-07		1.14E-03
			28.00		2.03E-07		1.15E-03
			29.00		2.10E-07		1.15E-03
			30.00		2.14E-07		1.14E-03

Table J6 The raw data of the determination of linear regime of Zeolite MOR at 24-25°C, 54-60% R.H.

Sample	Thickness	Applied voltage (v)		Measure Current (A)		Conductivity (S/cm)	
	(cm)	1	2	1	2	1	2
MOR	1) 0.02659	5.00	10.00	7.98E-08	1.72E-07	2.77E-03	2.94E-03
	2) 0.02706	6.00	11.00	1.15E-07	2.01E-07	3.33E-03	3.11E-03
		7.00	12.00	1.49E-07	2.32E-07	3.69E-03	3.29E-03
		8.00	13.00	1.82E-07	2.63E-07	3.95E-03	3.44E-03
		9.00	14.00	2.17E-07	2.96E-07	4.18E-03	3.61E-03
		10.00	15.00	2.51E-07	3.34E-07	4.35E-03	3.79E-03
		11.00	16.00	2.85E-07	3.71E-07	4.50E-03	3.95E-03
		12.00	17.00	3.07E-07	4.06E-07	4.43E-03	4.07E-03
		13.00	18.00	3.40E-07	4.44E-07	4.53E-03	4.20E-03
		14.00	19.00	3.69E-07	4.74E-07	4.57E-03	4.25E-03
		15.00	20.00	3.92E-07	5.07E-07	4.53E-03	4.32E-03
		16.00	21.00	4.26E-07	5.59E-07	4.61E-03	4.53E-03
		17.00	22.00	4.62E-07	6.01E-07	4.71E-03	4.65E-03
		18.00	23.00	4.90E-07	6.53E-07	4.72E-03	4.84E-03
		19.00	24.00	5.24E-07	6.95E-07	4.78E-03	4.93E-03
		20.00	25.00	5.51E-07	7.52E-07	4.78E-03	5.12E-03
		21.00	26.00	5.85E-07	7.90E-07	4.83E-03	5.17E-03
		22.00	27.00	6.12E-07	8.44E-07	4.82E-03	5.32E-03
		23.00	28.00	6.39E-07	9.00E-07	4.81E-03	5.48E-03
		24.00	29.00	6.80E-07	9.43E-07	4.91E-03	5.54E-03
		25.00	30.00	7.40E-07	9.67E-07	5.13E-03	5.49E-03
			31.00		1.01E-06		5.56E-03
			32.00		1.05E-06		5.58E-03
			33.00		1.07E-06		5.55E-03
			34.00		1.12E-06		5.59E-03
			35.00		1.16E-06		5.65E-03

Table J7 The raw data of the determination of linear regime of Zeolite BEA at 24-25°C, 54-60% R.H.

Sample	Thickness	Applied voltage (v)		Measure Current (A)		Conductivity (S/cm)	
	(cm)	1	2	1	2	1	2
BEA	1) 0.04493	40.00	40.00	2.64E-07	3.60E-07	6.77E-04	9.25E-04
	2) 0.04488	41.00	41.00	2.75E-07	3.71E-07	6.89E-04	9.28E-04
		42.00	42.00	2.87E-07	3.82E-07	7.00E-04	9.34E-04
		43.00	43.00	2.98E-07	3.94E-07	7.11E-04	9.40E-04
		44.00	44.00	3.09E-07	4.05E-07	7.20E-04	9.45E-04
		45.00	45.00	3.20E-07	4.19E-07	7.30E-04	9.56E-04
		46.00	46.00	3.31E-07	4.30E-07	7.38E-04	9.59E-04
		47.00	47.00	3.42E-07	4.39E-07	7.46E-04	9.60E-04
		49.00	48.00	3.62E-07	4.49E-07	7.57E-04	9.61E-04
		50.00	49.00	3.75E-07	4.60E-07	7.69E-04	9.65E-04
		51.00	50.00	3.86E-07	4.71E-07	7.76E-04	9.67E-04
		52.00	51.00	3.98E-07	4.82E-07	7.84E-04	9.70E-04
		53.00	52.00	4.10E-07	4.92E-07	7.93E-04	9.72E-04
		54.00	53.00	4.23E-07	5.03E-07	8.03E-04	9.75E-04
		55.00	54.00	4.36E-07	5.14E-07	8.12E-04	9.77E-04
		56.00	55.00	4.47E-07	5.25E-07	8.18E-04	9.80E-04
		57.00	56.00	4.58E-07	5.37E-07	8.24E-04	9.84E-04
		58.00	57.00	4.70E-07	5.49E-07	8.32E-04	9.88E-04
		59.00	58.00	5.17E-07	5.60E-07	9.00E-04	9.92E-04
		60.00	59.00	5.29E-07	5.71E-07	9.04E-04	9.94E-04
		61.00	60.00	5.49E-07	5.82E-07	9.23E-04	9.96E-04
		62.00		5.61E-07		9.28E-04	
		63.00		5.75E-07		9.36E-04	
		64.00		5.88E-07		9.42E-04	
		65.00		6.04E-07		9.53E-04	

Appendix K Density Measurement

The specific density (ρ_p) of the conductive polymer and zeolite can be measured by using a pyncometer. At first, we measured the weight of blank pyncometer and then we added the water to the pyncometer and the measured the total weight again. The specific density of water at testing temperature can calculate by equation (K.1).

$$\rho_w = \frac{(a-b)}{25} \qquad \text{(K.1)}$$

where ρ_w is specific density of water ($g.cm^{-3}$), a is the weigth of pyncometer with water (g), and b is the weigth of blank pyncometer (g).

Next step, we measured the weight of the blank pyncometer again and then we added polymer or zeolite powders and then remeasured the total weight. Then we added water into the pyncometer and then measured the total weight of pyncometer. The specific density of polymer and zeolite at testing temperature can be calculated from equations (K2) – (K.3).

$$A = \frac{(e-d)}{\rho_w} \qquad \text{(K.2)}$$

where A is the volume of water added into pyncometer (cm^3), ρ_w is the specific density of water ($g.cm^{-3}$), e is the weigth of the pyncometer with water and polymer or zeolite (g), and d is the weigth of polymer or zeolite powder and pyncometer (g).

$$\rho_m = \frac{(d-b)}{25-A} \qquad \text{(K.3)}$$

where ρ_m is the specific density of material ($g.cm^{-3}$), d is the weigth of plymer or zeolite powder and pyncometer (g), b is the weigth of blank pyncometer (g), and A is the volume of water which add into pyncometer (cm^3).

Table K1 Summary data of specific density of materials

Materials	ρ_w (g/cm^3)	Volume of water (A, cm^3)	ρ_m (g/cm^3)
Pth	0.9955	24.3768	1.6630
ZeoliteL	0.9964	24.4116	2.0885
Zeolit mordenite	0.9962	24.9787	2.1951
Zeolite beta	0.9963	24.8527	2.1574

Appendix L Determination the Amount of Cation in Zeolite

An atomic absorption spectrophotometer (Varian, spectr AA.300) was used to determine the amounts of cations in zeolites before and after ion exchange processes. About 0.05 g of zeolite was immersed in HCl solution with 1:1 by volume of HCl and H_2O and heated to about 60 °C. The solution after filtering was characterized. Standard, blank and sample solutions were prepared before testing of each cation type in zeolite. Each cation type in zeolite was identified by using the diferrent lamp sources. Mole % was calculated by following eqution L.1

$$\text{Mole \%} = \frac{W_{cat}/MW_{cat} \times 100}{\left(W_{cat}/MW_{cat}\right)+\left(W_{Na}/MW_{Na}\right)} \qquad \text{L.1}$$

where W_{cat} is weight of cation per gram of zeolite, W_{Na} is weight of Na per gram of zeolite, MW_{cat} is atomic weight of cation and MW_{Na} is atomic weight of cation.

Table L1 Degree of cation exchange of zolite Mordenite with Na^+

Sample	Weigth (g)	Determination of K^+			Determination of Na^+			Mole %
		Conc. (ppm)	g_{K+}/ g zeolite	Mole/ $kg_{zeolite}$	Conc. (ppm)	g_{Na+}/ g zeolite	Mole/ $kg_{zeolite}$	
MOR/1	0.0515				0.97	0.04709	2.0473	
MOR/2	0.0529				0.97	0.04584	1.9931	
$K1^{st}$/1	0.0514	0.72	0.07059	1.8055	0.48	0.004669	0.2030	89.89
$K1^{st}$/2	0.0506	0.79	0.07806	1.9966	0.46	0.004545	0.1976	90.99
							Avg.	90.44
							SD.	0.78
$K5^{th}$/1	0.0511	0.82	0.08137	2.0812	0.41	0.004012	0.1744	92.27
$K5^{th}$/2	0.0511	0.81	0.07926	2.0271	0.39	0.003816	0.1659	92.44
							Avg.	92.36
							SD.	0.12
$K9^{th}$/1	0.0506	0.68	0.06720	1.7189	0.27	0.002668	0.1160	93.68
$K9^{th}$/2	0.0517	0.68	0.06576	1.6820	0.26	0.002515	0.1093	93.90
							Avg.	93.79
							SD.	0.16
$K11^{th}$/1	0.0510	0.67	0.06569	1.68470	0.13	0.001275	0.0554	96.82
$K11^{th}$/2	0.0519	0.68	0.65510	1.67550	0.12	0.001156	0.0503	97.09
							Avg.	96.96
							SD.	0.19

Table L2 Degree of cation exchange of zolite Mordenite with Li^+

Sample	Weigth (g)	Determination of Li^+			Determination of Na^+			Mole %
		Conc. (ppm)	g_{Li+}/ g zeolite	Mole/ $kg_{zeolite}$	Conc. (ppm)	g_{Na+}/ g zeolite	Mole/ $kg_{zeolite}$	
MOR/1	0.0515				0.97	0.04709	2.0473	
MOR/2	0.0529				0.97	0.04584	1.9931	
Li1st/1	0.0510	0.23	0.01127	1.6243	0.21	0.010290	0.4476	78.40
Li1st/2	0.0502	0.23	0.01145	1.6502	0.18	0.008964	0.3897	80.90
							Avg.	79.65
							SD.	1.77
Li3rd/1	0.0515	0.29	0.01408	2.0282	0.11	0.00534	0.2322	89.73
Li3rd/2	0.0514	0.29	0.01411	2.0321	0.11	0.00535	0.2326	89.73
							Avg.	89.73
							SD.	0.00
Li5th/1	0.0513	0.31	0.01511	2.1765	0.14	0.006823	0.2966	88.10
Li5th/2	0.0503	0.30	0.01491	2.1481	0.10	0.004970	0.2161	90.86
							Avg.	89.48
							SD.	1.95

Table L3 Degree of cation exchange of zolite L with Na^+

Sample	Weigth (g)	Determination of Na^+			Determination of K^+			Mole %
		Conc. (ppm)	$g_{Na+}/g_{zeolite}$	Mole/ $kg_{zeolite}$	Conc. (ppm)	$g_{K+}/g_{zeolite}$	Mole/ $kg_{zeolite}$	
L/1	0.0510				1.76	0.1725	4.4132	
L/2	0.0506				1.72	0.1700	4.3470	
Na 1st/1	0.0508	0.17	0.01663	0.7232	1.66	0.1634	4.1789	14.75
Na 1st/2	0.0508	0.17	0.01663	0.7232	1.64	0.1614	4.2185	14.91
							Avg.	14.83
							SD.	0.11
Na 2nd/1	0.0514	0.22	0.02140	0.9305	1.56	0.1518	3.8813	19.34
Na 2nd/2	0.0508	0.18	0.01772	0.7703	1.16	0.1142	2.9202	20.87
							Avg.	20.11
							SD.	1.08
Na 3rd/1	0.0500	0.28	0.02800	1.2174	1.28	0.1280	3.2738	27.11
Na 3rd/2	0.0510	0.22	0.02157	0.9378	1.05	0.1029	2.6329	26.26
							Avg.	26.69
							SD.	0.60
Na 5th/1	0.0503	0.26	0.02584	1.1237	1.01	0.1004	2.5678	30.44
Na 5th/2	0.0502	0.29	0.02888	1.2558	1.06	0.1056	2.7003	31.74
							Avg.	31.09
							SD.	0.92
Na 8th/1	0.0500	0.29	0.02918	1.2685	1.02	0.1026	2.6246	32.58
Na 8th/2	0.0497	0.29	0.02918	1.2685	1.04	0.1046	2.6760	32.16
							Avg.	32.37
							SD.	0.30
Na19th/1	0.0516	0.39	0.03779	1.6431	0.7	0.06783	1.7349	48.64
Na19th/2	0.0516	0.44	0.04264	1.8537	0.72	0.06978	1.7844	50.95
							Avg.	49.80
							SD.	1.63

Appendix M Surface area and Pore size of Zeolite

Surface area and pore size of each zeolite were measured by BET (Sorptomatic 1990, Thermo Finnigan). Zeolite powder was weighed and out gassed at 300°C over night before the adsorption and the desorption with He and N_2 gases. During the operation, zeolite powder was cooling by liquid N_2.

The specific surface area can be determined by the equation M.1.

$$SS = \frac{Z \times a \times V_m}{W} \qquad (M.1)$$

where SS is the specific surface, W is the sample mass, Vm is the monolayer volume, Z is the avogadro number and a is the average molecular area of the adsorbate.

The pore size and pore volume of zeolite were determined by method of Horvath Kawazoe. This model originates from a thermodynamic point of view combined with the 10:4 potential functions of Lennard-Jones. Staring with the Gibbs free energy of adsorption.

$$\Delta G_{ads} = RT \ln(p/p^{\circ}) = \Delta H_{ads} - T\Delta S_{ads} \qquad (M.2)$$

with:

$$\Delta H_{ads} = -q_{diff} - RT + L\,(Ta_m/\theta)[\partial\pi/\partial T] \qquad (M.3)$$

As ΔS_{ads} is constant and ΔG_{ads} reaching p° is zero. The differentialheat of adsorption can be calculated from a molecular theoretyl way resulting in the eqution:

$$\Delta G_{ads} = RT \ln(p/p^{\circ}) = U_o + Pa \qquad (M.4)$$

where U_o is a measure for the potential of the adsorptive and P_a a measure for the potential of the adsorbate adsorbent interactions giving the sum of potential functions $f(r)$ that can be expressed in the following way:

$$\phi(r) = \frac{N_a A_a + N_A A_A}{2\sigma^4} \cdot \left[-\left(\frac{\sigma}{r}\right)^4 + \left(\frac{\sigma}{r}\right)^{10} - \left(\frac{\sigma}{l-r}\right)^4 + \left(\frac{\sigma}{l-r}\right)^{10} \right] = (U_0 + P_a/L) \quad \text{(M.5)}$$

The constant A_a and A_A from the Lennard Jones Potential can be calculated with the Kirkwood-Müller-equation:

$$A_a = \frac{6mc^2 \alpha_a \alpha_A}{\alpha_a/\chi_a + \alpha_A/\chi_A} \quad \text{(M.6)}$$

$$A_A = \frac{3mc^2 \alpha_A \chi_A}{2} \quad \text{(M.7)}$$

Thus the average potential of the one mole adsorbent can be integrated from eq. (M.5) according to the distance of the atom centers. With the limits of the minimal and maximal possible dis tance between the adsorbate-atoms and the adsorbent-atoms in a micropore (Figure M.1), the integal in eq. (M.8) can be solved to give eq. (M.9). This equation gives a function correlating the relative pressure with the pore radius:

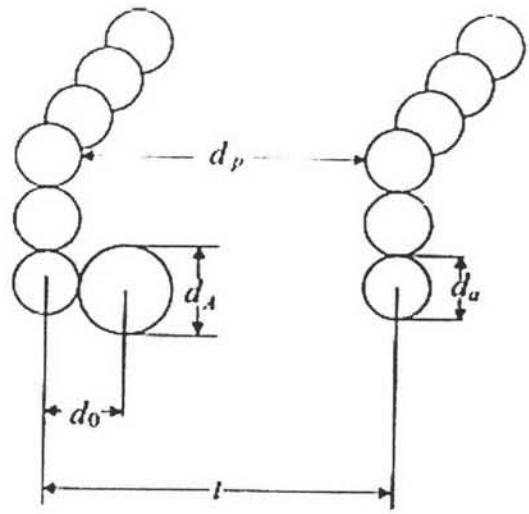

Figure M1 Model of a slit pore ; big circle adsorbate, small circle adsorbent

This function is determined by four constants that can be calculated from the tabulated physical constants setting $\sigma=0.858\ d_o$:

$$\ln(p/p^o)=\frac{L}{RT}\frac{N_a A_a+N_r A_r}{\sigma^4}\frac{1}{(l-(d_a+d_r))}\int_{d_a}^{l-d_r}\left[-\left(\frac{\sigma}{r}\right)^4+\left(\frac{\sigma}{r}\right)^{10}-\left(\frac{\sigma}{l-r}\right)^4+\left(\frac{\sigma}{l-r}\right)^{10}\right]dr \quad \text{M.8}$$

$$\ln(p/p^o)=\frac{L}{RT}\frac{N_a A_a+N_r A_r}{\sigma^4}\frac{1}{(l-2d_o)}\cdot\left[-\frac{\sigma^4}{3(l-d_o)^3}+\frac{\sigma^{10}}{9(l-d_o)^9}-\frac{\sigma^4}{3(d_o)^3}+\frac{\sigma^{10}}{9(d_o)^9}\right] \quad \text{M.9}$$

The pore width is correlated with the distance of the atom centers as $d_p=l-d_a$. Thus a function is available that converts the pore sizes to relative pressures, if the physical parameters of adsorbate and adsorbent are available. The reciprocal fuction enable the conversion of $p/p^o \Rightarrow d_p$ by a plot of $W(d_p)$ and $dW/dd_p(d_p)$.

$$\ln(p/p^o)=A\frac{1}{(l-2d_o)}\cdot\left[\frac{B}{(l-d_o)^3}-\frac{C}{(l-d_o)^9}-D\right] \quad \text{M.10}$$

Table M1 Surface area and pore size of zeolite

	Surface area (m^2/g)			Pore volume (cm^3/g)			Pore size (A°)		
	L	MOR	BEA	L	MOR	BEA	L	MOR	BEA
Tosoh Co.	280.00	360.00	580.00						
1st	290.07	341.09	583.25	0.20	0.25	0.40	5.45	5.90	6.57
2nd	275.99	330.84	527.15	0.33	0.22	0.35	6.28	6.46	6.01
Average	283.03	335.96	555.20	0.27	0.23	0.37	5.86	6.18	6.29
SD	9.95	7.24	39.67	0.09	0.02	0.04	0.59	0.40	0.39

Appendix N Electrical Conductivity Sensitivity Measurement

Sensitivity measurements of polythiophene and polythiophene/zeolite pellets were carried out by using the two point probe with pure hydrogen gas (99.999%) under the pressure of 1.3 atm, 57-67% relative humidity, and 29±1°C. The electrical conductivity response of sample was calculated from the difference between the equilibrium conductivity of sample upon exposed to H_2 and the steady state conductivity value of sample in N_2.

$$\Delta\sigma = \sigma_{H2} - \sigma_{initial\ N2} \qquad (N.1)$$

The sensitivity is defined as the electrical conductivity response divided by the conductivity itself at the N_2.

$$\text{Sensitivity} = \Delta\sigma/\sigma_{initial\ N2} \qquad (N.2)$$

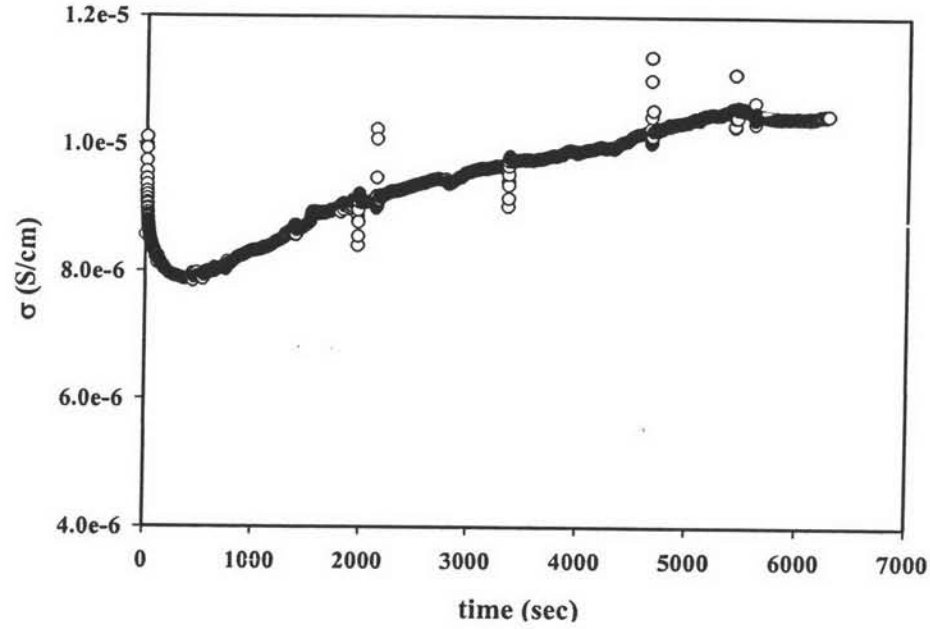

Figure N1 Specific conductivity of Pth_200:1(1) when exposed to H_2.

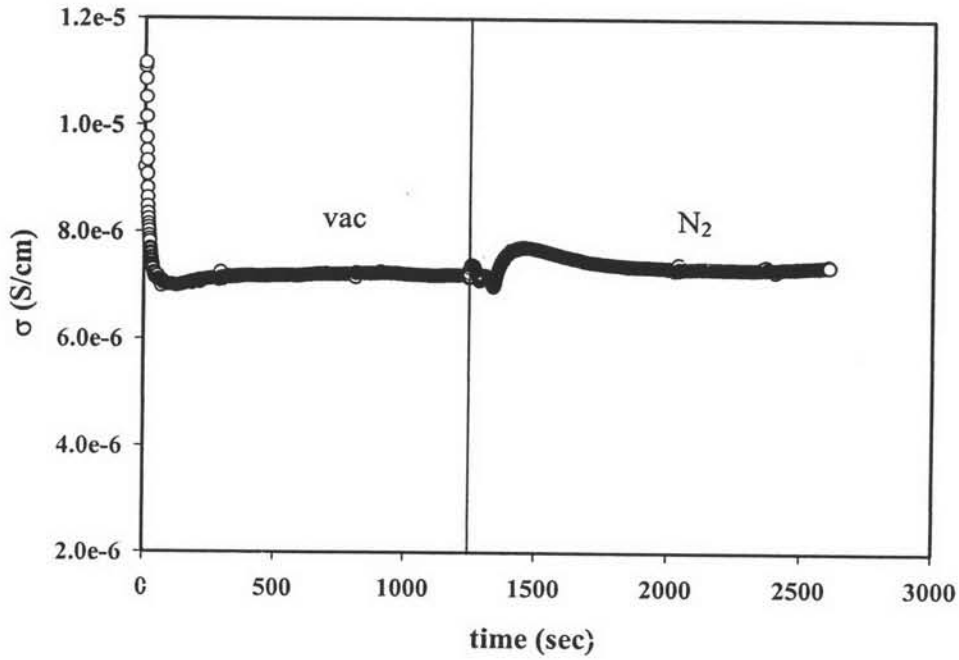

Figure N2 Specific conductivity of Pth_200:1(1) after evacuating H_2 and exposed to N_2.

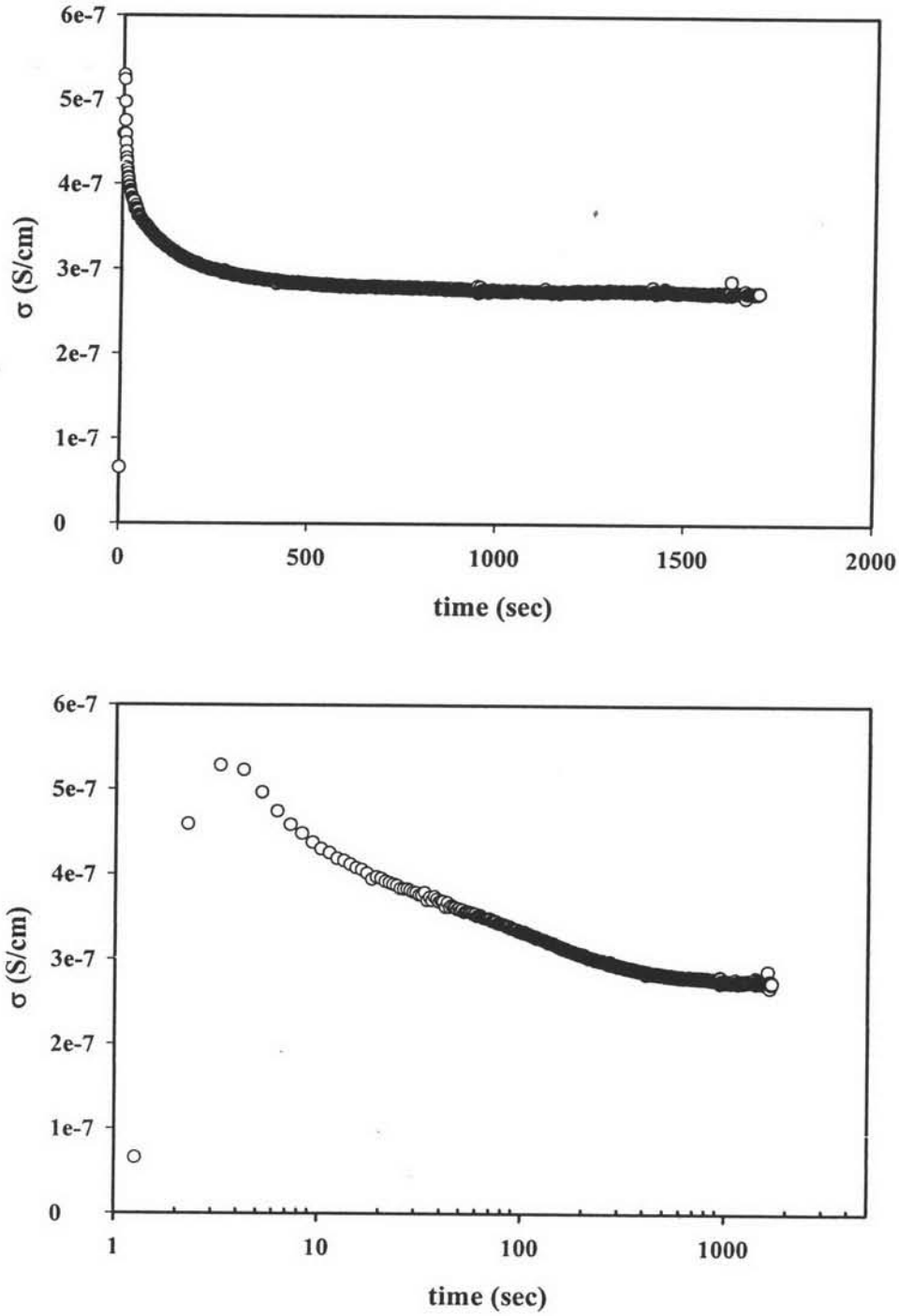

Figure N3 Specific conductivity of Pth_200:1/L_20(1) when exposed to H_2.

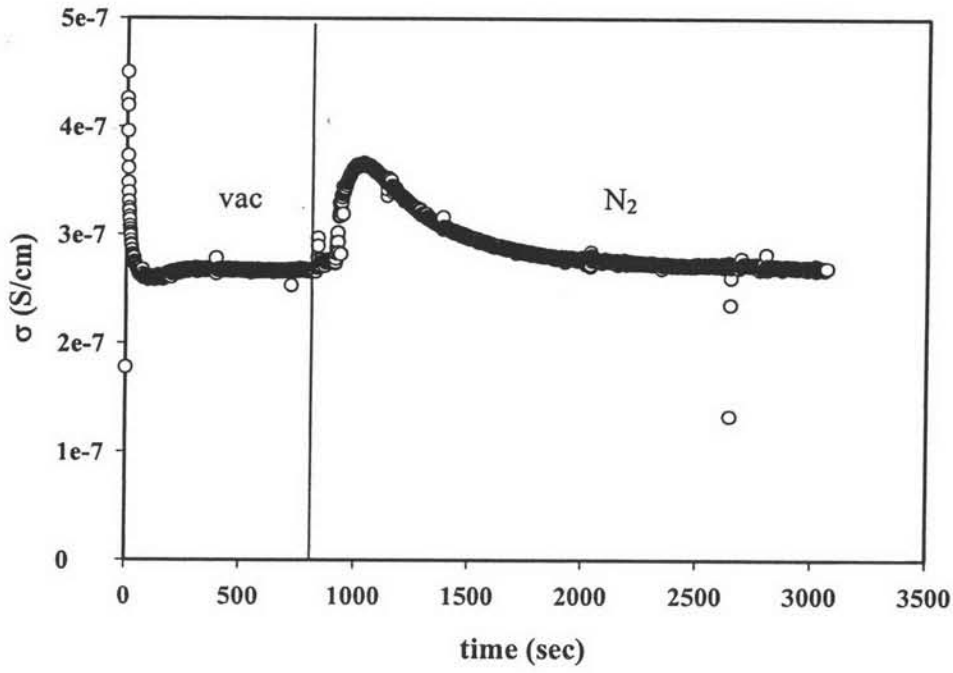

Figure N4 Specific conductivity of Pth_200:1/L_20(1) after evacuating H_2 and exposed to N_2.

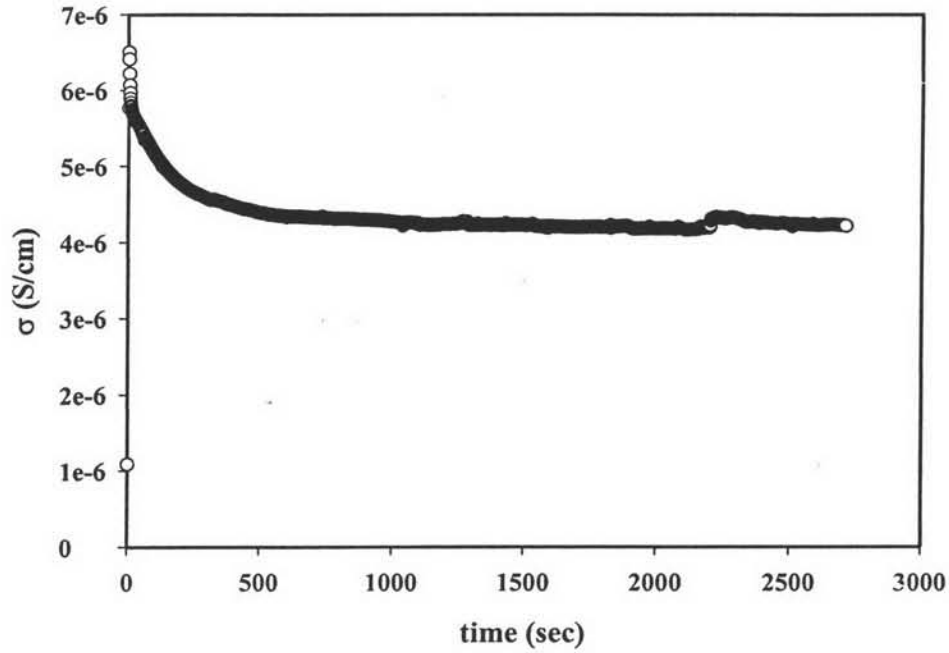

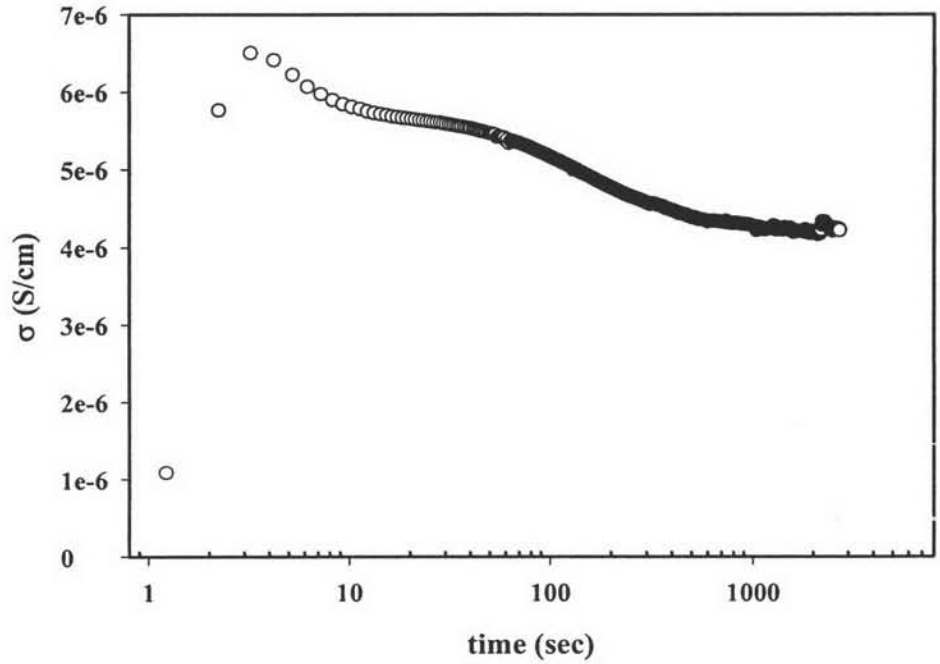

Figure N5 Specific conductivity of Pth_200:1/MOR_20(1) when exposed to H_2.

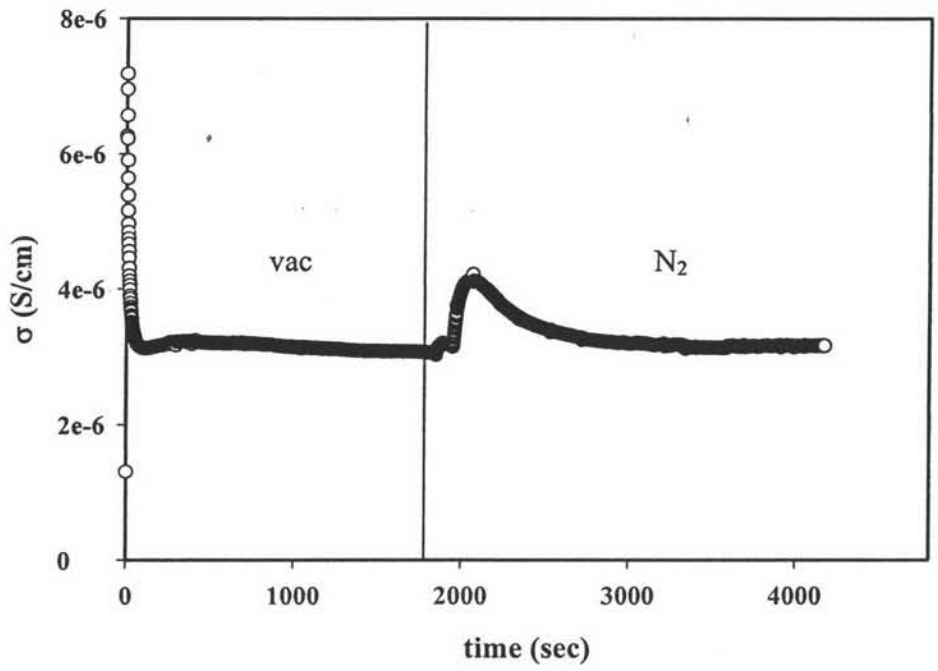

Figure N6 Specific conductivity of Pth_200:1/MOR_20(1) after evacuating H_2 and exposed to N_2.

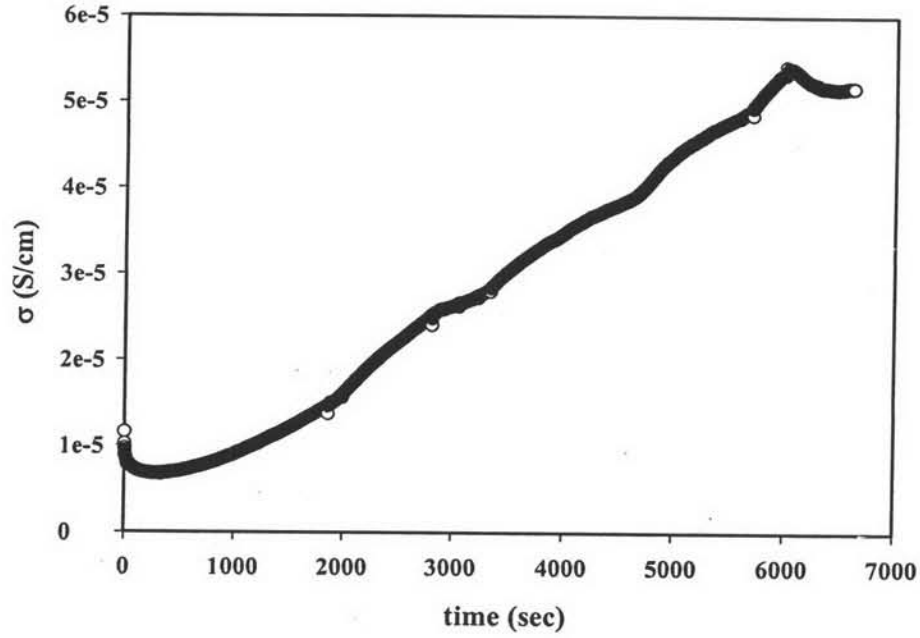

Figure N7 Specific conductivity of Pth_200:1/BEA_20(2) when exposed to H_2.

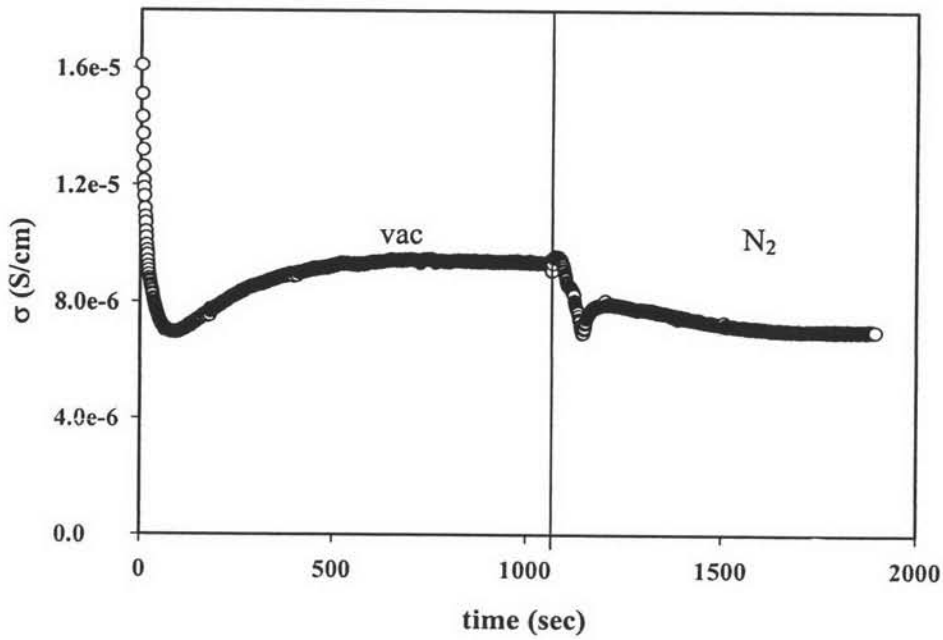

Figure N8 Specific conductivity of Pth_200:1/BEA_20(2) after evacuating H_2 and exposed to N_2.

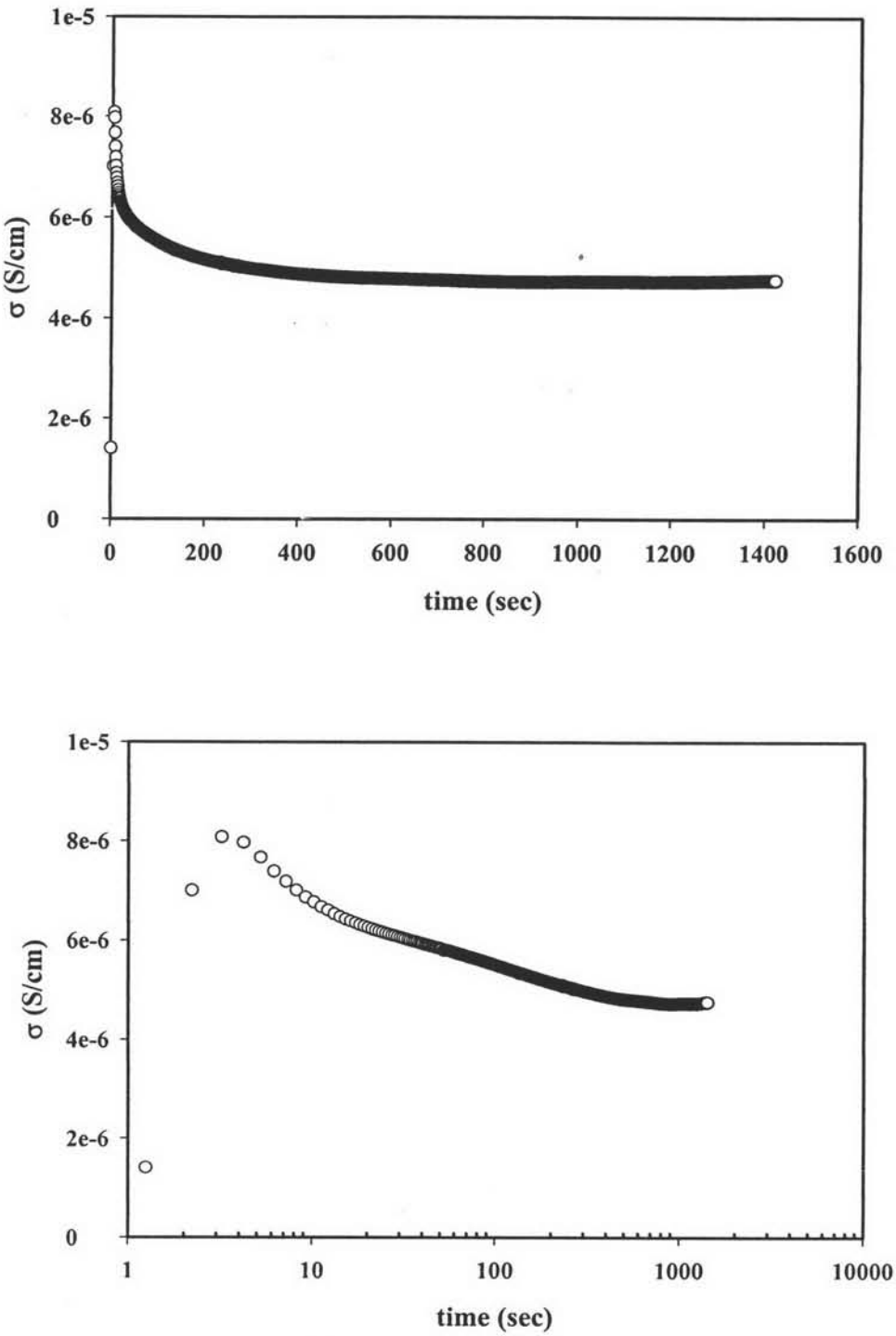

Figure N9 Specific conductivity of Pth_200:1/MOR_Li[90]20(1) when exposed to H_2.

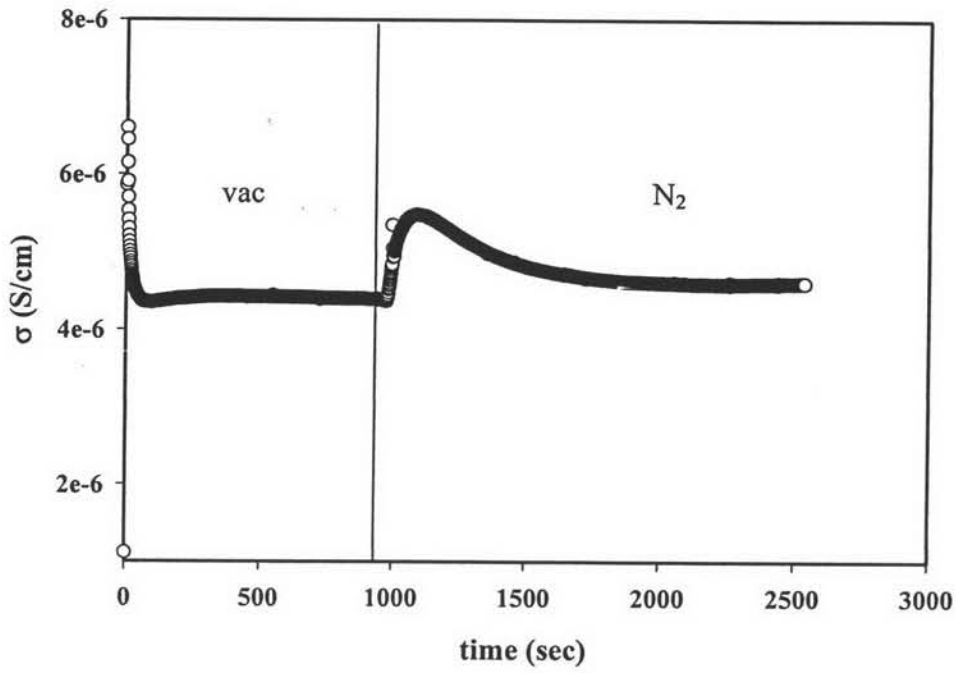

Figure N10 Specific conductivity of Pth_200:1/MOR_Li[90]_20(1) after evacuating H_2 and exposed to N_2.

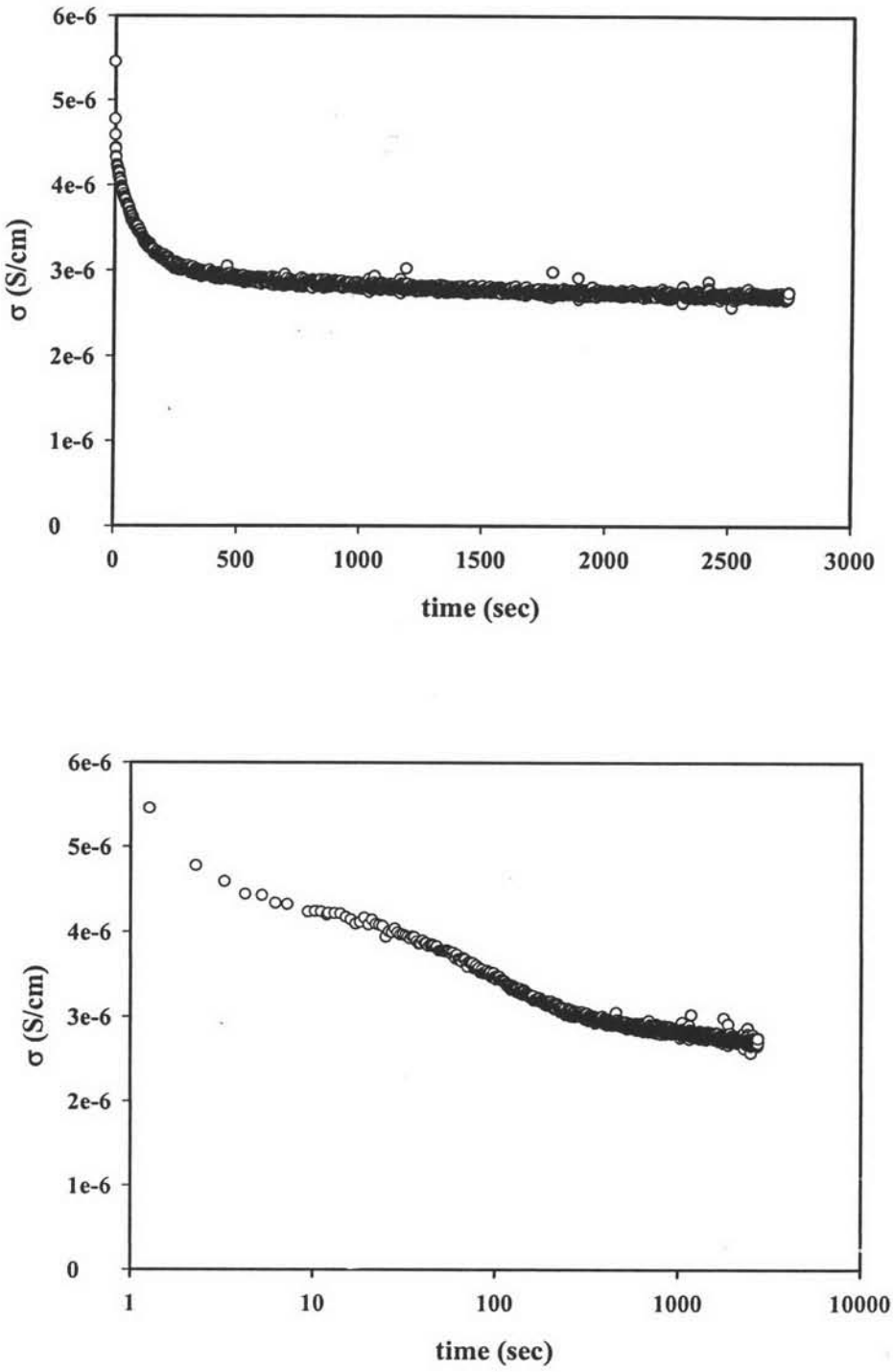

Figure N11 Specific conductivity of Pth_200:1/MOR_K[90]_20(1) when exposed to H_2.

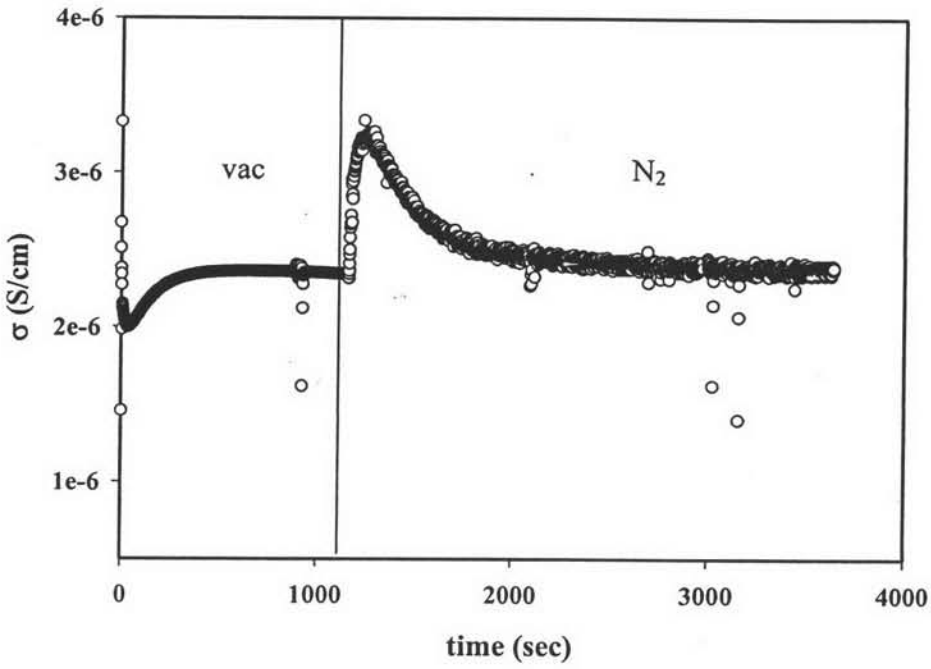

Figure N12 Specific conductivity of Pth_200:1/MOR_K[90]_20(1) after evacuating H_2 and exposed to N_2.

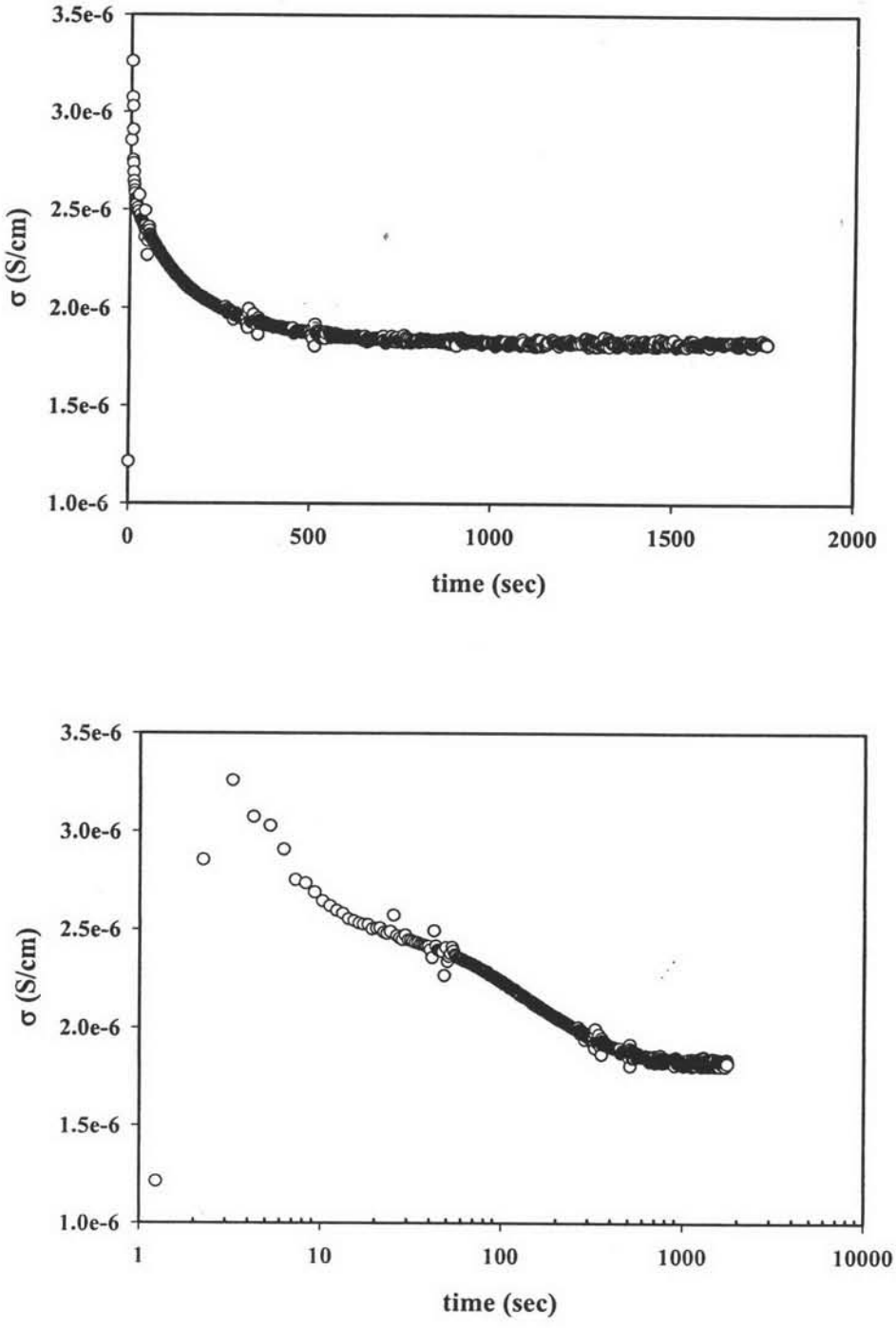

Figure N13 Specific conductivity of Pth_200:1/L_Na[15]_20(1) when exposed to H_2.

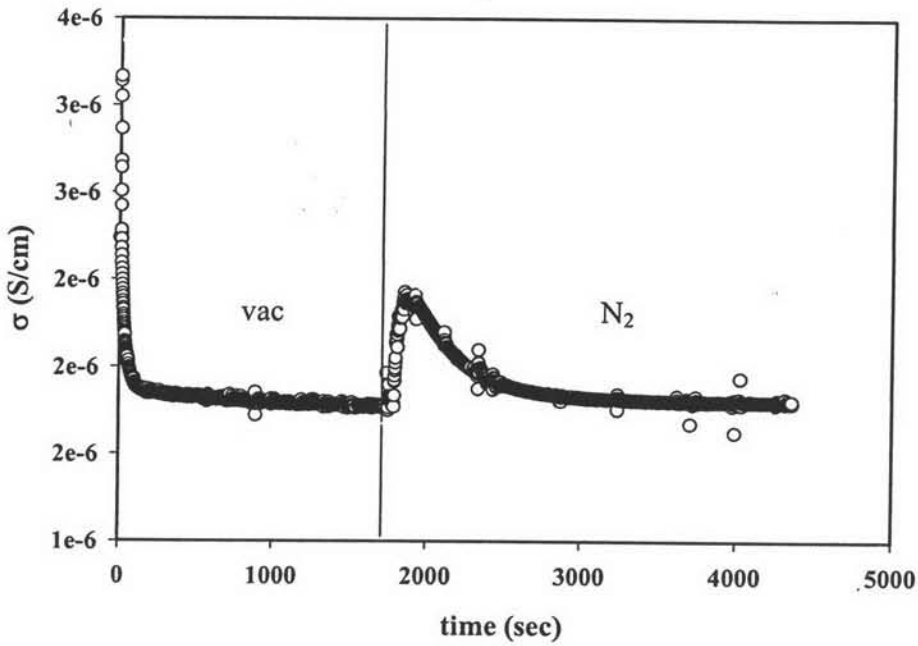

Figure N14 Specific conductivity of Pth_200:1/L_Na[15]_20(1) after evacuating H_2 and exposed to N_2.

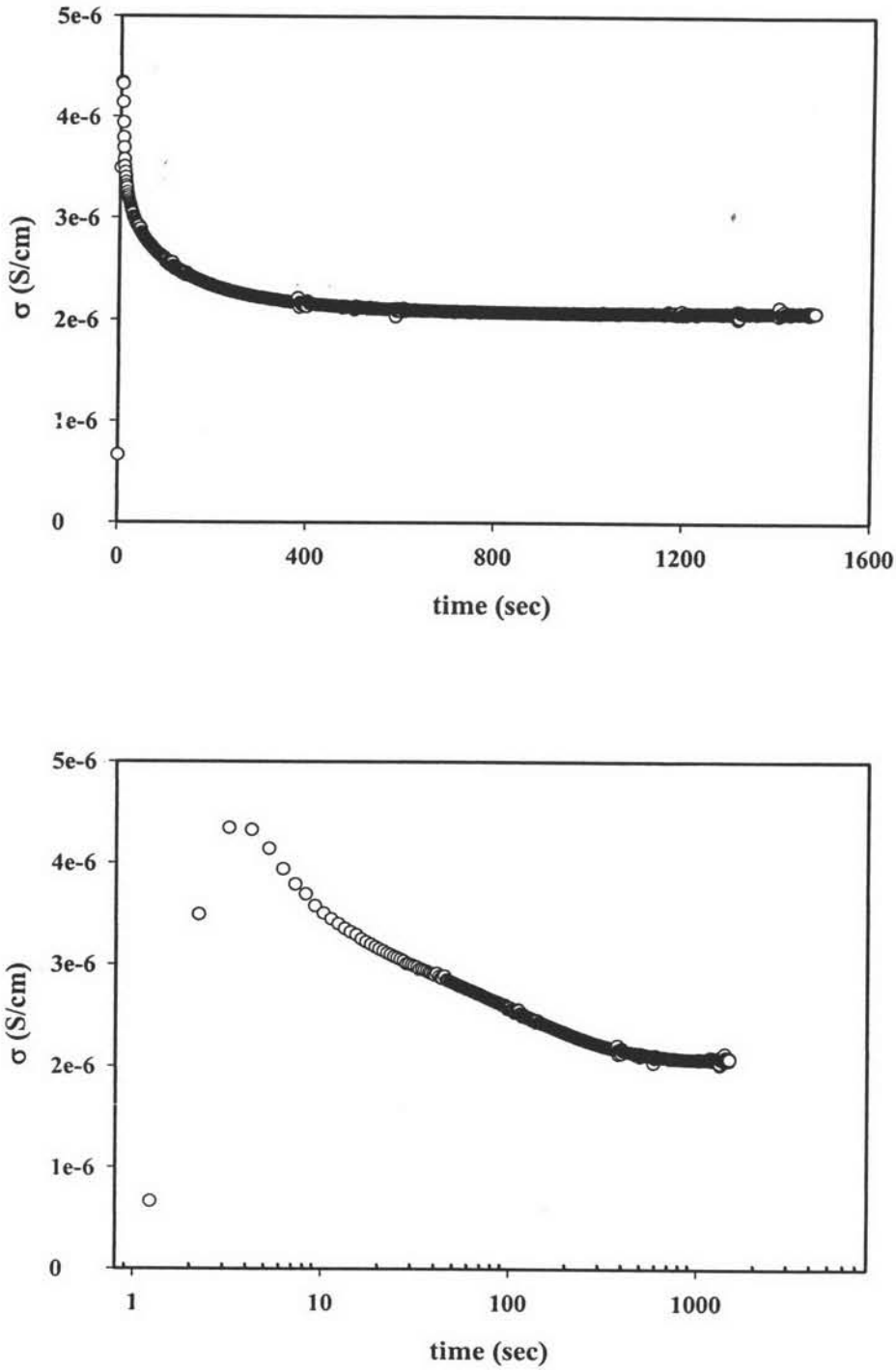

Figure N15 Specific conductivity of Pth_200:1/L_Na[20]_20(1) when exposed to H_2.

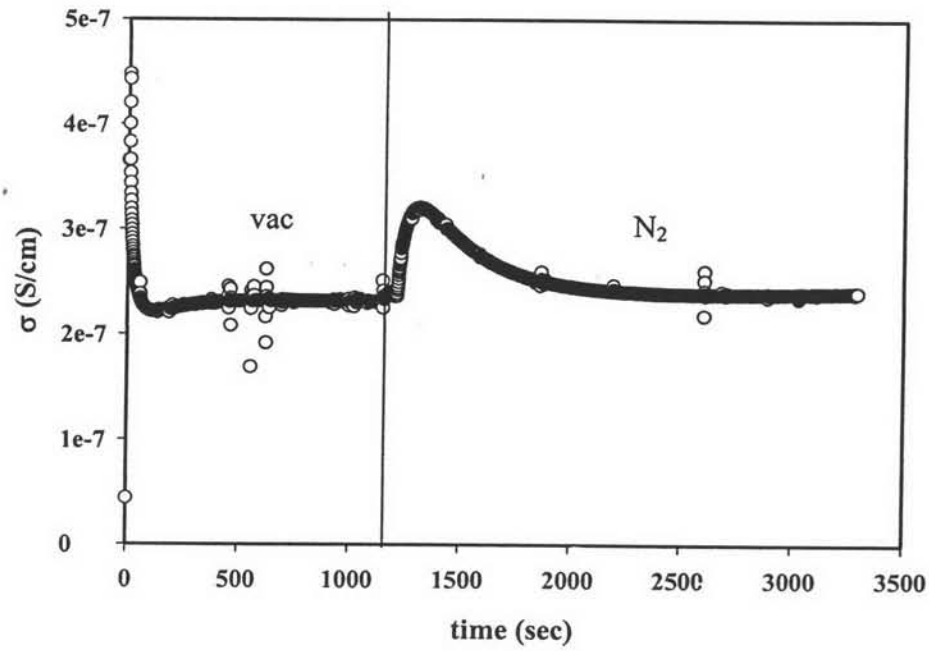

Figure N16 Specific conductivity of Pth_200:1/L_Na[20]_20(1) after evacuating H_2 and exposed to N_2.

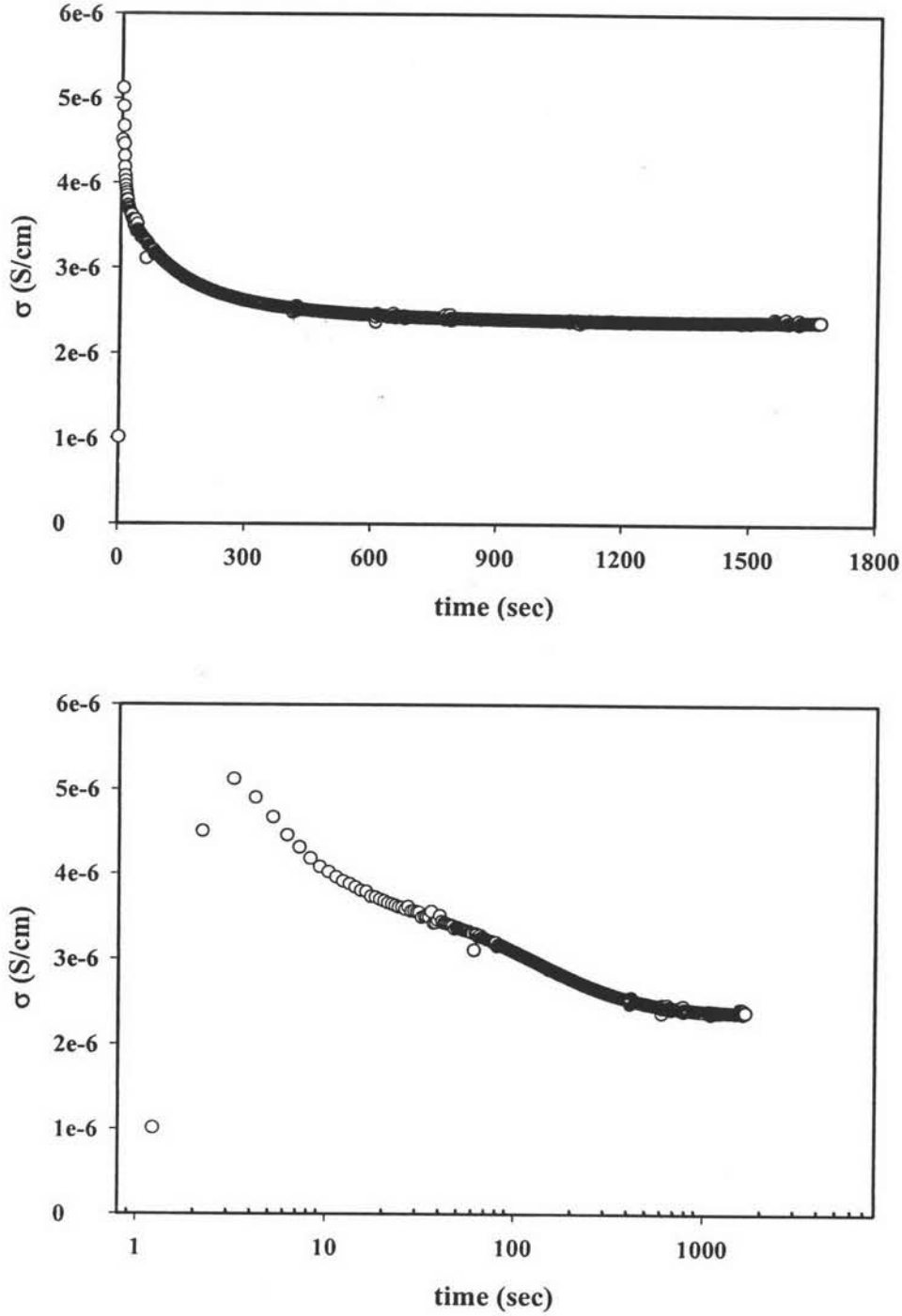

Figure N17 Specific conductivity of Pth_200:1/L_Na[30]_20(1) when exposed to H_2.

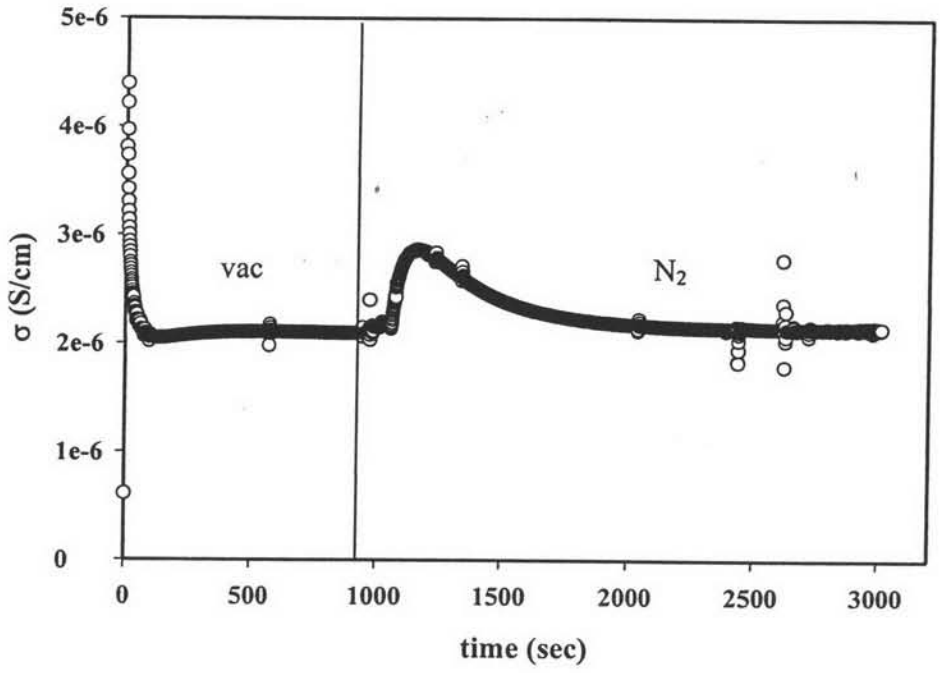

Figure N18 Specific conductivity of Pth_200:1/L_Na[30]_20(1) after evacuating H_2 and exposed to N_2.

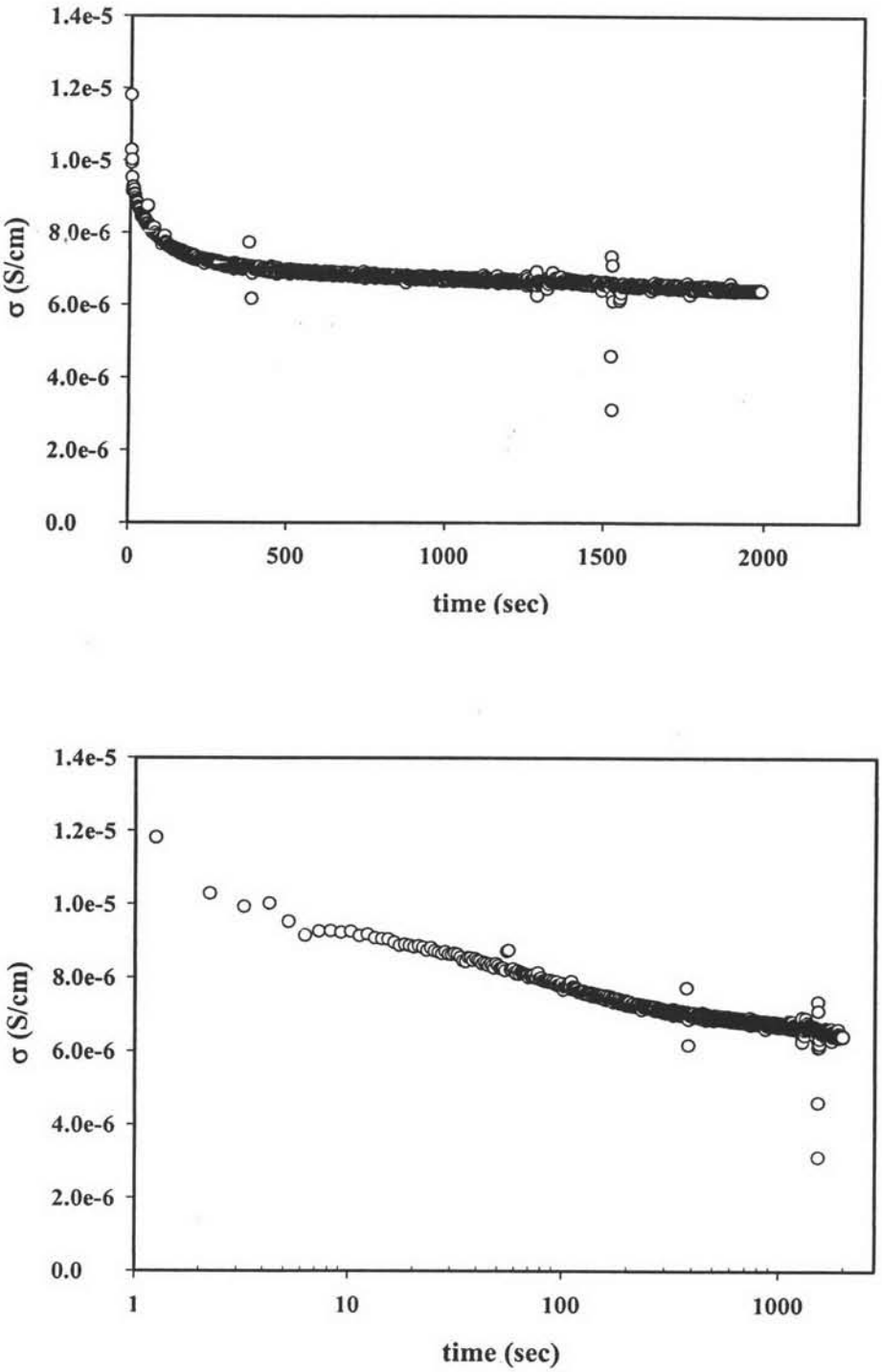

Figure N19 Specific conductivity of Pth_200:1/L_Na[50]_20(2) when exposed to H_2.

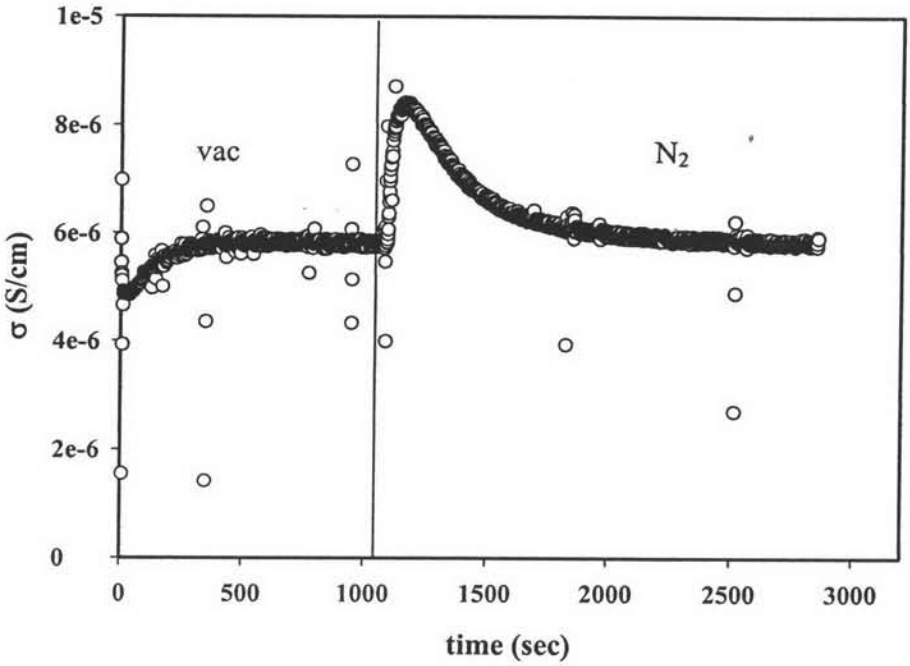

Figure N20 Specific conductivity of Pth_200:1/L_Na[50]_20(2) after evacuating H_2 and exposed to N_2.

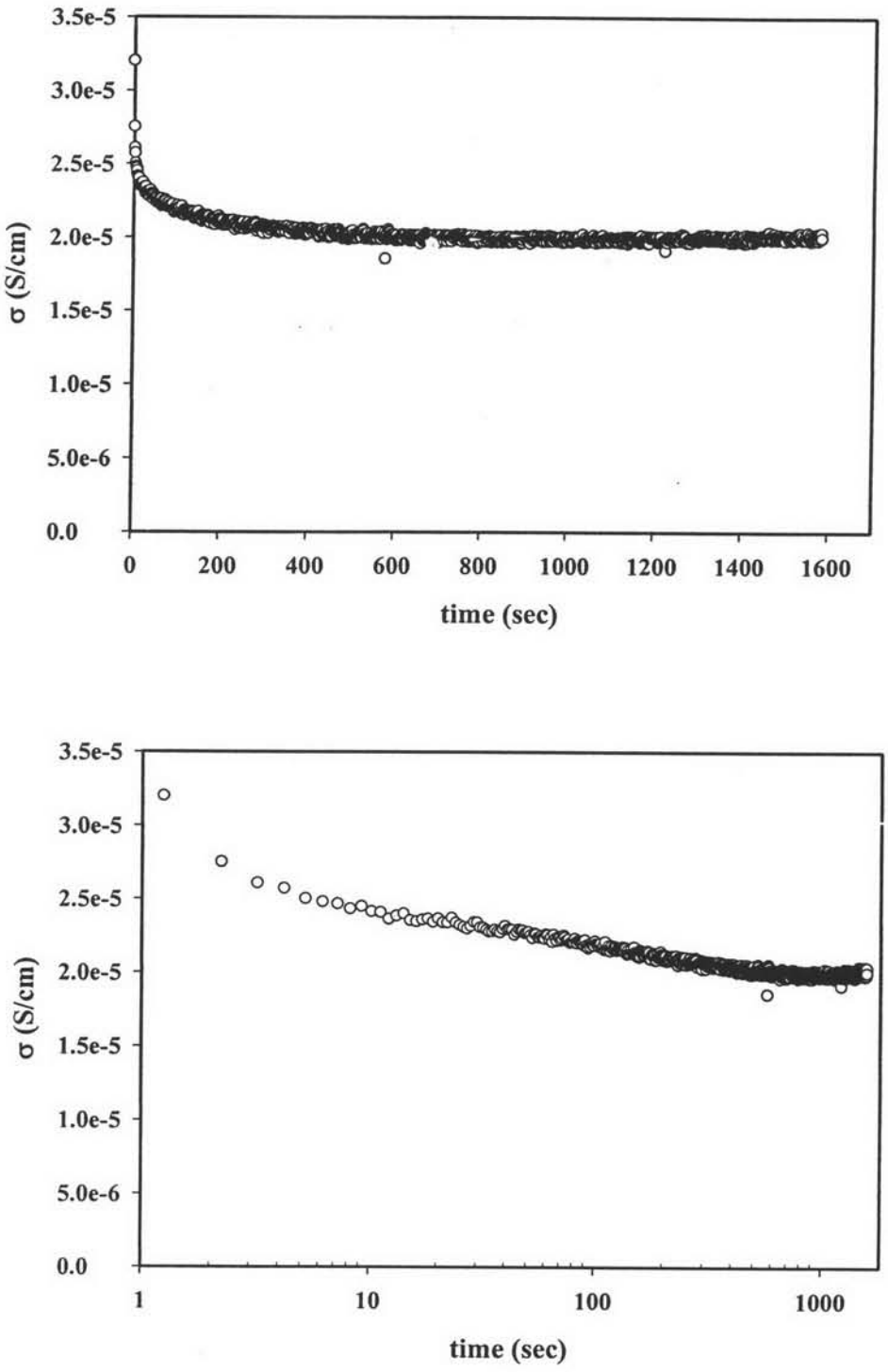

Figure N21 Specific conductivity of Pth_200:1/MOR_10(1) when exposed to H_2.

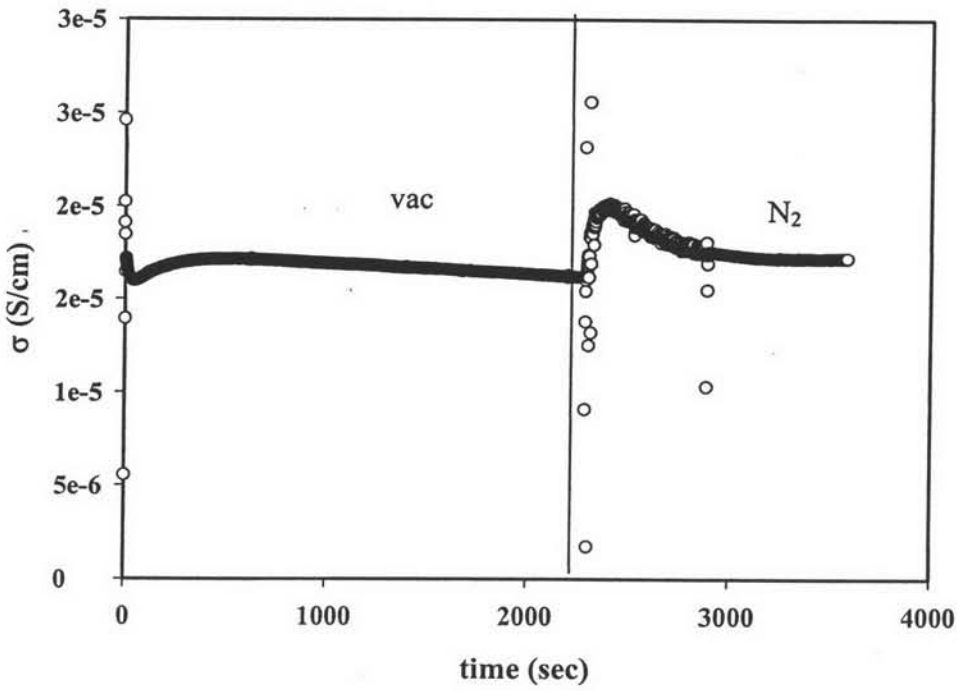

Figure N22 Specific conductivity of Pth_200:1/MOR_10(1) after evacuating H_2 and exposed to N_2.

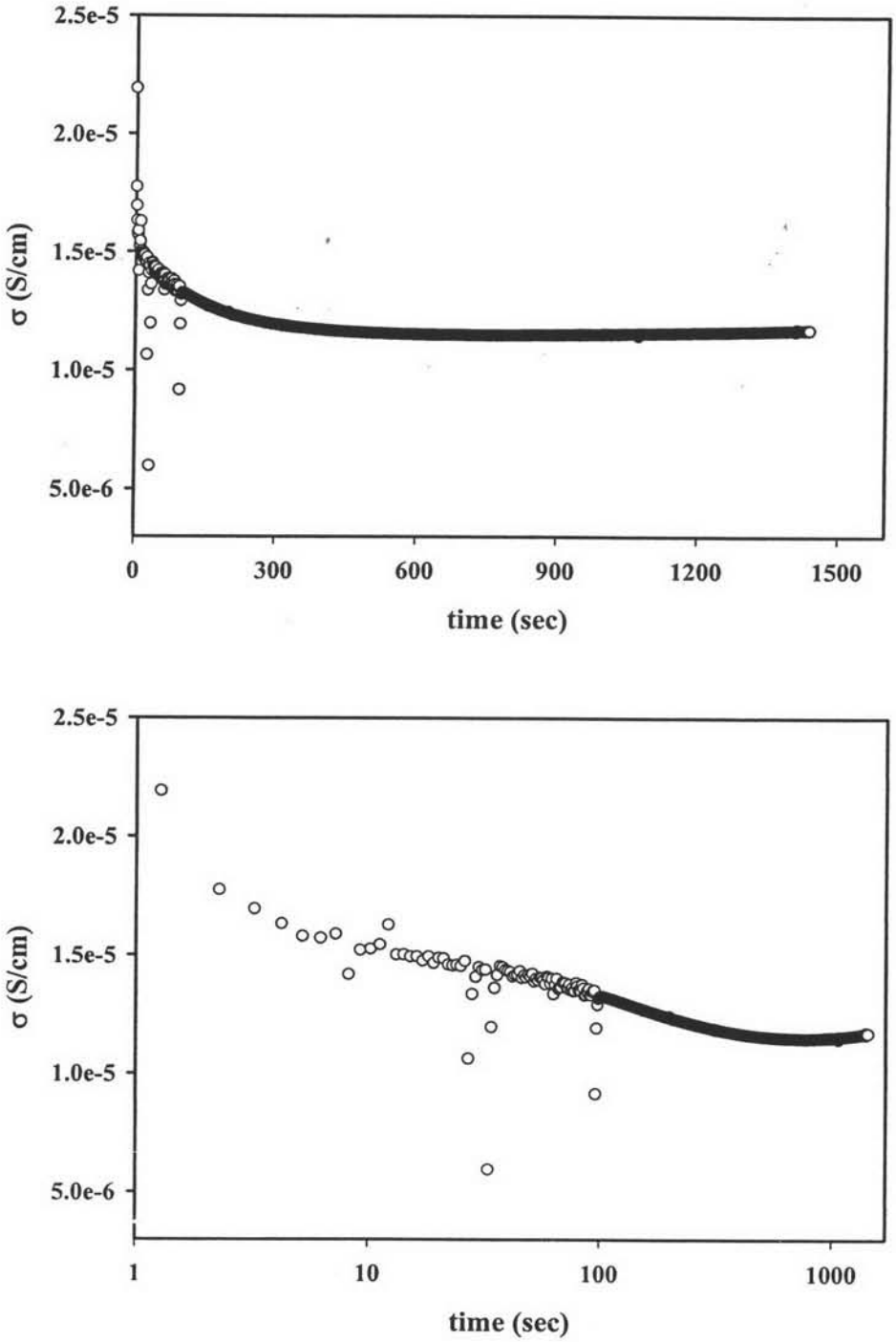

Figure N23 Specific conductivity of Pth_200:1/MOR_30(1) when exposed to H_2.

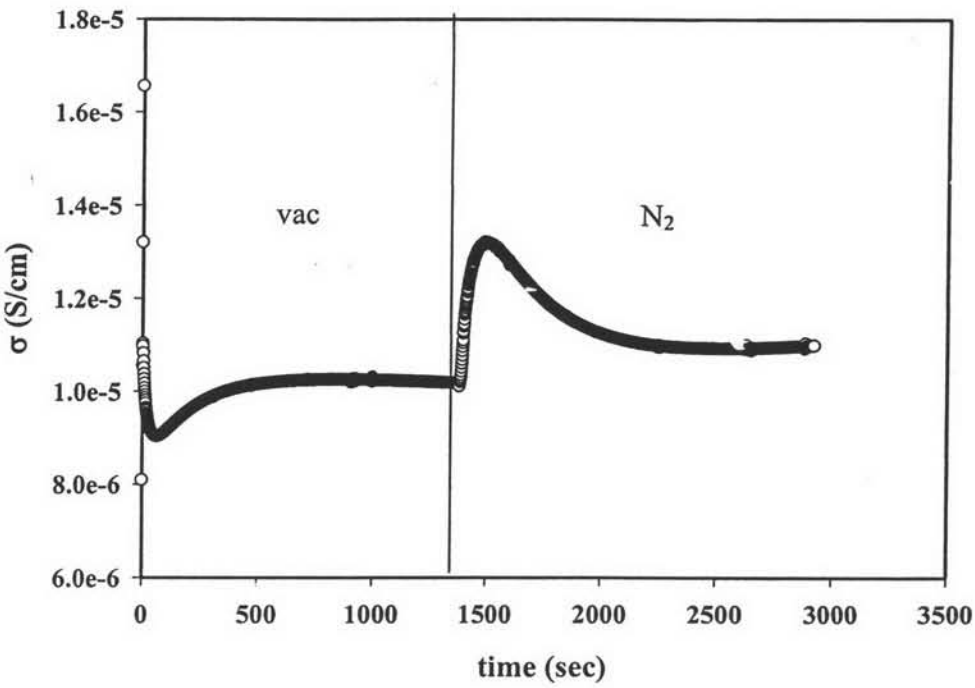

Figure N24 Specific conductivity of Pth_200:1/MOR_30(1) after evacuating H_2 and exposed to N_2.

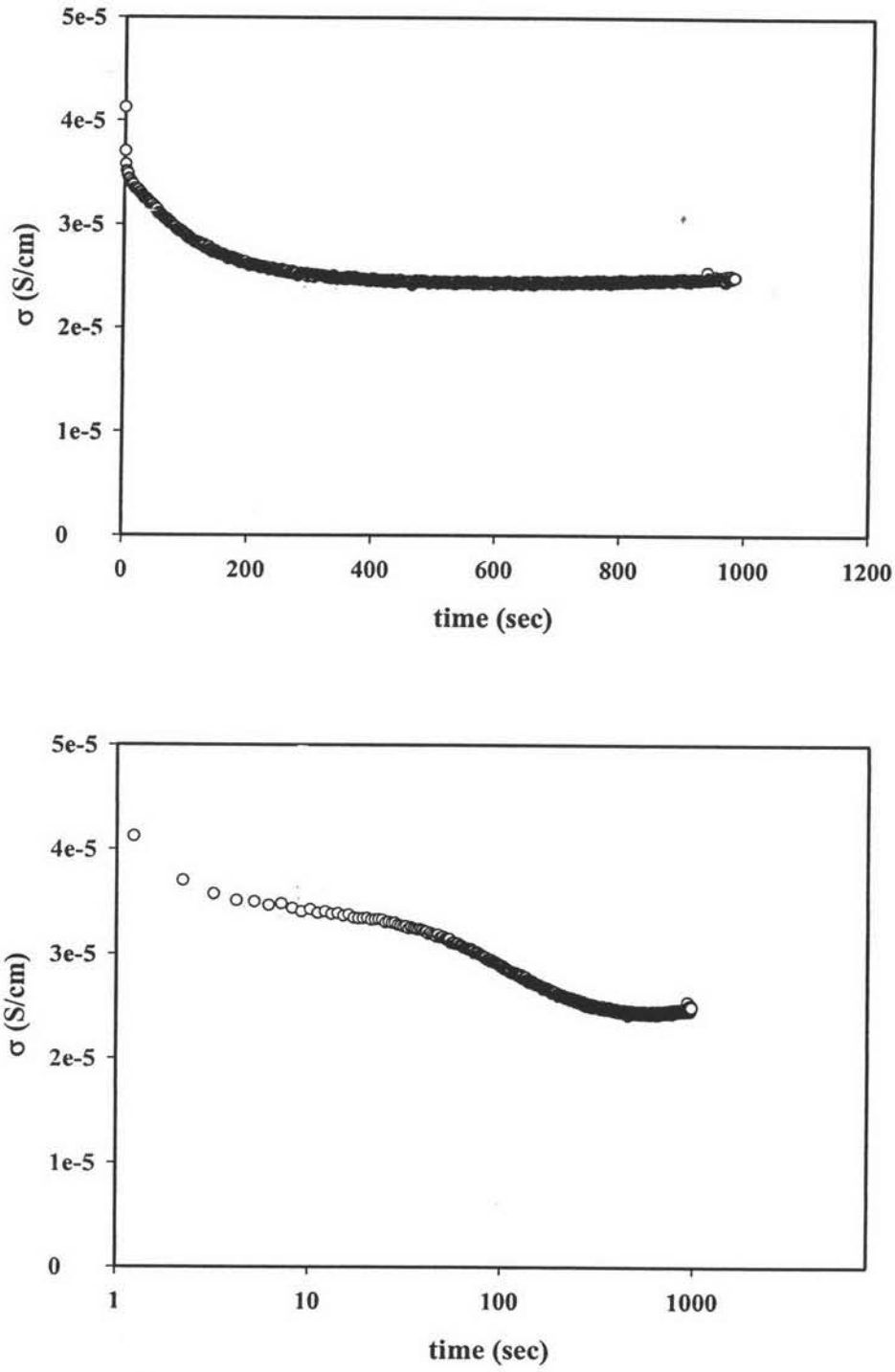

Figure N25 Specific conductivity of Pth_200:1/MOR_40(2) when exposed to H_2.

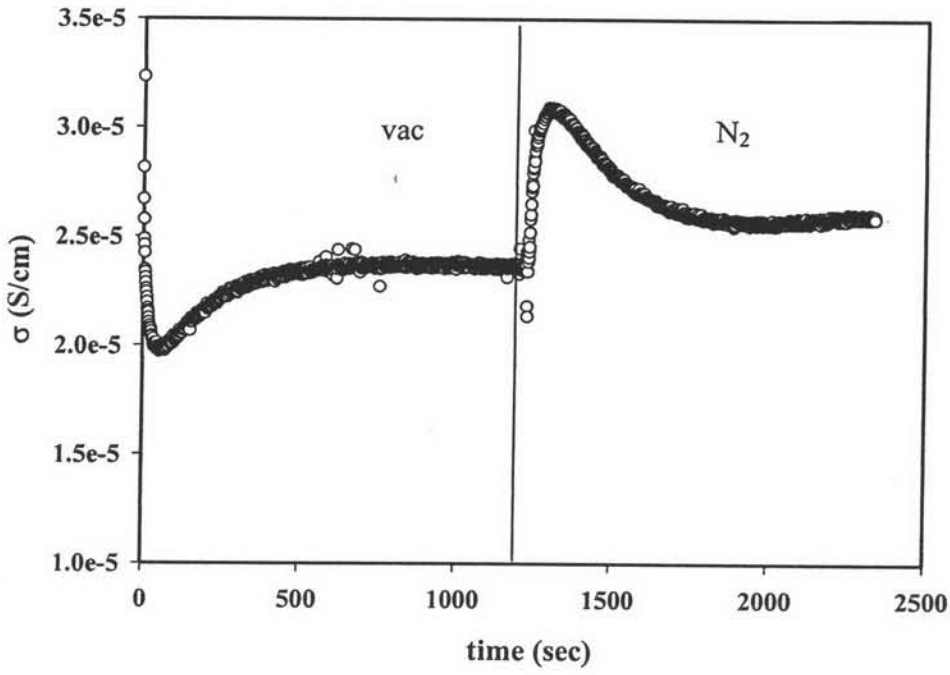

Figure N26 Specific conductivity of Pth_200:1/MOR_40(2) after evacuating H_2 and exposed to N_2.

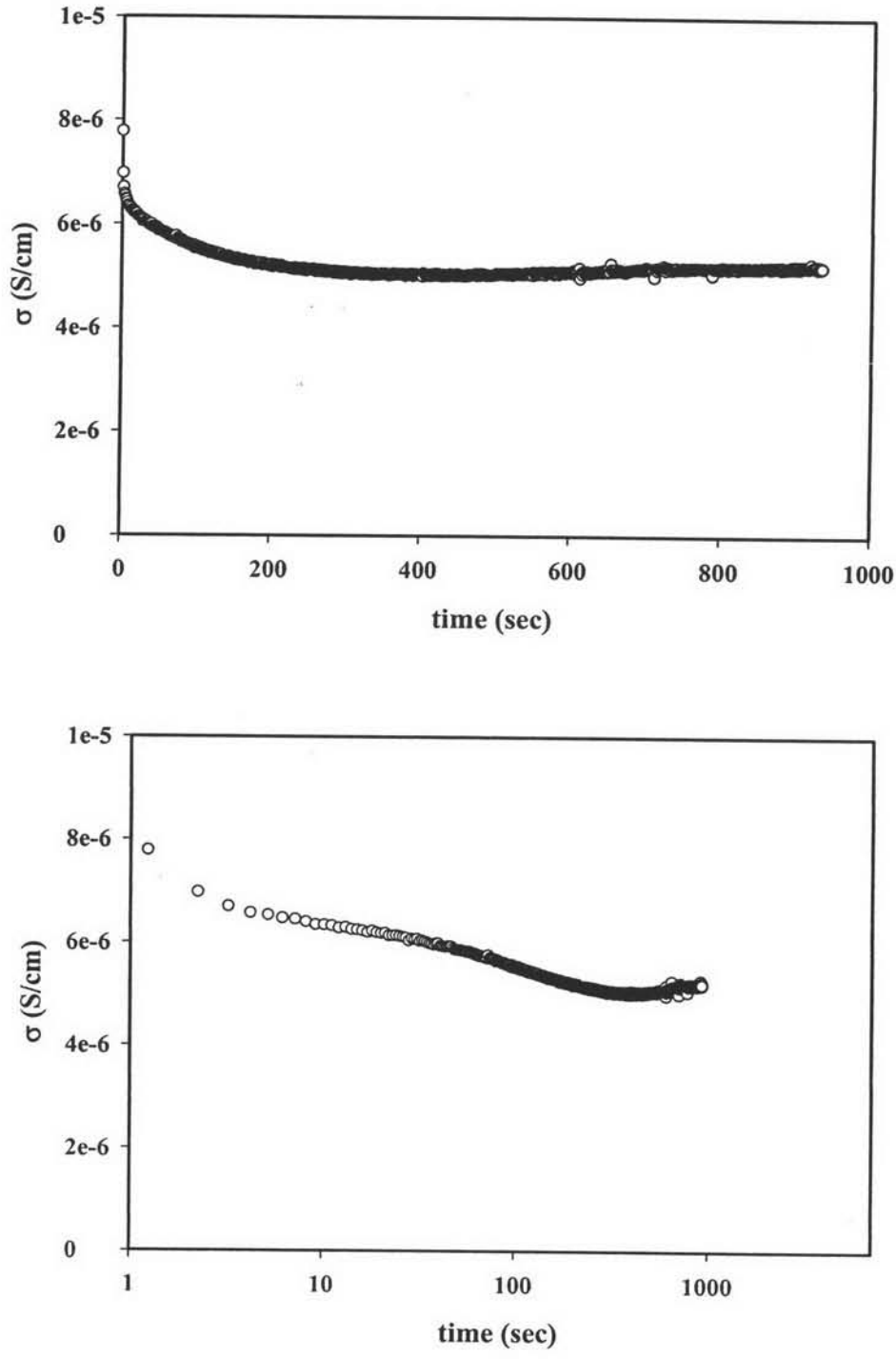

Figure N27 Specific conductivity of Pth_200:1/MOR_50(2) when exposed to H_2.

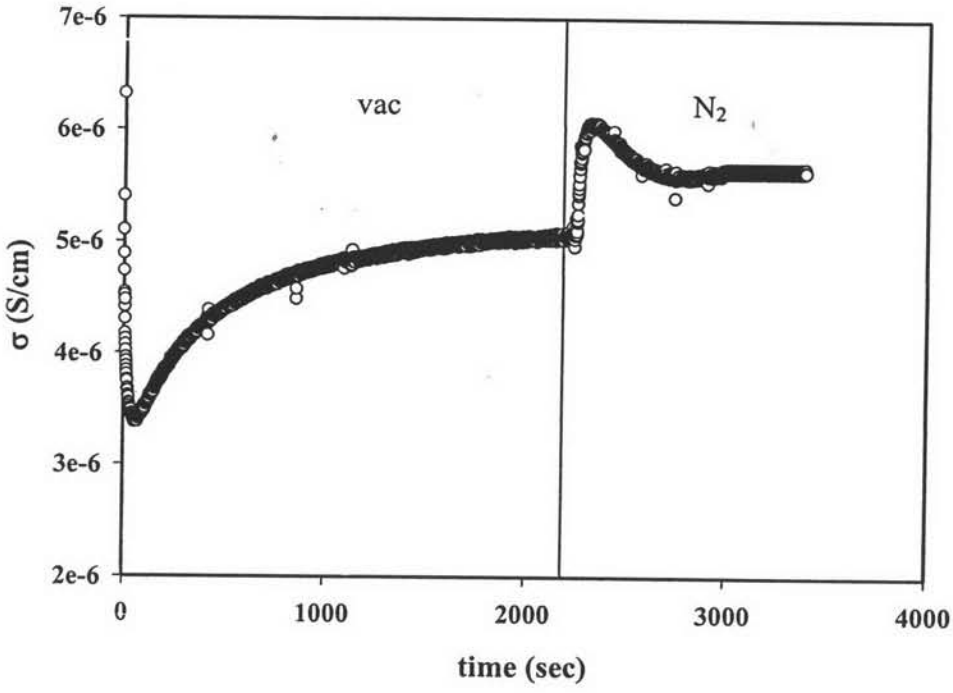

Figure N28 Specific conductivity of Pth_200:1/MOR_50(2) after evacuating H_2 and exposed to N_2.

Table N1 Specific conductivity and sensitivity of Pth_200:1 when exposed to H_2, [a] T_c = chamber temperature, [b] t_i = the time that σ_{H2} reaches equilibrium, [c] t_r = the time that σ reaches equilibrium after evacuate H_2

Vapplied (V) : 5 T_c[a] : 29±1 t_i[b] (min) : 105 t_r[c] (min) : 21

$K = 5.06\times10^{-5}$ for sample 1 $K = 2.17\times10^{-4}$ for sample 2

No.	Thickness	I (A)					σ (S/cm)					Δσ(S/cm)	$\Delta\sigma/\sigma_{N2}$
	(cm)	Air	Vac	$N_{2\ initial}$	$N_{2\ final}$	H_2	Air	Vac	$N_{2\ initial}$	$N_{2\ final}$	H_2		
1	0.01826	2.65E-06	3.68E-11	6.55E-11	3.40E-11	4.83E-11	5.73E-01	7.96E-06	1.42E-05	7.36E-06	1.04E-05	-3.73E-06	-2.63E-01
2	0.01821	6.93E-06	7.47E-11	1.15E-10	7.38E-11	9.48E-11	3.51E-01	3.78E-06	5.82E-06	3.74E-06	4.80E-06	-1.02E-06	-1.76E-01
Avg.		4.79E-06	5.57E-11	9.03E-11	5.39E-11	7.15E-11	4.62E-01	5.87E-06	1.00E-05	5.55E-06	7.62E-06	-2.38E-06	-2.19E-01
SD		3.02E-06	2.68E-11	3.51E-11	2.81E-11	3.29E-11	1.58E-01	2.95E-06	5.90E-06	2.56E-06	3.99E-06	1.91E-06	6.15E-02

Table N2 Specific conductivity and sensitivity of Pth_200:1/L_20 when exposed to H_2

Vapplied (V) : 4 T_c[a] : 29±1 t_i[b] (min) : 28 t_r[c] (min) : 15

$K = 4.27\times10^{-4}$ for sample 1 $K = 2.20\times10^{-4}$ for sample 2

No.	Thickness	I (A)					σ (S/cm)					Δσ(S/cm)	$\Delta\sigma/\sigma_{N2}$
	(cm)	Air	Vac	$N_{2\ initial}$	$N_{2\ final}$	H_2	Air	Vac	$N_{2\ initial}$	$N_{2\ final}$	H_2		
1	0.01619	1.42E-09	3.68E-11	8.09E-12	7.43E-12	7.55E-12	5.13E-05	2.72E-07	2.93E-07	2.69E-07	2.73E-07	-1.97E-08	-6.72E-02
2	0.01594	1.65E-09	7.47E-11	2.08E-12	1.70E-12	1.90E-12	1.17E-04	1.31E-07	1.50E-07	1.21E-07	1.35E-07	-1.43E-08	-8.60E-02
Avg.		1.53E-09	5.57E-11	5.08E-12	4.57E-12	4.72E-12	4.68E-05	9.94E-08	1.01E-07	1.04E-07	9.74E-08	-1.62E-08	-7.66E-02
SD		1.63E-10	2.68E-11	4.26E-12	4.05E-12	4.00E-12	4.68E-05	9.94E-08	1.01E-07	1.04E-07	9.74E-08	4.91E-09	1.33E-02

Table N3 Specific conductivity and sensitivity of Pth_200:1/MOR_20 when exposed to H_2

Vapplied (V) : 17 T_c[a] : 29±1 t_i[b] (min) : 45 t_r[c] (min) : 30

K = 5.06×10^{-5} for sample 1 K = 2.17×10^{-4} for sample 2

No.	Thickness (cm)	I (A)					σ (S/cm)					Δσ(S/cm)	$\Delta\sigma/\sigma_{N2}$
		Air	Vac	$N_{2\ initial}$	$N_{2\ final}$	H_2	Air	Vac	$N_{2\ initial}$	$N_{2\ final}$	H_2		
1	0.01609	4.32E-07	6.87E-11	3.68E-11	4.37E-11	5.85E-11	3.12E-02	4.97E-06	6.99E-06	3.16E-06	4.23E-06	-2.76E-06	-3.95E-01
2	0.01544	8.62E-07	1.46E-10	3.05E-10	1.17E-10	1.59E-10	1.51E-02	2.56E-06	5.35E-06	2.06E-06	2.79E-06	-2.56E-06	-4.79E-01
Avg.		6.47E-07	1.07E-10	1.71E-10	8.05E-11	1.09E-10	2.32E-02	3.76E-06	6.17E-06	2.61E-06	3.51E-06	-2.66E-06	-4.37E-01
SD		3.04E-07	5.44E-11	1.89E-10	5.21E-11	7.09E-11	1.14E-02	1.70E-06	1.16E-06	7.75E-07	1.02E-06	1.42E-07	5.91E-02

Table N4 Specific conductivity and sensitivity of Pth_200:1/BEA_20 when exposed to H_2

Vapplied (V) : 24 T_c : 29±1 t_i (min) : 111 t_r (min) : 20

K = 5.06×10^{-5} for sample 1 K = 2.17×10^{-4} for sample 2

No.	Thickness (cm)	I (A)					σ (S/cm)					Δσ(S/cm)	$\Delta\sigma/\sigma_{N2}$
		Air	Vac	$N_{2\ initial}$	$N_{2\ final}$	H_2	Air	Vac	$N_{2\ initial}$	$N_{2\ final}$	H_2		
1	0.01658	1.21E-06	7.47E-10	1.70E-08	5.03E-10	3.99E-09	5.99E-02	3.71E-05	8.44E-04	2.50E-05	1.98E-04	-6.45E-04	-7.65E-01
2	0.01564	2.50E-06	1.33E-09	1.38E-08	5.64E-10	4.16E-09	3.06E-02	1.64E-05	1.70E-04	6.92E-06	5.11E-05	-1.19E-04	-6.99E-01
Avg.		1.85E-06	1.04E-09	1.54E-08	5.33E-10	4.08E-09	4.53E-02	2.67E-05	5.07E-04	1.59E-05	1.25E-04	-3.82E-04	-7.32E-01
SD		9.12E-07	4.14E-10	2.23E-09	4.34E-11	1.19E-10	2.07E-02	1.47E-05	4.76E-04	1.28E-05	1.04E-04	3.72E-04	4.65E-02

Table N5 Specific conductivity and sensitivity of Pth_200:1/MOR_Li[90]_20 when exposed to H_2

Vapplied (V) : 19 T_c : 29±1 t_i (min) : 24 t_r (min) : 16

$K = 5.06\times10^{-5}$ for sample 1 $K = 2.17\times10^{-4}$ for sample 2

No.	Thickness	I (A)					σ (S/cm)					Δσ(S/cm)	$\Delta\sigma/\sigma_{N2}$
	(cm)	Air	Vac	$N_{2\ initial}$	$N_{2\ final}$	H_2	Air	Vac	$N_{2\ initial}$	$N_{2\ final}$	H_2		
1	0.01543	6.66E-07	7.17E-11	7.66E-11	6.82E-11	7.05E-11	4.49E-02	4.83E-06	5.17E-06	4.59E-06	4.75E-06	-4.14E-07	-8.02E-02
2	0.01595	4.45E-06	1.36E-10	1.52E-10	1.37E-10	1.41E-10	6.77E-02	2.06E-06	2.31E-06	2.08E-06	2.14E-06	-1.75E-07	-7.55E-02
Avg.		2.56E-06	1.04E-10	1.14E-10	1.02E-10	1.06E-10	5.63E-02	3.45E-06	3.74E-06	3.34E-06	3.44E-06	-2.94E-07	-7.78E-02
SD		2.68E-06	4.51E-11	5.33E-11	4.85E-11	4.96E-11	1.61E-02	1.96E-06	2.02E-06	1.78E-06	1.85E-06	1.69E-07	3.30E-03

Table N6 Specific conductivity and sensitivity of Pth_200:1/MOR_K[90]_20 when exposed to H_2

Vapplied (V) : 13 T_c : 29±1 t_i (min) : 46 t_r (min) : 19

$K = 4.27\times10^{-4}$ for sample 1 $K = 2.17\times10^{-4}$ for sample 2

No.	Thickness	I (A)					σ (S/cm)					* Δσ(S/cm)	$\Delta\sigma/\sigma_{N2}$
	(cm)	Air	Vac	$N_{2\ initial}$	$N_{2\ final}$	H_2	Air	Vac	$N_{2\ initial}$	$N_{2\ final}$	H_2		
1	0.01602	1.64E-08	2.13E-10	2.56E-10	1.72E-10	1.98E-10	1.84E-04	2.39E-06	2.88E-06	1.94E-06	2.22E-06	-6.58E-07	-2.28E-01
2	0.01602	2.62E-08	2.56E-10	3.04E-10	2.10E-10	2.40E-10	5.80E-04	5.66E-06	6.73E-06	4.65E-06	5.31E-06	-1.42E-06	-2.11E-01
Avg.		2.13E-08	2.34E-10	2.80E-10	1.91E-10	2.19E-10	3.82E-04	4.03E-06	4.81E-06	3.29E-06	3.77E-06	-1.04E-06	-2.20E-01
SD		6.96E-09	3.03E-11	3.38E-11	2.67E-11	2.99E-11	2.80E-04	2.31E-06	2.72E-06	1.92E-06	2.18E-06	5.38E-07	1.24E-02

Table N7 Specific conductivity and sensitivity of Pth_200:1/L_Na[15]_20 when exposed to H_2

Vapplied (V) : 7 T_c : 29±1 t_i (min) : 29 t_r (min) : 29

K = 5.06×10^{-5} for sample 1 K = 2.17×10^{-4} for sample 2

No.	Thickness	I (A)					σ (S/cm)					Δσ(S/cm)	$\Delta\sigma/\sigma_{N2}$
	(cm)	Air	Vac	$N_{2\ initial}$	$N_{2\ final}$	H_2	Air	Vac	$N_{2\ initial}$	$N_{2\ final}$	H_2		
1	0.01410	3.50E-08	8.58E-12	9.27E-12	8.99E-12	9.07E-12	8.31E-04	1.72E-06	1.86E-06	1.80E-06	1.82E-06	-3.89E-08	-2.10E-02
2	0.01468	4.28E-08	6.57E-11	7.38E-11	6.25E-11	7.02E-11	1.89E-03	2.95E-06	3.31E-06	2.80E-06	3.15E-06	-1.63E-07	-4.91E-02
Avg.		3.89E-08	3.72E-11	4.15E-11	3.57E-11	3.96E-11	1.36E-03	2.33E-06	2.58E-06	2.30E-06	2.48E-06	-1.01E-07	-3.51E-02
SD		5.48E-09	4.04E-11	4.56E-11	3.78E-11	4.32E-11	7.50E-04	8.70E-07	1.03E-06	7.09E-07	9.41E-07	8.74E-08	1.99E-02

Table N8 Specific conductivity and sensitivity of Pth_200:1/ L_Na[20]_20 when exposed to H_2

Vapplied (V) : 18 T_c : 29±1 t_i (min) : 25 t_r (min) : 13

K = 5.06×10^{-5} for sample 1 K = 2.17×10^{-4} for sample 2

No.	Thickness	I (A)					σ (S/cm)					Δσ(S/cm)	$\Delta\sigma/\sigma_{N2}$
	(cm)	Air	Vac	$N_{2\ initial}$	$N_{2\ final}$	H_2	Air	Vac	$N_{2\ initial}$	$N_{2\ final}$	H_2		
1	0.01522	3.55E-08	2.86E-11	3.24E-11	2.81E-11	2.87E-11	3.03E-04	2.06E-06	2.34E-06	2.02E-06	2.07E-06	-2.65E-07	-1.13E-01
2	0.01489	2.40E-08	1.30E-10	1.46E-10	1.26E-10	1.29E-10	4.13E-04	2.23E-06	2.50E-06	2.17E-06	2.22E-06	-2.84E-07	-1.13E-01
Avg.		2.97E-08	7.91E-11	8.90E-11	7.72E-11	7.89E-11	3.58E-04	2.15E-06	2.42E-06	2.10E-06	2.15E-06	-2.74E-07	-1.13E-01
SD		8.09E-09	7.15E-11	8.01E-11	6.95E-11	7.10E-11	7.77E-05	1.17E-07	1.19E-07	1.06E-07	1.06E-07	1.35E-08	2.46E-05

Table N9 Specific conductivity and sensitivity of Pth_200:1/ L_Na[30]_20 when exposed to H_2

Vapplied (V) : 13 T_c : 29±1 t_i (min) : 28 t_r (min) : 16

K = 5.06×10^{-5} for sample 1 K = 2.17×10^{-4} for sample 2

No.	Thickness (cm)	I (A)					σ (S/cm)					Δσ(S/cm)	$\Delta\sigma/\sigma_{N2}$
		Air	Vac	$N_{2\ initial}$	$N_{2\ final}$	H_2	Air	Vac	$N_{2\ initial}$	$N_{2\ final}$	H_2		
1	0.01543	1.58E-08	2.51E-11	3.07E-11	2.17E-11	2.42E-11	1.56E-03	2.47E-06	3.02E-06	2.13E-06	2.38E-06	-6.41E-07	-2.12E-01
2	0.01544	3.34E-08	6.25E-11	8.48E-11	6.22E-11	6.76E-11	7.66E-04	1.43E-06	1.95E-06	1.43E-06	1.55E-06	-3.95E-07	-2.03E-01
Avg.		2.46E-08	4.38E-11	5.77E-11	4.19E-11	4.59E-11	1.16E-03	1.95E-06	2.48E-06	1.78E-06	1.97E-06	-5.18E-07	-2.08E-01
SD		1.24E-08	2.64E-11	3.83E-11	2.86E-11	3.07E-11	5.59E-04	7.34E-07	7.60E-07	5.00E-07	5.86E-07	1.74E-07	6.58E-03

Table N10 Specific conductivity and sensitivity of Pth_200:1/ L_Na[50]_20 when exposed to H_2

Vapplied (V) : 12 T_c : 29±1 t_i (min) : 32 t_r (min) : 18

K = 5.06×10^{-5} for sample 1 K = 2.17×10^{-4} for sample 2

No.	Thickness (cm)	I (A)					σ (S/cm)					Δσ(S/cm)	$\Delta\sigma/\sigma_{N2}$
		Air	Vac	$N_{2\ initial}$	$N_{2\ final}$	H_2	Air	Vac	$N_{2\ initial}$	$N_{2\ final}$	H_2		
1	0.01560	3.06E-08	2.39E-10	2.70E-10	1.95E-10	2.21E-10	3.23E-03	2.52E-05	2.85E-05	2.07E-05	2.33E-05	-5.20E-06	-1.82E-01
2	0.01570	1.30E-07	2.80E-10	3.22E-10	2.38E-10	2.63E-10	3.18E-03	6.85E-06	7.89E-06	5.81E-06	6.44E-06	-1.45E-06	-1.83E-01
Avg.		8.02E-08	2.59E-10	2.96E-10	2.16E-10	2.42E-10	3.20E-03	1.60E-05	1.82E-05	1.33E-05	1.49E-05	-3.32E-06	-1.83E-01
SD		7.02E-08	2.92E-11	3.69E-11	3.03E-11	3.00E-11	3.48E-05	1.30E-05	1.46E-05	1.05E-05	1.19E-05	2.66E-06	6.53E-04

Table N11 Specific conductivity and sensitivity of Pth_200:1/ MOR_10 when exposed to H_2

Vapplied (V) : 13 T_c : 29±1 t_i (min) : 26 t_r (min) : 38

$K = 5.06\times10^{-5}$ for sample 1 $K = 2.17\times10^{-4}$ for sample 2

No.	Thickness	I (A)					σ (S/cm)					Δσ(S/cm)	$\Delta\sigma/\sigma_{N2}$
	(cm)	Air	Vac	$N_{2\ initial}$	$N_{2\ final}$	H_2	Air	Vac	$N_{2\ initial}$	$N_{2\ final}$	H_2		
1	0.01808	4.08E-07	2.61E-10	3.58E-10	2.04E-10	2.37E-10	3.43E-02	2.20E-05	3.01E-05	1.72E-05	1.99E-05	-1.02E-05	-3.37E-01
2	0.01816	1.23E-06	3.38E-10	5.44E-10	3.27E-10	3.52E-10	2.40E-02	6.60E-06	1.06E-05	6.39E-06	6.87E-06	-3.74E-06	-3.52E-01
Avg.		8.20E-07	3.00E-10	4.51E-10	2.66E-10	2.95E-10	2.92E-02	1.43E-05	2.04E-05	1.18E-05	1.34E-05	-6.95E-06	-3.45E-01
SD		5.82E-07	5.44E-11	1.31E-10	8.71E-11	8.12E-11	7.28E-03	1.09E-05	1.38E-05	7.61E-06	9.25E-06	4.54E-06	1.07E-02

Table N12 Specific conductivity and sensitivity of Pth_200:1/ MOR_30 when exposed to H_2

Vapplied (V) : 16 T_c : 29±1 t_i (min) : 24 t_r (min) : 23

$K = 5.06\times10^{-5}$ for sample 1 $K = 2.17\times10^{-4}$ for sample 2

No.	Thickness	I (A)					σ (S/cm)					Δσ(S/cm)	$\Delta\sigma/\sigma_{N2}$
	(cm)	Air	Vac	$N_{2\ initial}$	$N_{2\ final}$	H_2	Air	Vac	$N_{2\ initial}$	$N_{2\ final}$	H_2		
1	0.01875	1.78E-07	1.80E-10	2.08E-10	1.66E-10	1.75E-10	1.18E-02	1.18E-05	1.37E-05	1.09E-05	1.15E-05	-2.17E-06	-1.58E-01
2	0.01834	4.73E-07	2.84E-10	3.72E-10	3.03E-10	3.41E-10	7.43E-03	4.45E-06	5.84E-06	4.75E-06	5.36E-06	-4.80E-07	-8.21E-02
Avg.		3.26E-07	2.32E-10	2.90E-10	2.34E-10	2.58E-10	9.59E-03	8.15E-06	9.77E-06	7.85E-06	8.45E-06	-1.32E-06	-1.20E-01
SD		2.08E-07	7.34E-11	1.16E-10	9.65E-11	1.18E-10	3.06E-03	5.23E-06	5.56E-06	4.38E-06	4.36E-06	1.19E-06	5.39E-02

Table N13 Specific conductivity and sensitivity of Pth_200:1/ MOR_40 when exposed to H_2

Vapplied (V) : 25 T_c : 29±1 t_i (min) : 17 t_r (min) : 21

K = 5.06×10^{-5} for sample 1 K = 2.17×10^{-4} for sample 2

No.	Thickness (cm)	I (A)					σ (S/cm)					Δσ(S/cm)	$\Delta\sigma/\sigma_{N2}$
		Air	Vac	$N_{2\ initial}$	$N_{2\ final}$	H_2	Air	Vac	$N_{2\ initial}$	$N_{2\ final}$	H_2		
1	0.02097	8.32E-07	5.84E-10	7.40E-10	5.99E-10	6.93E-10	3.14E-02	2.20E-05	2.79E-05	2.26E-05	2.61E-05	-1.77E-06	-6.35E-02
2	0.02057	1.51E-06	7.73E-10	7.93E-10	6.85E-10	6.56E-10	1.35E-02	6.93E-06	7.11E-06	6.14E-06	5.88E-06	-1.23E-06	-1.73E-01
Avg.		1.17E-06	6.78E-10	7.67E-10	6.42E-10	6.74E-10	2.24E-02	1.45E-05	1.75E-05	1.44E-05	1.60E-05	-1.50E-06	-1.18E-01
SD		4.79E-07	1.34E-10	3.75E-11	6.10E-11	2.62E-11	1.26E-02	1.07E-05	1.47E-05	1.16E-05	1.43E-05	3.84E-07	7.73E-02

Table N14 Specific conductivity and sensitivity of Pth_200:1/ MOR_50 when exposed to H_2

Vapplied (V) : 21 T_c : 29±1 t_i (min) : 16 t_r (min) : 37

K = 5.06×10^{-5} for sample 1 K = 2.17×10^{-4} for sample 2

No.	Thickness (cm)	I (A)					σ (S/cm)					Δσ(S/cm)	$\Delta\sigma/\sigma_{N2}$
		Air	Vac	$N_{2\ initial}$	$N_{2\ final}$	H_2	Air	Vac	$N_{2\ initial}$	$N_{2\ final}$	H_2		
1	0.02339	3.77E-07	4.89E-10	5.24E-10	5.14E-10	4.59E-10	1.52E-02	1.97E-05	2.11E-05	2.07E-05	1.85E-05	-2.64E-06	-1.25E-01
2	0.02462	1.46E-06	6.60E-10	6.16E-10	6.32E-10	5.82E-10	1.30E-02	5.88E-06	5.49E-06	5.64E-06	5.19E-06	-3.07E-07	-5.59E-02
Avg.		9.16E-07	5.74E-10	5.70E-10	5.73E-10	5.20E-10	1.41E-02	1.28E-05	1.33E-05	1.32E-05	1.18E-05	-1.47E-06	-9.05E-02
SD		7.63E-07	1.20E-10	6.50E-11	8.35E-11	8.71E-11	1.55E-03	9.76E-06	1.10E-05	1.06E-05	9.39E-06	1.65E-06	4.90E-02

Appendix O The Interaction between Pth, L, MOR, BEA and H_2 by FTIR

FTIR spectra of Pth_200:1, Pth_200:1/MOR_20, L, MOR and BEA were taken by KBr pellet technique. The sample pellet was placed on sample holder and put it into the gas cell. The spectrums of samples were recorded, before H_2 exposure, when exposed to H_2, and after the H_2 exposure, in order to study interaction between these samples and H_2.

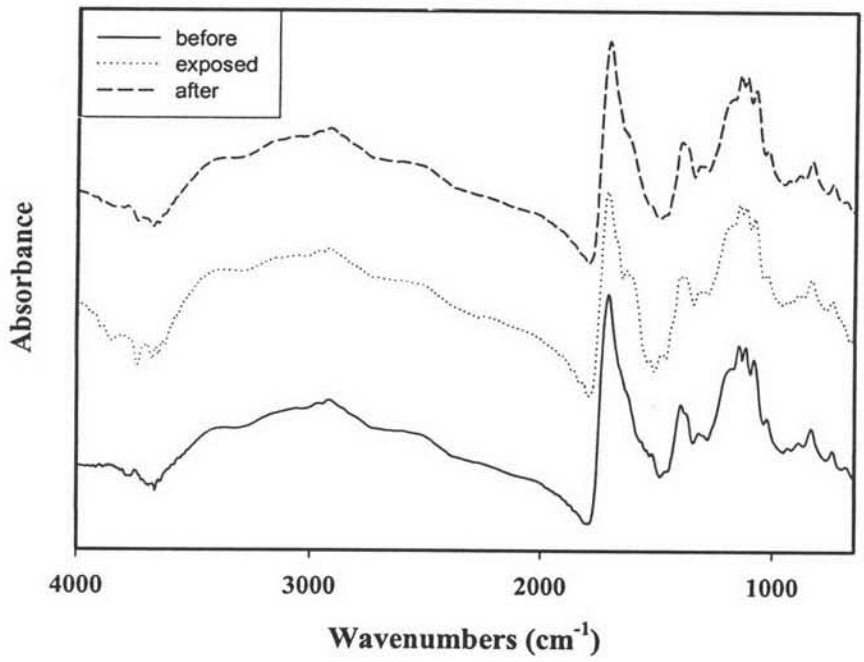

Figure O1 The FT-IR spectra of Pth_200:1: before, exposed and after exposed to H_2.

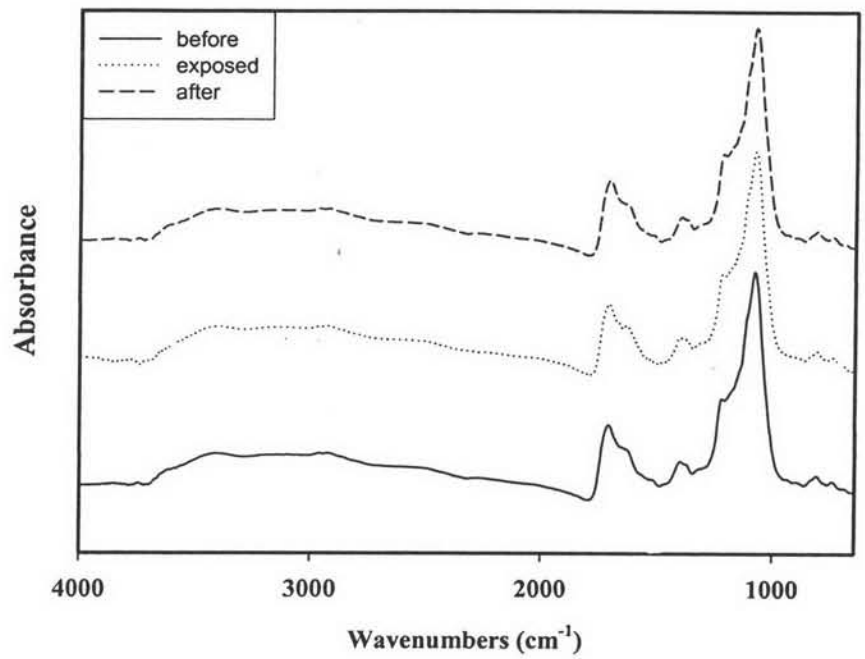

Figure O2 The FT-IR spectra of Pth_200:1/MOR_20: before, exposed and after exposed to H_2.

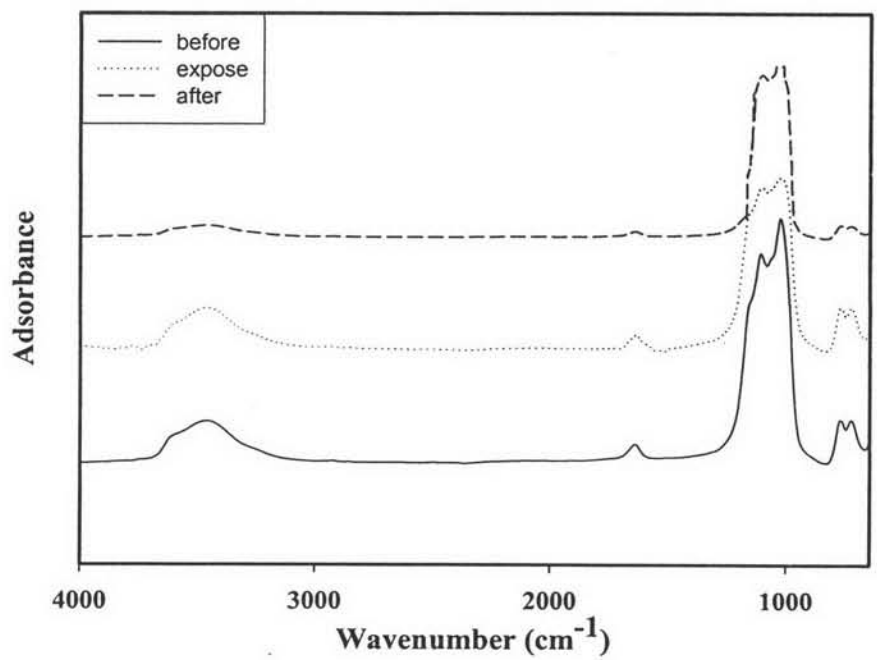

Figure O3 The FT-IR spectra of zeolite L: before, exposed and after exposed to H_2.

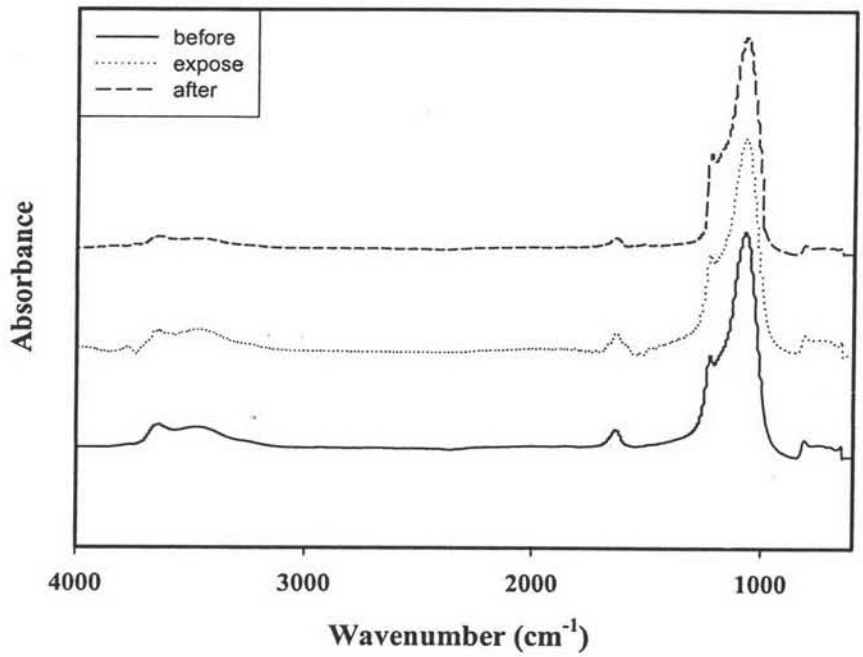

Figure O4 The FT-IR spectra of MOR: before, exposed and after exposed to H_2.

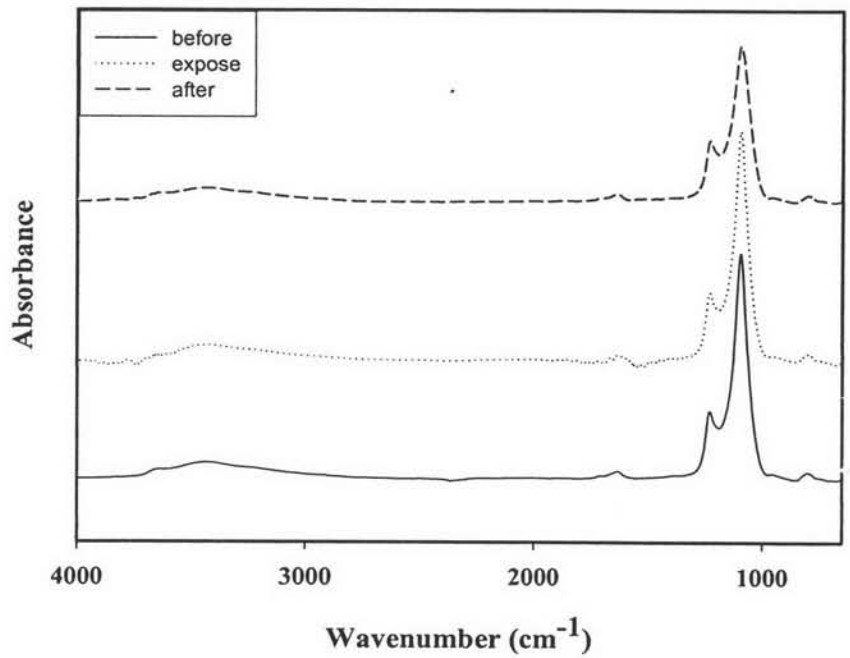

Figure O5 The FT-IR spectra of BEA: before, expose and after expose to H_2.

Table O1 Peak position in FT-IR spectra of Pth_200:1 before, exposed and after exposed to H_2.

Characteristic	Ref.	Wavenumber (cm^{-1})		
		before	exposed	after
CH str of thiophene ring	3200-3000[a]	2960	2966	2962
CH str of aliphatic	3000-2800[a]	2919	2921	2920
C=O str	1700[a]	1707	1711	1709
C=C str	1700-1575[b]	N/A	1632	N/A
C=C str asym, thiophene ring	1468[c]	1465	1470	1467
thiophene ring str	1410[a]	1396	1404	1398
C-C str, thiophene ring	1350[c]	1319	1322	1320
C-O str	1300-1200[a]	1180	1181	1180
ClO_4^-	1140-1060[d]	1146	1147	1147
thiophene cycle deformation	1015[c]	1026	1025	1026
C-S str, thiophene ring	962 [c]	936	936	935
N/A		890	890	890
N/A		835	835	835
N/A		743	744	744

[a] Kim et al., 1999, [b] Skoog and Leary, 1992, [c] Van et al., 2001, [d] Gunzler and Gremlich, 2002, [e] Weitkamp and Puppe, 1999

Table O2 Peak position in FT-IR spectra of Pth_200:1/MOR_20 before, exposed and after exposed to H_2.

Characteristic	Ref.	Wavenumber (cm^{-1})		
		before	exposed	after
CH str of thiophene ring	3200-3000[a]	2961	2962	2961
CH str of aliphatic	3000-2800[a]	2926	2922	2924
C=O str	1700[a]	1708	1709	1709
C=C str	1700-1575[b]	1627	1631	1639
C=C str asym, thiophene ring	1468[c]	1463	1469	1467
thiophene ring str	1410[a]	1397	1400	1399
C-C str, thiophene ring	1350[c]	1320	1325	1321
O-T-O ex asym	1150-1050[e] sh	1220	1217	1221
O-T-O in asym	1250-950[e]	1081	1081	1081
O-T-O ex sym	820-750[e]	813	813	813

Table O3 Peak position in FT-IR spectra of L before, exposed and after exposed to H_2.

Characteristic	Ref.	Wavenumber (cm^{-1})		
	(Weitkamp and Puppe, 1999)	before	exposed	after
-OH str.	N/A	3458	3462	3449
	N/A	1639	1636	1642
O-T-O ex asym	1150-1050 sh	1109	1105	1108
O-T-O in asym	1250-950	1027	1024	1017
O-T-O ex sym	820-750	772	772	772
O-T-O in sym	720-650	727	727	728

T= Si or Al, ex = external linkages, in = internal tetrahedra, sh = shoulder
asym = asymmetric stretching vibration, sym = asymmetric stretching vibration

Table O4 Peak position in FT-IR spectra of MOR before, exposed and after exposed to H_2.

Characteristic	Ref. (Weitkamp and Puppe, 1999)	Wavenumber (cm^{-1})		
		before	exposed	after
-OH str.	N/A	3636	3636	3648
-OH str.	N/A	3461	3466	3465
	N/A	1633	1631	1631
O-T-O ex asym	1150-1050 sh	1226	1226	1226
O-T-O in asym	1250-950	1074	1075	1068
O-T-O ex sym	820-750	811	810	811

Table O5 Peak position in FT-IR spectra of BEA before, exposed and after exposed to H_2.

Characteristic	Ref. (Weitkamp and Puppe, 1999)	Wavenumber (cm^{-1})		
		before	exposed	after
-OH str.	N/A	3658	3661	3646
-OH str.	N/A	3431	3433	3445
	N/A	1629	1624	1630
O-T-O ex asym	1150-1050 sh	1229	1229	1229
O-T-O in asym	1250-950	1096	1096	1096
O-T-O ex sym	820-750	801	800	789

Appendix P Temperature Program Desorption (TPD)

Adsorption property of sample powder Zeolite L, MOR and BEA, Pth_200:1 and Pth_200:1/MOR, was investigated by TPD. Sample powder was weighted about 0.1-0.2 g and pretreated under N_2 atmosphere, and adsorbed with H_2 at 50°C. Then H_2 was desorbed from the samples and the data was analyzed.

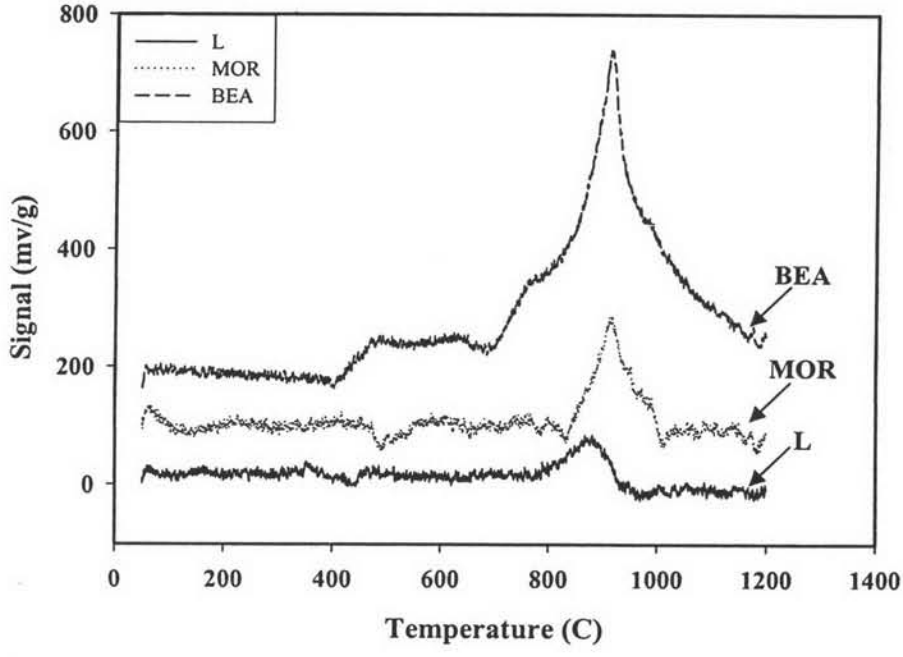

Figure P1 TPD signals of Zeolite L, MOR and BEA for the adsorption at 50°C.

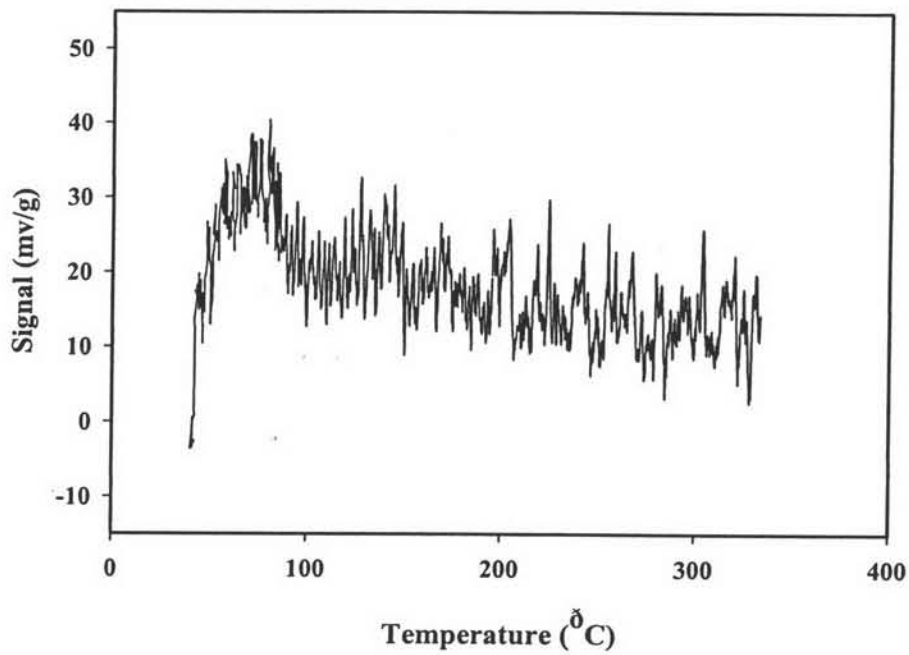

Figure P2 TPD signal of Pth_200:1 for the adsorption at 50°C.

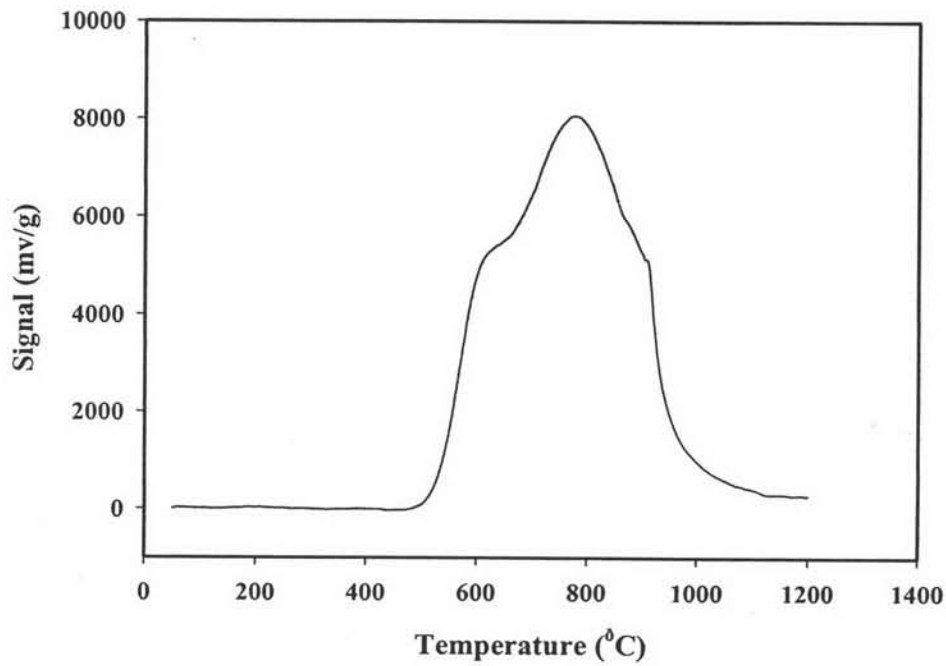

Figure P3 TPD signal of Pth_200:1/MOR_20 for the adsorption at 50°C

CURRICULUM VITAE

Name: Ms. Kanuengnit Thuwachaosuan

Date of Birth: November 5, 1981

Nationality: Thai

University Education:

2000-2004 Bachelor Degree of Petrochemical Engineer and Polymeric Materials, Faculty of Engineering and Industrial Technology, Silpakorn University, Nakornphathom, Thailand